

# Intrinsic Spin-Charge Conversion in Excitonic Pseudospin Superfluid

Yeyang Zhang<sup>1, 2</sup> and Ryuichi Shindou<sup>1, 2, \*</sup>

<sup>1</sup>International Center for Quantum Materials, School of Physics, Peking University, Beijing 100871, China

<sup>2</sup>Collaborative Innovation Center of Quantum Matter, Beijing 100871, China

(Dated: June 24, 2022)

Dissipationless spin-charge conversion phenomenon is proposed in excitonic pseudospin superfluid in an electron-hole double layer system. Magnetic exchange fields lift singlet-triplet degeneracy of exciton levels in the double layer system. Condensation of the singlet-triplet hybridized level breaks both a U(1) gauge symmetry and pseudospin rotational symmetry around the field, leading to spin-charge coupled superflow in the double layer system. We derive spin-charge coupled Josephson equations from a quantum-dot model, where a finite spatial variation of the exchange fields leads to a novel time dependence of electric currents.

*Introduction.*— Bosonic quasiparticles [1] condensed in momentum space acquire superfluidity [2, 3]. Depending on properties of the quasiparticles, the superfluid may carry mass [4, 5], electric charge [6, 7], spin magnetic moment [8–20] or pseudospin magnetic moment [21–27]. Spin Josephson effect [10, 11, 28–30] in spin superfluidity [31–39] converts spin voltage into spin supercurrent, offering practical loss-free methods of information transport [40–45]. Nonetheless, the previous works on the spin superfluidity is limited to pure spin transport, where the conversion of the spin current into a detectable charge current is implemented *externally* through the inverse spin Hall effect [46–51].

Exciton condensates in two-dimensional (2D) electron-hole double-layer (EHDL) system meet these two needs at the same time. In the 2D EHDL, electron and hole layers are separated from each other by an insulating layer [52–55]. Electrons and holes interact only through the Coulomb attraction, which binds them into a bound state (exciton). The condensation of the exciton breaks a relative U(1) gauge symmetry between the two layers, giving rise to electric supercurrents flowing in opposite directions in the two layers [52, 56, 57]. An experimental observation of the supercurrents in the zero magnetic field remains illusive at this moment [54, 58], while it has been observed in the quantum limit [59–66].

In this paper, we propose an intrinsic spin-charge conversion in the 2D EHDL system under magnetic *exchange* fields. The exchange fields induce polarization of exciton pseudospin in the exciton levels (electrons and holes with opposite spins). The condensation of such exciton levels breaks a pseudospin rotational symmetry and the U(1) gauge symmetry [22, 26, 67–69]. We clarify a relation between the pseudospin polarizations and physical symmetries in the condensates, and derive charge-spin coupled Josephson equations from a quantum-dot junction model [70, 71]. Based on the coupled Josephson equations, we show that a finite static spin voltage leads to an unconventional time-dependent (a.c.) charge supercurrent, giving a microscopic mechanism of the intrinsic

spin-charge conversion.

Spin-orbit interaction (SOI) facilitates rich photoluminescence measurements of the condensation in the EHDL [23–25, 69, 72–77]. 2D EHDL system breaks spatial inversion symmetry, causing an effective Rashba spin-orbit interaction (SOI) in the electron band [78–81]. We clarify that the Rashba interaction gives rise to spatial textures of the pseudospin polarization in the condensates [69], where a sliding phase of the texture (‘phason’) is given by the gapless pseudospin precessional mode. Accordingly, the finite static spin voltage induces not only the charge supercurrent but also a dissipationless sliding of the spatial textures of the exciton pseudospin.

*Models.*—The 2D EHDL system (in  $xy$  plane) comprises of an electron layer with a positive effective mass  $m_a (> 0)$  and a hole layer with a negative effective mass  $-m_b (< 0)$ . Electrons in these two layers are coupled only through a screened interlayer Coulomb interaction [69]:

$$\begin{aligned}
 K \equiv & H - \mu N \\
 = & \int d^2\vec{r} \mathbf{a}^\dagger(\vec{r}) [(-\frac{\hbar^2 \nabla^2}{2m_a} - E_g - \mu) \boldsymbol{\sigma}_0 + H_a \boldsymbol{\sigma}_x] \mathbf{a}(\vec{r}) \\
 + & \int d^2\vec{r} \mathbf{b}^\dagger(\vec{r}) [(\frac{\hbar^2 \nabla^2}{2m_b} + E_g - \mu) \boldsymbol{\sigma}_0 + H_b \boldsymbol{\sigma}_x] \mathbf{b}(\vec{r}) \\
 + & g \sum_{\sigma, \sigma'=\uparrow, \downarrow} \int d^2\vec{r} a_\sigma^\dagger(\vec{r}) b_{\sigma'}^\dagger(\vec{r}) b_{\sigma'}(\vec{r}) a_\sigma(\vec{r}). \quad (1)
 \end{aligned}$$

$\mathbf{a} \equiv (a_\uparrow, a_\downarrow)$ ,  $\mathbf{b} \equiv (b_\uparrow, b_\downarrow)$ ,  $H_a$  and  $H_b$  are annihilations of electrons and magnetic exchange fields in the two layers. The exchange fields can be experimentally induced by magnetic proximity effect from magnetic substrates. The interlayer interaction is modelled by the short-range interaction with a coupling constant  $g$ . The interaction leads to an interlayer *s*-wave exciton pairing, that can be described by a four-components exciton pairing field  $\phi_\mu \equiv \frac{g}{2} \langle \mathbf{b}^\dagger \boldsymbol{\sigma}_\mu \mathbf{a} \rangle$  with pseudospin singlet ( $\mu = 0$ ) and triplet ( $\mu = x, y, z$ ) components. The exchange fields lift the four-fold degeneracy, causing a singlet-triplet hybridization.

The singlet-triplet hybridization can be seen from a  $\phi^4$ -type effective Lagrangian for the four-component exciton

\* rshindou@pku.edu.cn

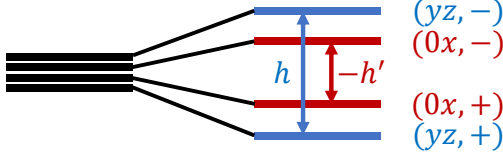


FIG. 1. The four-fold spin degeneracy is lifted by the exchange fields. When  $|h| > |h'|$  ( $|h| < |h'|$ ), the lowest band is transverse (longitudinal) hybrid mode, where the pseudospin polarization is in the  $yz$  ( $0x$ ) plane.  $(yz/0x, \pm)$  are exciton levels whose pseudospin polarization field  $\vec{\phi}$  are in the  $0x/yz$  plane and  $\pm$  specifies a relative position between the real and imaginary part of the four-components exciton field  $\vec{\phi}$  within the  $yz$  ( $0x$ ) plane. The figure is for  $h > h' > 0$ .

pairing field  $\vec{\Phi} \equiv (-i\phi_0, \phi_x, \phi_y, \phi_z)$  [69, 82]:

$$\begin{aligned} \mathcal{L} = & -\eta\vec{\Phi}^\dagger \cdot \partial_\tau \vec{\Phi} - \left(\alpha - \frac{2}{g}\right)|\vec{\Phi}|^2 - \gamma\left[(\vec{\Phi}'^2)^2 + (\vec{\Phi}''^2)^2\right. \\ & \left.+ 6\vec{\Phi}'^2\vec{\Phi}''^2 - 4(\vec{\Phi}' \cdot \vec{\Phi}'')^2\right] + \lambda|\nabla\vec{\Phi}|^2 \\ & - 2h(\Phi'_y\Phi''_z - \Phi'_z\Phi''_y) + 2h'(\Phi'_0\Phi''_x - \Phi'_x\Phi''_0) + \mathcal{O}(H^2), \end{aligned} \quad (2)$$

with  $|\vec{\Phi}|^2 \equiv \vec{\Phi}^\dagger \cdot \vec{\Phi}$ . Here  $\vec{\Phi}'$  and  $\vec{\Phi}''$  are real and imaginary parts of the complex-valued four-component exciton field  $\vec{\Phi} \equiv \vec{\Phi}' + i\vec{\Phi}''$ .  $h$  and  $h'$  are proportional to weighted average exchange fields, while their coefficients as well as other coupling constants in the Lagrangian depend on microscopic details. We assume that  $\eta < 0$ ,  $\gamma < 0$ , and  $\lambda > 0$  [69].

The spin degeneracy is lifted by the  $h$  and  $h'$  terms (Fig. 1). Energy levels of singlet-triplet hybridized modes depend on a competition between  $h$  and  $h'$  terms, which favor  $\vec{\Phi}$  polarized within the  $yz$  and  $0x$  planes respectively. Both of them favor a perpendicular arrangement of  $\vec{\Phi}'$  and  $\vec{\Phi}''$  in the respective planes. When a mass of the lowest hybridized mode becomes negative, the exciton undergoes a condensation. In the condensate phase with finite amplitude of  $\vec{\Phi}$ , the  $\gamma(\vec{\Phi}' \cdot \vec{\Phi}'')^2$  term in the action competes with the exchange terms; the quartic term favors a parallel arrangement of  $\vec{\Phi}'$  and  $\vec{\Phi}''$ , while the two exchange terms favor the perpendicular arrangements. The competition results in an acute angle between  $\vec{\Phi}'$  and  $\vec{\Phi}''$ , which increases linearly in  $h$  or  $h'$  and changes its sign under sign changes of the exchange fields.

The nature of the excitonic condensates can be clarified by a minimization of the action  $S = \int d\tau d^2\vec{r} \mathcal{L}$  by a  $\tau$ -independent classical configuration [82]. For  $|h| > |h'|$ , the action is minimized by a transverse configuration:

$$\begin{aligned} \vec{\phi}_{yz}(\theta, \varphi, \varphi_0) = & \rho \cos\theta(\cos\varphi_0 \vec{e}_y + \sin\varphi_0 \vec{e}_z) \\ & + i\rho \sin\theta[\cos(\varphi + \varphi_0) \vec{e}_y + \sin(\varphi + \varphi_0) \vec{e}_z], \end{aligned} \quad (3)$$

while for  $|h| < |h'|$ , it is minimized by a longitudinal

configuration,

$$\begin{aligned} \vec{\phi}_{0x}(\theta, \varphi, \varphi_0) = & \rho[-\sin\theta \cos(\varphi + \varphi_0) \vec{e}_0 + \cos\theta \sin\varphi_0 \vec{e}_x] \\ & + i\rho[\cos\theta \cos\varphi_0 \vec{e}_0 + \sin\theta \sin(\varphi + \varphi_0) \vec{e}_x], \end{aligned} \quad (4)$$

with  $\rho \equiv \sqrt{h_c/(2|\gamma|)}$  and  $h_c \equiv \alpha - 2/g$ . Here  $\vec{e}_\mu$  ( $\mu = 0, x, y, z$ ) are unit vectors in the four-components vector space. The angle between  $\vec{\Phi}'$  and  $\vec{\Phi}''$  in these two configurations is given by  $\varphi$  and it increases linearly in the exchange fields;

$$\tilde{h} \equiv \sin\varphi \sin 2\theta = h \equiv \begin{cases} h/h_c & \text{for } \vec{\phi}_{yz} \\ -h'/h_c & \text{for } \vec{\phi}_{0x} \end{cases} \quad (5)$$

We call the exciton condensates with these two configurations as transverse ( $yz$ ) and longitudinal ( $0x$ ) phases respectively. Both configurations have two arbitrary phase variables. One is a  $U(1)$  phase variable  $\varphi_0$ , and the other is a combination of  $\theta$  and  $\varphi$  that satisfies the constraint of Eq. (5). The two are nothing but gapless Goldstone modes associated with broken continuous symmetries.

*Spontaneously Broken Symmetries.*— Both  $yz$  and  $0x$  phases break the relative  $U(1)$  gauge symmetry between the two layers.  $yz/0x$  phases also break the pseudospin rotational symmetry in which spins in the electron and hole layers are rotated around the field in same/opposite direction to each other. The two arbitrary  $U(1)$  phase variables in Eqs. (3-5) correspond to two Goldstone modes associated with these symmetry breaking. In fact, they can be absorbed into the relative gauge transformation and the pseudospin rotation by way of a mean-field coupling,  $\vec{\phi}_\lambda(\theta, \varphi, \varphi_0) \cdot \mathbf{a}^\dagger \vec{\sigma} \mathbf{b}$  ( $\lambda = yz, 0x$ ). The coupling is invariant under the spin rotation around the  $x$  axis together with a change of  $\varphi_0$  by  $\delta\varphi_0$ ,

$$\begin{aligned} \vec{\phi}_\lambda(\theta, \varphi, \varphi_0) & \rightarrow \vec{\phi}_\lambda(\theta, \varphi, \varphi_0 + \delta\varphi_0), \\ \mathbf{a} \rightarrow e^{i\varphi_a \sigma_x} \mathbf{a}, \quad \mathbf{b} \rightarrow e^{i\varphi_b \sigma_x} \mathbf{b} & = e^{\mp i(\varphi_a + \delta\varphi_0) \sigma_x} \mathbf{b}. \end{aligned} \quad (6)$$

Here the “ $\mp$ ” signs in Eq. (6) are for the  $\lambda = yz, 0x$  respectively. The coupling is also invariant under the relative gauge transformation together with a combination of changes of  $\theta$ ,  $\varphi$  and  $\varphi_0$  under the constraint Eq. (5),

$$\begin{aligned} \vec{\phi}_\lambda(\theta, \varphi, \varphi_0) & \rightarrow e^{i\psi} \vec{\phi}_\lambda(\theta, \varphi, \varphi_0) \equiv \vec{\phi}_\lambda(\theta(\psi), \varphi(\psi), \varphi_0(\psi)), \\ \mathbf{a} \rightarrow e^{i\psi_a} \mathbf{a}, \quad \mathbf{b} \rightarrow e^{i\psi_b} \mathbf{b} & = e^{i(\psi_a - \psi)} \mathbf{b}. \end{aligned} \quad (7)$$

Here  $(\theta(\psi), \varphi(\psi), \varphi_0(\psi))$  satisfies the constraint Eq. (5) for arbitrary  $U(1)$  phase  $\psi$ . A continuous variation of  $(\theta(\psi), \varphi(\psi), \varphi_0(\psi))$  as a function of  $\psi$  is shown in Fig. 6(a) of the supplemental material [82]. To emphasize the dependence of  $\vec{\phi}_\lambda$  on the two arbitrary  $U(1)$  phase variables, we use  $\vec{\phi}_\lambda(\psi, \tilde{h}, \varphi_0)$  instead of  $\vec{\phi}_\lambda(\theta, \varphi, \varphi_0)$  where  $\tilde{h}$  is a massive mode defined in Eq. (5). We further omit  $\tilde{h}$  from the arguments of  $\vec{\phi}_\lambda$  in the followings.

*Coupled Josephson effects.*— As an analogy to superfluidity [17, 19], the two Goldstone modes,  $\varphi_0$  and  $\psi$ , are related to spin and charge supercurrents respectively via

symmetries. Without the exciton pairings, the electron and hole layers have the spin rotational symmetry:

$$\mathbf{c} \rightarrow e^{i\varphi_c \sigma_x} \mathbf{c}, \quad H_c \rightarrow H_c - \hbar \partial_t \varphi_c, \quad (8)$$

and the U(1) gauge symmetry:

$$\mathbf{c} \rightarrow e^{i\psi_c} \mathbf{c}, \quad V_c \rightarrow V_c - \hbar \partial_t \psi_c, \quad (9)$$

where  $\mathbf{c} = \mathbf{a}/b$ ,  $c = a/b$ ,  $V_{a/b}$  and  $H_{a/b}$  are electric potential and exchange field along  $x$  in the electron/hole layer.  $V_{a/b}/(-e)$  and  $H_{a/b}/(-e)$  correspond to charge voltage and spin voltage in the electron/hole layer. In the excitonic condensates, Eqs. (8,9) should be combined with Eqs. (6,7). The combination reveals the methods to control the Goldstone modes and realize spin-charge coupled Josephson effect.

The spin-charge coupled Josephson effect can be understood by a quantum-dot junction model [70, 82]. The model comprises of two domains and a junction between them in the 2D coordinate space. Each domain can be regarded as a bilayer (electron-hole double-layer) quantum dot. The two domains ( $i = 1, 2$ ) have exciton pairing  $\vec{\phi}_\lambda(\psi, \varphi_0)$  ( $\lambda = yz, 0x$ ) with different values of  $\psi$  and  $\varphi_0$ , i.e.  $\psi_i$  and  $\varphi_{0i}$  ( $i = 1, 2$ ). The charge and spin voltages change across the junction in the electron/hole layer by  $V_{Ca/b}$  and  $V_{Sa/b}$  respectively.  $e|V_{Sa/b}|$  is assumed to be much smaller than the average exchange field  $H_{a/b}$ , so that variations of the gapped modes ( $\rho$  and  $\tilde{h}$ ) can be neglected. An action for the model is given by a functional of  $V_{Cc}$ ,  $V_{Sc}$ ,  $\psi_i$  and  $\varphi_{0i}$  ( $c = a, b$ ,  $i = 1, 2$ ), that takes a quadratic form of the creation operators in the electron and hole layers in the two domains,  $\mathbf{a}_i^\dagger(\vec{r})$  ( $i = 1, 2$ ) and  $\mathbf{b}_i^\dagger(\vec{r})$  ( $i = 1, 2$ ). The action comprises of two parts:

$$\begin{aligned} \mathcal{S}[\mathbf{a}_i, \mathbf{a}_i^\dagger, \mathbf{b}_i, \mathbf{b}_i^\dagger, \psi_i, \varphi_{0i}; V_{Cc}, V_{Sc}] &= \mathcal{S}_T[\mathbf{a}_i, \mathbf{a}_i^\dagger, \mathbf{b}_i, \mathbf{b}_i^\dagger] \\ &+ \mathcal{S}_{\text{mf}}[\mathbf{a}_i, \mathbf{a}_i^\dagger, \mathbf{b}_i, \mathbf{b}_i^\dagger, \psi_i, \varphi_{0i}; V_{Cc}, V_{Sc}], \end{aligned} \quad (10)$$

where the mean-field part:

$$\begin{aligned} \mathcal{S}_{\text{mf}} = \int d\tau \sum_{i=1,2} \sum_{\alpha} & \{ \mathbf{a}_{i\alpha}^\dagger [\hbar \partial_\tau + \mathbf{H}_{a\alpha} - \mu - i \frac{\eta_i}{2} e (V_{Ca} + V_{Sa} \sigma_x)] \mathbf{a}_{i\alpha} \\ & + \mathbf{b}_{i\alpha}^\dagger [\hbar \partial_\tau + \mathbf{H}_{b\alpha} - \mu - i \frac{\eta_i}{2} e (V_{Cb} + V_{Sb} \sigma_x)] \mathbf{b}_{i\alpha} \\ & - [\vec{\phi}_\lambda(\psi_i, \varphi_{0i}) \cdot \mathbf{a}_{i\alpha}^\dagger \vec{\sigma} \mathbf{b}_{1\alpha} + \text{h.c.}] \}, \end{aligned} \quad (11)$$

and a tunneling part:

$$\mathcal{S}_T = \int d\tau \sum_{\alpha\beta} [\mathbf{a}_{1\alpha}^\dagger T_{\alpha\beta}^{(a)} \mathbf{a}_{2\beta} + \mathbf{b}_{1\alpha}^\dagger T_{\alpha\beta}^{(b)} \mathbf{b}_{2\beta} + \text{h.c.}], \quad (12)$$

with  $\eta_1 = -\eta_2 = 1$ ,  $\mathbf{a}_i(\vec{r}) \equiv \sum_{\alpha} u_{ai\alpha}(\vec{r}) \mathbf{a}_{i\alpha}$  and  $\mathbf{b}_i(\vec{r}) \equiv \sum_{\alpha} u_{bi\alpha}(\vec{r}) \mathbf{b}_{i\alpha}$ . Here  $u_{cia}(\vec{r})$  is a single-particle eigenstate of the kinetic energy part of Eq. (1) for the electron/hole layer in the  $i$ -th domain region ( $c = a/b$ ,  $i = 1, 2$ ) with a proper boundary condition, together with

its eigen-energy  $\mathbf{H}_{c\alpha} \equiv E_{c\alpha} \sigma_0 + H_c \sigma_x$ . Tunneling matrices between the two domains are given by the single-particle eigenstates,  $T_{\alpha\beta}^{(c)} \equiv \langle u_{c1\alpha} | \mathcal{T}^{(c)} | u_{c2\beta} \rangle$ , where  $\mathcal{T}^{(c)}$  is the kinetic energy part for the electron/hole layer in the junction region ( $c = a/b$ ). We assume that  $\mathcal{T}^{(c)}$  is free from spin and electron-hole mixings.

A perturbative treatment of the tunneling term in the junction model leads to the spin-charge coupled Josephson equations. In the equations, the charge and spin currents,  $I_C^{a/b}$  and  $I_S^{a/b}$ , are induced across the junction in the electron/hole layer by the charge and spin voltages,  $V_C \equiv V_{Cb} - V_{Ca}$  and  $V_S \equiv V_{Sb} \pm V_{Sa}$ . Phase differences of the gapless phase variables between the two domains,  $\tilde{\varphi}_0 \equiv \varphi_{01} - \varphi_{02}$ , and  $\tilde{\psi} \equiv \psi_1 - \psi_2$  [82], play the central role in the equations. The first Josephson equations are:

$$\begin{aligned} -I_C^{(a)} = I_C^{(b)} &= -e I_0 [\sin(\tilde{\psi} - \frac{e}{\hbar c} \Psi) \cos \tilde{\varphi}_0 \\ &- \bar{h}_{\pm} \cos(\tilde{\psi} - \frac{e}{\hbar c} \Psi) \sin \tilde{\varphi}_0], \end{aligned} \quad (13)$$

$$\begin{aligned} I_S^{(a)} = \pm I_S^{(b)} &= -e I_0 [\sin \tilde{\varphi}_0 \cos(\tilde{\psi} - \frac{e}{\hbar c} \Psi) \\ &- \bar{h}_{\pm} \cos \tilde{\varphi}_0 \sin(\tilde{\psi} - \frac{e}{\hbar c} \Psi)], \end{aligned} \quad (14)$$

where the spin currents are defined as differences of charge currents contributed by spin-up and spin-down electrons [82]. The second Josephson equations are:

$$\frac{d\tilde{\psi}}{dt} = -\frac{e}{\hbar} V_C, \quad \frac{d\tilde{\varphi}_0}{dt} = \mp \frac{e}{\hbar} V_S. \quad (15)$$

Here upper and lower signs are for transverse and longitudinal phase respectively.  $\Psi$  is an external magnetic flux trapped in the junction region.  $I_0$  and  $\bar{h}_{\pm}$  are constants and  $\bar{h}_{\pm}$  is proportional to  $\hbar$ , while  $\bar{h}_+ \neq \bar{h}_-$ .

The Josephson equations reveal the spin-charge coupled Josephson effects. The term proportional to  $\sin(\tilde{\psi} - \frac{e}{\hbar c} \Psi)$  in Eq. (13) and the term proportional to  $\sin(\tilde{\varphi}_0)$  in Eq. (14) represent the well-known pure charge and pure spin Josephson effects respectively [19, 29, 30]. The terms proportional to  $\bar{h}_{\pm}$  in Eqs. (13,14) shows that in the presence of the exchange fields, the spin (charge) phase difference can also lead to charge (spin) supercurrent. This intrinsic spin-charge coupling is because the condensation of the exciton with the pseudospin polarization breaks the spin rotational symmetry. Namely, the exciton carries the spin polarization, so does the supercurrent.

To propose the dissipationless spin-charge conversion in a feasible experimental setup, we consider to put two magnetic substrates with different magnetizations along the same ( $x$ ) direction under the hole layer (Fig. 2(a)). The two substrates introduce the two domains in the EHDL system, whose hole layers experience the magnetic exchange fields through the proximity effect. The difference results in a finite d.c. spin voltage  $V_S$  across the junction in the hole layer. The d.c. spin voltage results in a linear increase of  $\tilde{\varphi}_0$ ,  $\tilde{\varphi}_0 = \mp \frac{e}{\hbar} V_S t$  ( $\tilde{\varphi}_0 = 0$  at  $t = 0$  is

taken without loss of generality). The time-dependence of  $\tilde{\varphi}_0$  gives rise to a.c. electric currents in the counter-propagating direction in the electron and hole layers respectively. The electric currents induce the a.c. charge voltages across the junction in the electron and hole layers as  $I_C^{(a)}R_a$  and  $I_C^{(b)}R_b$ , where  $R_a$  and  $R_b$  are external resistances (Fig. 2(a)). The exciton U(1) phase  $\tilde{\psi}$  couples only with the difference between the charge voltages in the two layer,  $V_C = I_C^{(a)}R_a - I_C^{(b)}R_b$ . Thus, Eqs. (13,15) give an equation of motion (EOM) for  $\tilde{\psi}$ :

$$I_C(s) \frac{R}{V_S} = \frac{d\tilde{\psi}}{ds} = -k[\sin(\tilde{\psi})\cos(s) \pm \bar{h}_\pm \cos(\tilde{\psi})\sin(s)], \quad (16)$$

with a normalized time  $s \equiv eV_S t/\hbar$ ,  $k \equiv eI_0 R/V_S$ ,  $R \equiv R_a + R_b$ , and  $I_C \equiv I_C^{(b)} = -I_C^{(a)}$ .

The EOM has two dimensionless parameters,  $k$  and  $\bar{h}_\pm$ . Solutions at  $|\bar{h}_\pm| = 0, 1$  is obtained analytically, while solution for general  $k$  and  $\bar{h}_\pm$  are obtained numerically [82]. The solutions of  $\tilde{\psi}(s)$  show two distinct behaviours (Fig. 2(b)): (i) oscillating behaviour for  $|\bar{h}_\pm| < 1/|k|$  and (ii) stepping behaviour for  $|\bar{h}_\pm| > 1/|k|$ . The oscillating behaviour can be understood by the solution at  $\bar{h}_\pm = 0$ .  $\tilde{\psi}(s)$  therein is oscillatory with  $2\pi$  periodicity in  $s$  [82]. The  $\bar{h}_\pm$  term in Eq. (16) with  $\mp k\bar{h}_\pm > 0$  ( $< 0$ ) gives rise to a component of  $\tilde{\psi}(s)$  that increases (decreases) in the time  $s$  linearly. As a result,  $\tilde{\psi}(s)$  for  $0 < |\bar{h}_\pm| < 1/|k|$  comprises of a fast oscillatory mode with the period of  $2\pi$  and a slow oscillatory mode with a longer period. The slow oscillatory mode comes from the linear component, that increases (decreases)  $\tilde{\psi}(s)$  by  $\pi$  over the long period [82]. When  $|\bar{h}_\pm| > 1/|k|$ , the long period converges to the short period, where  $\tilde{\psi}(s)$  shows the stepping behaviour:  $\tilde{\psi}(s)$  increases by  $\pi$  at every step and the step appear at every  $\pi$  in  $s$ . The spin voltage  $V_S$  can be experimentally measured from the (short) period of the a.c. electric current (Fig. 2(b)).

*Spin-orbit coupling.*—2D EHDL system has structural inversion asymmetry (SIA), causing Rashba interaction in the electron band with spin  $S_z = \pm 1/2$ ,

$$H_R = \xi_e \int d^2\vec{r} \mathbf{a}^\dagger(\vec{r}) (-i\partial_y \boldsymbol{\sigma}_x + i\partial_x \boldsymbol{\sigma}_y) \mathbf{a}(\vec{r}). \quad (17)$$

The Rashba interaction is also induced in the heavy hole band with spin  $J_z = \pm 3/2$ , while it is generally negligible [79–81]. The SOI results in an antisymmetric vector-product (AVP) type coupling among the four-components excitonic field  $\vec{\Phi}$ . The previous study of Eq. (2) in the presence of the AVP type coupling [69] is generalized in the supplemental materials [82]. The effect of the AVP interaction is to replace  $\varphi_0$  in the classical solutions of Eqs. (3,4) by  $\varphi_0 - Ky$ , where  $y$  is the spatial coordinate perpendicular to the exchange field. Thus, the pseudospin polarization in the  $yz/0x$  phase acquires

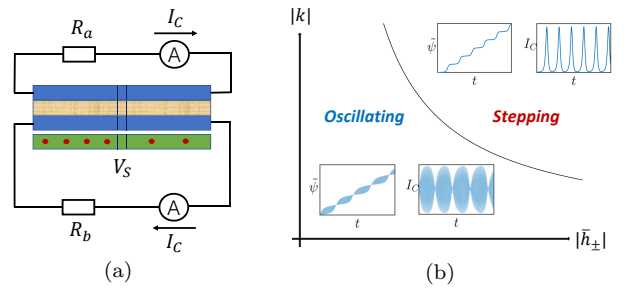


FIG. 2. Charge current ( $I_C$ ) induced by spin voltage ( $V_S$ ). (a) The spin voltage is added at the Josephson junction in the hole layer. The charge currents can be measured by the two external circuits attached to electron and hole layers respectively. (b) The ac behavior of  $\tilde{\psi}(t)$  and  $I_C(t)$  according to Eq. (16) for small  $|\bar{h}_\pm|$ .  $\tilde{\psi}(t)$  shows oscillating behaviour in  $|\bar{h}_\pm k| < 1$  and a stepping behaviour in  $|\bar{h}_\pm k| > 1$ .

a spatial texture, that breaks the translational symmetry (helicoidal/helical phase) [69, 82].

The helicoidal/helical phases have two gapless Goldstone modes ( $\psi$  and  $\varphi_0$ ) with similar physical meanings as in the  $yz/0x$  phase. In the presence of the Rashba interaction in the electron layer, however, the gapless  $\varphi_0$  mode originates purely from the spin rotational symmetry in the hole layer. Note also that  $\varphi_0$  appears together with the spatial coordinate ( $y$ ), so that  $\varphi_0$  is a sliding mode (phason) as well as the spin rotational mode. Charge and (hole-layer) spin voltages control the Goldstone modes  $\psi$  and  $\varphi_0$  in the helical/helicoidal phases as well; Eq. (15). Charge and spin currents can be also generated by spatial gradients of the two gapless Goldstone modes in the textured excitonic phases. One can see the latter from the effective action of  $\vec{\phi}$  with the Rashba SOI [82], where the charge and spin Noether currents in the hole layer are calculated as:

$$J_i^C = -\frac{\lambda h_c}{|\gamma|} [(\partial_i \psi - \frac{e}{\hbar c} \tilde{A}_i) - \hbar \partial_i \varphi_0], \quad (18)$$

$$J_i^S = \mp \frac{\lambda h_c}{|\gamma|} [\partial_i \varphi_0 - \hbar (\partial_i \psi - \frac{e}{\hbar c} \tilde{A}_i)], \quad (19)$$

with  $i = x, y$  respectively. Here  $\tilde{A}$  is the difference of the vector potential between the two layers. Eqs. (18,19) are consistent with Eqs. (13,14) in a small-phase-difference limit up to the coefficients ( $I_0$  and  $\bar{h}_\pm$ ) respectively. The consistency concludes that the qualitative properties of the spin-charge coupled Josephson effect holds true also in the presence of the SOI in the electron layer.

*Summary.*—In this letter, we clarify coupled spin and charge Josephson effects in the EHDL exciton system under magnetic exchange field, where the charge Josephson current can be a response of the spin voltage. This intrinsic spin-charge coupling effect enriches possible spintronics applications of the excitonic pseudospin superfluidity. A layered InAs/AlSb/GaInSb semiconductor

heterostructure is an ideal EHDL system whose electron layer has a large SOI [78–81]. The pseudospin rotational symmetry and the spin-charge coupled superflow property are robust against the SOI in the electron layer.

Y. Z. and R. S. thanks the fruitful discussion with

Junren Shi, Rui-Rui Du, Xi Lin, Ke Chen, Zhenyu Xiao and Lingxian Kong. The work was supported by the National Basic Research Programs of China (No. 2019YFA0308401) and by National Natural Science Foundation of China (No.11674011 and No. 12074008).

- 
- [1] E. Kaxiras, *Atomic and Electronic Structure of Solids* (Cambridge University Press, Cambridge, 2003).
- [2] F. London and H. London, The electromagnetic equations of the superconductor, *Proceedings of the Royal Society A* **149**, 71 (1935).
- [3] F. London, *Superfluids* (Wiley, New York, 1950).
- [4] P. Kapitza, Viscosity of liquid helium below the  $\lambda$ -point, *Nature* **141**, 74 (1938).
- [5] D. D. Osheroff, R. C. Richardson, and D. M. Lee, Evidence for a new phase of solid  $\text{He}^3$ , *Phys. Rev. Lett.* **28**, 885 (1972).
- [6] J. Bardeen, L. N. Cooper, and J. R. Schrieffer, Theory of superconductivity, *Phys. Rev.* **108**, 1175 (1957).
- [7] J. G. Bednorz and K. A. Müller, Possible high  $T_c$  superconductivity in the Ba-La-Cu-O system, *Z. Physik B–Condensed Matter* **64**, 189 (1986).
- [8] M. Vuorio, Condensate spin currents in helium-3, *Journal of Physics C: Solid State Physics* **7**, L5 (1974).
- [9] M. Vuorio, Relaxation by magnetic counterflow in superfluid  $^3\text{He}$ , *Journal of Physics C: Solid State Physics* **9**, L267 (1976).
- [10] E. Sonin, Phase fixation, excitonic and spin superfluidity of electron-hole pairs and antiferromagnetic chromium, *Solid State Communication* **25**, 253 (1978).
- [11] E. B. Sonin, Analogs of superfluid flows for spins and electron-hole pairs, *Sov. Phys. JETP* **47**, 1091 (1978).
- [12] E. B. Sonin, Relaxation of longitudinal magnetization in the  $^3\text{He}$  A-phase and superfluid spin flux, *JETP Lett.* **30**, 662 (1978).
- [13] L. R. Corruccini and D. D. Osheroff, Nuclear susceptibility of superfluid  $B$ - $^3\text{He}$ , *Phys. Rev. Lett.* **34**, 695 (1975).
- [14] A. S. Borovik-Romanov, Y. M. Bunkov, V. V. Dmitriev, and Y. M. Mukharskii, Long-lived induction signal in superfluid  $^3\text{He}$ - $B$ , *JETP Lett.* **40**, 1033 (1984).
- [15] I. A. Fomin, Long-lived induction signal and spatially nonuniform spin precession in  $^3\text{He}$ - $B$ , *JETP Lett.* **40**, 1037 (1984).
- [16] Y. M. Bunkov, Spin supercurrent and novel properties of NMR in  $^3\text{He}$ , in *Progress in Low Temperature Physics*, Vol. 14 (1995) pp. 69–158.
- [17] G. E. Volovik, *The Universe in a Helium Droplet* (Clarendon Press, Oxford, 2003).
- [18] J. König, M. C. Bønsager, and A. H. MacDonald, Dissipationless spin transport in thin film ferromagnets, *Phys. Rev. Lett.* **87**, 187202 (2001).
- [19] E. Sonin, Spin currents and spin superfluidity, *Advanced Physics* **59**, 181 (2010).
- [20] S. B. Chung, S. K. Kim, K. H. Lee, and Y. Tserkovnyak, Cooper-pair spin current in a strontium ruthenate heterostructure, *Phys. Rev. Lett.* **121**, 167001 (2018).
- [21] L. N. Kozlov and L. A. Maximov, The metal-dielectric divalent crystal phase transition, *Sov. Phys. JETP* **21**, 790 (1965).
- [22] B. I. Halperin and T. M. Rice, Possible anomalies at a semimetal-semiconductor transition, *Rev. Mod. Phys.* **40**, 755 (1968).
- [23] T. Hakioğlu and M. Şahin, Excitonic condensation under spin-orbit coupling and BEC-BCS crossover, *Phys. Rev. Lett.* **98**, 166405 (2007).
- [24] M. A. Can and T. Hakioğlu, Unconventional pairing in excitonic condensates under spin-orbit coupling, *Phys. Rev. Lett.* **103**, 086404 (2009).
- [25] Y.-P. Shim and A. H. MacDonald, Spin-orbit interactions in bilayer exciton-condensate ferromagnets, *Phys. Rev. B* **79**, 235329 (2009).
- [26] Q.-F. Sun, Z.-T. Jiang, Y. Yu, and X. C. Xie, Spin superconductor in ferromagnetic graphene, *Phys. Rev. B* **84**, 214501 (2011).
- [27] Q.-F. Sun and X. C. Xie, Spin-polarized  $\nu = 0$  state of graphene: A spin superconductor, *Phys. Rev. B* **87**, 245427 (2013).
- [28] B. D. Josephson, Possible new effects in superconductive tunnelling, *Physics Letters* **1**, 251 (1962).
- [29] B. D. Josephson, The discovery of tunnelling supercurrents, *Rev. Mod. Phys.* **46**, 251 (1974).
- [30] S. Takei, Y. Tserkovnyak, and M. Mohseni, Spin superfluid Josephson quantum devices, *Phys. Rev. B* **95**, 144402 (2017).
- [31] S. A. Bender, R. A. Duine, and Y. Tserkovnyak, Electronic pumping of quasiequilibrium Bose-Einstein-condensed magnons, *Phys. Rev. Lett.* **108**, 246601 (2012).
- [32] S. Takei and Y. Tserkovnyak, Superfluid spin transport through easy-plane ferromagnetic insulators, *Phys. Rev. Lett.* **112**, 227201 (2014).
- [33] S. Takei, B. I. Halperin, A. Yacoby, and Y. Tserkovnyak, Superfluid spin transport through antiferromagnetic insulators, *Phys. Rev. B* **90**, 094408 (2014).
- [34] H. Chen, A. D. Kent, A. H. MacDonald, and I. Sodemann, Nonlocal transport mediated by spin supercurrents, *Phys. Rev. B* **90**, 220401 (2014).
- [35] K. Nakata, K. A. van Hoogdalem, P. Simon, and D. Loss, Josephson and persistent spin currents in Bose-Einstein condensates of magnons, *Phys. Rev. B* **90**, 144419 (2014).
- [36] S. Hoffman and Y. Tserkovnyak, Magnetic exchange and nonequilibrium spin current through interacting quantum dots, *Phys. Rev. B* **91**, 245427 (2015).
- [37] R. A. Duine, A. Brataas, S. A. Bender, and Y. Tserkovnyak, Spintronics and magnon Bose-Einstein condensation (2015), arXiv:1505.01329 [cond-mat.mes-hall].
- [38] S. Takei, A. Yacoby, B. I. Halperin, and Y. Tserkovnyak, Spin superfluidity in the  $\nu = 0$  quantum Hall state of graphene, *Phys. Rev. Lett.* **116**, 216801 (2016).
- [39] Y. Liu, G. Yin, J. Zang, R. K. Lake, and Y. Barlas, Spin-Josephson effects in exchange coupled antiferromagnetic insulators, *Phys. Rev. B* **94**, 094434 (2016).
- [40] S. K. Kim and Y. Tserkovnyak, Topological effects on

- quantum phase slips in superfluid spin transport, *Phys. Rev. Lett.* **116**, 127201 (2016).
- [41] S. K. Kim, S. Takei, and Y. Tserkovnyak, Thermally activated phase slips in superfluid spin transport in magnetic wires, *Phys. Rev. B* **93**, 020402 (2016).
- [42] Y. Tserkovnyak, Perspective: (beyond) spin transport in insulators, *Journal of Applied Physics* **124**, 190901 (2018).
- [43] Y. Tserkovnyak and J. Zou, Quantum hydrodynamics of vorticity, *Phys. Rev. Research* **1**, 033071 (2019).
- [44] J. Zou, S. K. Kim, and Y. Tserkovnyak, Topological transport of vorticity in heisenberg magnets, *Phys. Rev. B* **99**, 180402 (2019).
- [45] S. Dasgupta, S. Zhang, I. Bah, and O. Tchernyshyov, Quantum statistics of vortices from a dual theory of the  $xy$  ferromagnet, *Phys. Rev. Lett.* **124**, 157203 (2020).
- [46] E. Saitoh, M. Ueda, H. Miyajima, and G. Tatara, Conversion of spin current into charge current at room temperature: Inverse spin-hall effect, *Applied Physics Letters* **88**, 182509 (2006).
- [47] M. V. Costache, M. Sladkov, S. M. Watts, C. H. van der Wal, and B. J. van Wees, Electrical detection of spin pumping due to the precessing magnetization of a single ferromagnet, *Phys. Rev. Lett.* **97**, 216603 (2006).
- [48] T. Kimura, Y. Otani, T. Sato, S. Takahashi, and S. Maekawa, Room-temperature reversible spin Hall effect, *Phys. Rev. Lett.* **98**, 156601 (2007).
- [49] S. Takei and Y. Tserkovnyak, Nonlocal magnetoresistance mediated by spin superfluidity, *Phys. Rev. Lett.* **115**, 156604 (2015).
- [50] L. J. Cornelissen, J. Liu, R. A. Duine, J. B. Youssef, and B. J. van Wees, Long-distance transport of magnon spin information in a magnetic insulator at room temperature, *Nature Physics* **11**, 1022 (2015).
- [51] W. Yuan, Q. Zhu, T. Su, Y. Yao, W. Xing, Y. Chen, Y. Ma, X. Lin, J. Shi, R. Shindou, X. C. Xie, and W. Han, Experimental signatures of spin superfluid ground state in canted antiferromagnet  $\text{Cr}_2\text{O}_3$  via nonlocal spin transport, *Science Advances* **4**, eaat1098 (2018).
- [52] X. Zhu, P. B. Littlewood, M. S. Hybertsen, and T. M. Rice, Exciton condensate in semiconductor quantum well structures, *Phys. Rev. Lett.* **74**, 1633 (1995).
- [53] Y. Naveh and B. Laikhtman, Excitonic instability and electric-field-induced phase transition towards a two-dimensional exciton condensate, *Phys. Rev. Lett.* **77**, 900 (1996).
- [54] X. Wu, W. Lou, K. Chang, G. Sullivan, and R.-R. Du, Resistive signature of excitonic coupling in an electron-hole double layer with a middle barrier, *Phys. Rev. B* **99**, 085307 (2019).
- [55] X.-J. Wu, W. Lou, K. Chang, G. Sullivan, A. Ikhlassi, and R.-R. Du, Electrically tuning many-body states in a coulomb-coupled InAs/InGaSb double layer, *Phys. Rev. B* **100**, 165309 (2019).
- [56] Y. E. Lozovik and V. I. Yudson, Feasibility of superfluidity of paired spatially separated electrons and holes; a new superconductivity mechanism, *JETP Lett.* **22**, 274 (1975).
- [57] J. P. Eisenstein and A. H. MacDonald, Bose-Einstein condensation of excitons in bilayer electron systems, *Nature* **432**, 691 (2004).
- [58] G. W. Burg, N. Prasad, K. Kim, T. Taniguchi, K. Watanabe, A. H. MacDonald, L. F. Register, and E. Tutuc, Strongly enhanced tunneling at total charge neutrality in double-bilayer graphene-WSe<sub>2</sub> heterostructures, *Phys. Rev. Lett.* **120**, 177702 (2018).
- [59] I. B. Spielman, J. P. Eisenstein, L. N. Pfeiffer, and K. W. West, Resonantly enhanced tunneling in a double layer quantum Hall ferromagnet, *Phys. Rev. Lett.* **84**, 5808 (2000).
- [60] E. Tutuc, M. Shayegan, and D. A. Huse, Counterflow measurements in strongly correlated GaAs hole bilayers: Evidence for electron-hole pairing, *Phys. Rev. Lett.* **93**, 036802 (2004).
- [61] M. Kellogg, J. P. Eisenstein, L. N. Pfeiffer, and K. W. West, Vanishing Hall resistance at high magnetic field in a double-layer two-dimensional electron system, *Phys. Rev. Lett.* **93**, 036801 (2004).
- [62] R. D. Wiersma, J. G. S. Lok, S. Kraus, W. Dietsche, K. von Klitzing, D. Schuh, M. Bichler, H.-P. Tranitz, and W. Wegscheider, Activated transport in the separate layers that form the  $\nu_T = 1$  exciton condensate, *Phys. Rev. Lett.* **93**, 266805 (2004).
- [63] Y. Yoon, L. Tiemann, S. Schmult, W. Dietsche, K. von Klitzing, and W. Wegscheider, Interlayer tunneling in counterflow experiments on the excitonic condensate in quantum Hall bilayers, *Phys. Rev. Lett.* **104**, 116802 (2010).
- [64] D. Nandi, A. D. K. Finck, J. P. Eisenstein, L. N. Pfeiffer, and K. W. West, Exciton condensation and perfect coulomb drag, *Nature* **488**, 481 (2012).
- [65] X. Liu, K. Watanabe, T. Taniguchi, B. I. Halperin, and P. Kim, Quantum hall drag of exciton condensate in graphene, *Nature Physics* **13**, 746 (2017).
- [66] J. I. A. Li, T. Taniguchi, K. Watanabe, J. Hone, and C. R. Dean, Excitonic superfluid phase in double bilayer graphene, *Nature Physics* **13**, 751 (2017).
- [67] J. Frenkel, On the transformation of light into heat in solids. II, *Phys. Rev.* **37**, 1276 (1931).
- [68] N. F. Mott, The transition to the metallic state, *Philosophical Magazine* **6**, 287 (1961).
- [69] K. Chen and R. Shindou, Helicoidal excitonic phase in an electron-hole double-layer system, *Phys. Rev. B* **100**, 035130 (2019).
- [70] A. Altland and B. D. Simons, *Condensed Matter Field Theory* (Cambridge University Press, Cambridge, 2010).
- [71] U. Eckern, G. Schön, and V. Ambegaokar, Quantum dynamics of a superconducting tunnel junction, *Phys. Rev. B* **30**, 6419 (1984).
- [72] A. Zrenner, L. V. Butov, M. Hagn, G. Abstreiter, G. Böhm, and G. Weimann, Quantum dots formed by interface fluctuations in AlAs/GaAs coupled quantum well structures, *Phys. Rev. Lett.* **72**, 3382 (1994).
- [73] L. V. Butov, A. Zrenner, G. Abstreiter, G. Böhm, and G. Weimann, Condensation of indirect excitons in coupled AlAs/GaAs quantum wells, *Phys. Rev. Lett.* **73**, 304 (1994).
- [74] L. V. Butov, C. W. Lai, A. L. Ivanov, A. C. Gossard, and D. S. Chemla, Towards Bose-Einstein condensation of excitons in potential traps, *Nature* **417**, 47 (2002).
- [75] L. V. Butov, A. C. Gossard, and D. S. Chemla, Macroscopically ordered state in an exciton system, *Nature* **418**, 751 (2002).
- [76] A. A. High, J. R. Leonard, A. T. Hammack, M. M. Fogler, L. V. Butov, A. V. Kavokin, K. L. Campman, and A. C. Gossard, Spontaneous coherence in a cold exciton gas, *Nature* **483**, 584 (2012).
- [77] M. M. Fogler, L. V. Butov, and K. S. Novoselov, High-

- temperature superfluidity with indirect excitons in van der Waals heterostructures, *Nature Communications* **5**, 4555 (2014).
- [78] R. Winkler, *Spin-Orbit Coupling Effects in Two-Dimensional Electron and Hole Systems* (Springer, Heidelberg, 2003).
- [79] C. Liu, T. L. Hughes, X.-L. Qi, K. Wang, and S.-C. Zhang, Quantum spin Hall effect in inverted type-II semiconductors, *Phys. Rev. Lett.* **100**, 236601 (2008).
- [80] C.-X. Liu, X.-L. Qi, H. Zhang, X. Dai, Z. Fang, and S.-C. Zhang, Model Hamiltonian for topological insulators, *Phys. Rev. B* **82**, 045122 (2010).
- [81] D. I. Pikulin and T. Hyart, Interplay of exciton condensation and the quantum spin Hall effect in InAs/GaSb bilayers, *Phys. Rev. Lett.* **112**, 176403 (2014).
- [82] See Supplemental Material at [URL will be inserted by publisher].
- [83] M. E. Peskin and D. V. Schroeder, *An Introduction to Quantum Field Theory* (Westview, Boulder, 1995).
- [84] C. Liu and S.-C. Zhang, Models and materials for topological insulators, in *Contemporary Concepts of Condensed Matter Science*, Vol. 6 (2013) Chapter 3, pp. 59–89.

---

## SUPPLEMENTARY MATERIAL FOR “INTRINSIC SPIN-CHARGE CONVERSION IN EXCITONIC PSEUDOSPIN SUPERFLUID”

In the main text, the  $\phi^4$ -type effective Lagrangian is introduced for the four-component excitonic fields. The  $\phi^4$ -type Lagrangian is derived from Eqs. (1,17) perturbatively in the exchange fields and in the Rashba interaction  $\xi_e$ . The Lagrangian is minimized in terms of a classical solution of the excitonic fields, leading to the prediction of transverse, longitudinal, helicoidal and helical phases. All of them are excitonic pseudospin superfluid phases. Using a coupled quantum dots model or the effective Lagrangian, we derive spin-charge coupled Josephson equations in these excitonic pseudospin superfluid phases. In this supplemental material, we explain these derivations and minimizations as well as related details.

The structure of this supplemental material is as follows. In the next section, we give the perturbative derivation of the  $\phi^4$ -type effective Lagrangian. In Sec. B, we describe the minimization of the Lagrangian in the case of  $\xi_e = 0$ , where the classical ground-state phase diagram of transverse and longitudinal phases are presented. In Sec. C and D, we clarify what global continuous symmetries are broken in the transverse and longitudinal phases, and we associate the broken symmetries with the gapless Goldstone modes in these phases. In sec. E, we derive a spin-charge coupled Josephson equations based on the coupled quantum dots model. In sec. F, we describe solutions of the Josephson equation under a physical circumstance. In Sec. G, we describe the minimization of the Lagrangian in the case of  $\xi_e \neq 0$ , where the classical ground-state phase diagram of helicoidal and helical phases are presented. In Sec. H, we derive the spin-charge coupled Josephson equation in the case of  $\xi_e \neq 0$ , using the  $\phi^4$ -type effective Lagrangian. In Sec. I, we discuss a possible magnetism in the helicoidal and helical phases, in the presence of the spin-orbit interaction in the hole layer. In Sec. J and Sec. K, we give supplemental details of Sec. E and Sec. G respectively.

There are some notation simplifications in this supplemental material. First, we take the exchange fields of the two layers to be the same ( $H_a = H_b \equiv H$ ) in Sec. A and Sec. E. The result can be easily generalized into the other cases of  $H_a \neq H_b$ . Second, we take  $\hbar = c = e = 1$ , unless dictated otherwise (we recover these fundamental physical constants in the very last expressions of important physical equations).

### A. Derivation of $\phi^4$ type effective Lagrangian

In this section, we describe a derivation of the effective Lagrangian from Eqs. (1,17). The derivation is perturbative in the exchange fields in Eq. (1) and in the Rashba interaction in Eq. (17). Since both the exchange field and the Rashba interaction are often much smaller than the typical energy scale of the electron and hole bands, we include only their first-order perturbation effect.

The partition function of the four-components exciton pairing fields  $\vec{\phi}_\mu = \frac{g}{2} \langle \mathbf{b}^\dagger \boldsymbol{\sigma}_\mu \mathbf{a} \rangle$  ( $\mu = 0, x, y, z$ ) can be derived from Eq. (1) together with the Rashba interaction in the electron band Eq. (17);

$$Z = \int \mathcal{D}\phi^\dagger \mathcal{D}\phi \exp \left\{ -\frac{2}{g} |\vec{\phi}|^2 + \text{Tr} [G_0 G_R^{-1} G_0 \Psi G_0 \Psi + G_0 G_H^{-1} G_0 \Psi G_0 \Psi - \frac{1}{2} G_0 \Psi G_0 \Psi - \frac{1}{4} G_0 \Psi G_0 \Psi G_0 \Psi G_0 \Psi] \right\}, \quad (\text{A.1})$$

where

$$G_0^{-1}(q) \equiv \begin{pmatrix} (-i\omega_n + \mathcal{E}_a(\vec{k}) - \mu) \boldsymbol{\sigma}_0 & 0 \\ 0 & (-i\omega_n + \mathcal{E}_b(\vec{k}) - \mu) \boldsymbol{\sigma}_0 \end{pmatrix} \equiv \begin{pmatrix} g_a^{0-1}(k) & 0 \\ 0 & g_b^{0-1}(k) \end{pmatrix}, \quad (\text{A.2})$$

$$G_R^{-1}(q) \equiv \begin{pmatrix} \xi_e(k_y\boldsymbol{\sigma}_x - k_x\boldsymbol{\sigma}_y) & 0 \\ 0 & 0 \end{pmatrix}, \quad G_H^{-1}(q) \equiv \begin{pmatrix} H\boldsymbol{\sigma}_x & 0 \\ 0 & H\boldsymbol{\sigma}_x \end{pmatrix}, \quad (\text{A.3})$$

$$\Psi(q) = \frac{1}{\sqrt{\beta V}} \begin{pmatrix} 0 & -\vec{\phi}(-k) \cdot \vec{\sigma} \\ -\vec{\phi}^*(k) \cdot \vec{\sigma} & 0 \end{pmatrix}, \quad (\text{A.4})$$

with  $\mathcal{E}_a(\vec{k}) \equiv \frac{\hbar^2 \vec{k}^2}{2m_e} - E_g$ ,  $\mathcal{E}_b(\vec{k}) \equiv -\frac{\hbar^2 \vec{k}^2}{2m_h} + E_g$ ,  $q \equiv (i\omega_n, \vec{k})$  and  $\vec{k} = (k_x, k_y)$ . The expansion is perturbative in the excitonic field  $\Psi(q)$ , the Rashba interaction  $G_R^{-1}(q)$  and the exchange fields  $G_H^{-1}(q)$ . From the gauge symmetry, the expansion contains only the even order in  $\Psi(q)$ . For the 2nd order in  $\Psi(q)$ , we expand the exchange fields and the Rashba interaction up to the first order. We ignore their effect in the quartic order in  $\Psi(q)$ .

The expansion has been previously carried out only for triplet-components excitonic field in Ref. [69]. In the following, we describe the expansion for singlet-component as well.  $\text{Tr}'[\dots]$  denotes an additional contribution from the singlet-component  $\phi_0 \boldsymbol{\sigma}_0$ ,

$$\text{Tr}'[\dots] \equiv \text{Tr}[\dots] - \text{Tr}[\dots]_{\phi_0=0}, \quad (\text{A.5})$$

and  $\hat{\phi}$  and  $\hat{\boldsymbol{\sigma}}$  denote the three-component (spin-triplet) vectors. The leading-order terms in the expansion are as follows:

$$\text{Tr}'[G_0 G_R^{-1} G_0 \Psi G_0 \Psi] = -iD \int d\tau d^2 \vec{r} \vec{e}_z \cdot [(\hat{\phi}^* \times \nabla) \phi_0 - \phi_0^* (\nabla \times \hat{\phi})], \quad (\text{A.6})$$

$$\text{Tr}'[G_0 G_H^{-1} G_0 \Psi G_0 \Psi] = -h' \int d\tau d^2 \vec{r} \vec{e}_x \cdot (\phi_0^* \hat{\phi} + \phi_0 \hat{\phi}^*), \quad (\text{A.7})$$

$$\text{Tr}'[-\frac{1}{4}(G_0 \Psi)^4] = \gamma \int d\tau d^2 \vec{r} [|\phi_0|^4 + 4|\phi_0|^2 |\hat{\phi}|^2 + (\phi_0^*)^2 (\hat{\phi})^2 + (\phi_0)^2 (\hat{\phi}^*)^2], \quad (\text{A.8})$$

$$\text{Tr}'[-\frac{1}{2}G_0 \Psi G_0 \Psi] = \alpha \int d\tau d^2 \vec{r} |\phi_0|^2 + \eta \int d\tau d^2 \vec{r} \phi_0^* \partial_\tau \phi_0 + \lambda \int d\tau d^2 \vec{r} \phi_0^* \nabla^2 \phi_0. \quad (\text{A.9})$$

These terms share the same coefficients as those in the leading-order terms in Ref. [69], except for  $h'$ . For the later convenience, we give the expressions of  $D$ ,  $h$  and  $h'$  as follows:

$$D = -\frac{2\xi_e}{\beta V} \frac{\hbar^2}{m_b} \sum_k k_x^2 g_a^0(k)^2 g_b^0(k)^2, \quad (\text{A.10})$$

$$h = \frac{2H}{\beta V} \sum_k g_a^0(k) g_b^0(k) (g_b^0(k) - g_a^0(k)), \quad (\text{A.11})$$

$$h' = \frac{2H}{\beta V} \sum_k g_a^0(k) g_b^0(k) [g_a^0(k) + g_b^0(k)] = -\frac{2H}{V} \sum_{\vec{k}} \frac{1}{\mathcal{E}_a - \mathcal{E}_b} \left[ \frac{\beta}{2 + 2\cosh\beta(\mathcal{E}_a - \mu)} - \frac{\beta}{2 + 2\cosh\beta(\mathcal{E}_b - \mu)} \right]. \quad (\text{A.12})$$

Putting Eqs. (A.6-A.9) into Eq. (A.1) and add them into the triplet component (Eq. (5) of Ref. [69]), we obtain the  $\phi^4$ -type effective Lagrangian for the four-components excitonic field:

$$\begin{aligned} S = & \int d\tau d^2 \vec{r} \{ -\eta \vec{\phi}^\dagger \partial_\tau \vec{\phi} + \lambda |\nabla \vec{\phi}|^2 - (\alpha - \frac{2}{g}) |\vec{\phi}|^2 - \gamma [2|\hat{\phi}|^4 - (\hat{\phi}^*)^2 (\hat{\phi})^2 + |\hat{\phi}_0|^4 + 4|\phi_0|^2 |\hat{\phi}|^2 + (\phi_0^*)^2 (\hat{\phi})^2 + (\phi_0)^2 (\hat{\phi}^*)^2] \\ & - D[\vec{e}_y \cdot (\hat{\phi}^* \times \partial_x \hat{\phi}) - \vec{e}_x \cdot (\hat{\phi}^* \times \partial_y \hat{\phi}) - i\vec{e}_z \cdot ((\hat{\phi}^* \times \nabla) \phi_0 - \phi_0^* (\nabla \times \hat{\phi}))] + ih\vec{e}_x \cdot (\hat{\phi}^* \times \hat{\phi}) + h' \vec{e}_x \cdot (\phi_0^* \hat{\phi} + \phi_0 \hat{\phi}^*) \}, \end{aligned} \quad (\text{A.13})$$

where  $\vec{\phi} \equiv (\phi_0, \hat{\phi}) = (\phi_0, \phi_x, \phi_y, \phi_z)$ , and  $\nabla = (\partial_x, \partial_y, 0)$ . In terms of  $\vec{\Phi} \equiv (-i\phi_0, \hat{\phi}) \equiv \vec{\Phi}' + i\vec{\Phi}''$ , the Lagrangian takes a more symmetric form:

$$\begin{aligned} S = & \int_0^\beta d\tau \int d^2\vec{r} \{ -\eta \vec{\Phi}^\dagger \partial_\tau \vec{\Phi} - (\alpha - \frac{2}{g}) |\vec{\Phi}|^2 - \gamma [(\vec{\Phi}'^2)^2 + (\vec{\Phi}''^2)^2 + 6\vec{\Phi}'^2 \vec{\Phi}''^2 - 4(\vec{\Phi}' \cdot \vec{\Phi}'')^2] + \lambda [(\nabla \vec{\Phi}')^2 + (\nabla \vec{\Phi}'')^2] \\ & - D(\Phi'_z \partial_x \Phi'_x - \Phi'_x \partial_z \Phi'_z + \Phi'_z \partial_y \Phi'_y - \Phi'_y \partial_z \Phi'_z) - D(\Phi'_0 \partial_x \Phi'_y - \Phi'_y \partial_x \Phi'_0 + \Phi'_x \partial_y \Phi'_0 - \Phi'_y \partial_x \Phi'_x) \\ & - D(\Phi''_z \partial_x \Phi''_x - \Phi''_x \partial_z \Phi''_z + \Phi''_z \partial_y \Phi''_y - \Phi''_y \partial_z \Phi''_z) - D(\Phi''_0 \partial_x \Phi''_y - \Phi''_y \partial_x \Phi''_0 + \Phi''_x \partial_y \Phi''_0 - \Phi''_y \partial_x \Phi''_x) \\ & - 2h(\Phi'_y \Phi''_z - \Phi'_z \Phi''_y) + 2h'(\Phi'_0 \Phi''_x - \Phi'_x \Phi''_0) \} + \mathcal{O}(\xi_e^2, H^2, \xi_e H), \end{aligned} \quad (\text{A.14})$$

with  $|\vec{\Phi}|^2 \equiv \vec{\Phi}'^2 + \vec{\Phi}''^2$ . In absence of the Rashba term ( $D = 0$ ), this reduces to Eq. (2) in the main text.

Before closing this section, we like to mention a relation between  $\lambda$  and  $D$  and that between  $h$  and  $h'$ .  $\lambda$ ,  $\alpha$  and  $\eta$  in the action comes from an expansion of the bare polarization function in frequency and momentum,

$$\alpha_q \equiv -\frac{2}{\beta\Omega} \sum_k g_b^0(k - \frac{q}{2}) g_a^0(k + \frac{q}{2}) = \alpha_q^{(0)} + \alpha_q^{(1)} i\omega_m + \alpha_q^{(2)} \vec{q}^2 + \dots \quad (\text{A.15})$$

In terms of a relation,

$$\sum_k g_b^0(k - \frac{q_x}{2}) g_a^0(k + \frac{q_x}{2}) = \sum_k g_b^0(k - q_x) g_a^0(k) = \sum_k g_b^0(k) g_a^0(k + q_x), \quad (\text{A.16})$$

$\lambda$  is calculated as follows:

$$\lambda = -\alpha_q^{(2)} = -\frac{1}{\beta V} \sum_k g_b^0(k)' g_a^0(k)' = \frac{1}{\beta V} \frac{\hbar^4}{m_a m_b} \sum_k k_x^2 g_a^0(k)^2 g_b^0(k)^2, \quad (\text{A.17})$$

with  $g_a^0(k)' \equiv \partial_{k_x} g_a^0(k)$ . A comparison to Eq. (A.10) gives the relation between  $\lambda$  and  $D$  as

$$K \equiv \frac{D}{2\lambda} = -\frac{\xi_e m_a}{\hbar^2}, \quad (\text{A.18})$$

where we recover  $\hbar$  in Eq. (A.18) by substitutions  $1/m_{a/b} \rightarrow \hbar^2/m_{a/b}$  in Eqs. (A.10,A.17,A.18). The ratio between  $h'$  and  $h$  are determined by  $m_b/m_a$  and  $\beta E_g$ . Using Eqs. (A.11,A.12), we calculate  $h'/h$  as a function of  $\beta E_g$  and  $m_b/m_a$  (Fig. 3(a)). In sec. B, we show that when  $|h'| > |h| / |h| > |h'|$ , the classical effective Lagrangian Eq. (2) is minimized by longitudinal/transverse phase (Fig. 5(a)). We combine Fig. 3(b) and Fig. 5(a), to have a finite- $T$  phase diagram, Fig. 3(b). Note that the phase diagram is valid for the case with  $H_a = H_b = H$  and  $\xi_e = 0$ . In the case with  $H_a = H_b = H$  and  $\xi_e \neq 0$ , the transverse and longitudinal phases are replaced by helicoidal and helical phases respectively. Note also that the zero-temperature limit of the phase diagram ( $\beta \rightarrow \infty$ ) indicates the classical ground state of the 2D EHDL system under the exchange fields with  $H_a = H_b = H$  is the transverse phase.

## B. Derivation of classical ground-state phase diagram without Rashba interaction

In this section, we describe the minimization of Eq. (2) of the main text, while we describe the minimization of Eq. (A.14) in Sec. G. Note first that spatial derivative term in Eq. (2) is positive definite,  $\lambda |\nabla \vec{\Phi}|^2 \geq 0$ . Thus, only a spatially uniform solution of  $\vec{\Phi}$  minimizes the action,

$$\begin{aligned} \mathcal{L} = & A(\Phi'^2 + \Phi''^2) + B[\Phi'^4 + \Phi''^4 + 6\Phi'^2 \Phi''^2] \\ & - 4B\Phi'^2 \Phi''^2 (\cos\eta_1 \cos\eta_2 \cos\alpha_1 + \sin\eta_1 \sin\eta_2 \cos\alpha_2)^2 + 2h' \Phi' \Phi'' \cos\eta_1 \cos\eta_2 \sin\alpha_1 - 2h \Phi' \Phi'' \sin\eta_1 \sin\eta_2 \sin\alpha_2, \\ \equiv & A(\Phi'^2 + \Phi''^2) + B[\Phi'^4 + \Phi''^4 + 6\Phi'^2 \Phi''^2] - 2\Phi' \Phi'' g(\eta_1, \eta_2, \alpha_1, \alpha_2) \end{aligned} \quad (\text{B.1})$$

with  $A \equiv -(\alpha - 2/g) < 0$  and  $B = -\gamma > 0$ . Here  $\Phi'$  and  $\Phi''$  are the norm of the four-component vector fields  $\vec{\Phi}'$  and  $\vec{\Phi}''$  respectively.  $\eta_1$ ,  $\eta_2$ ,  $\alpha_1$  and  $\alpha_2$  define relative angles among  $\vec{\Phi}'$ ,  $\vec{\Phi}''$  and a  $0x$  plane subtended by  $\vec{e}_x$  and  $\vec{e}_0$  (Figs. 4(a),4(b),4(c),4(d)).  $\eta_1$  ( $\eta_2$ ) is an angle between  $\vec{\Phi}'$  ( $\vec{\Phi}''$ ) and the  $0x$  plane (Figs. 4(a),4(b)). To define  $\alpha_1$  and  $\alpha_2$ , we decompose  $\vec{\Phi}'$  and  $\vec{\Phi}''$  into a component parallel to the  $0x$  plane and the other,  $\vec{\Phi}' = \vec{\Phi}'_{0x} + \vec{\Phi}'_{yz}$ ,  $\vec{\Phi}'' = \vec{\Phi}''_{0x} + \vec{\Phi}''_{yz}$ .  $\alpha_1$  is an angle between  $\vec{\Phi}'_{0x}$  and  $\vec{\Phi}''_{0x}$  and  $\alpha_2$  is an angle between  $\vec{\Phi}'_{yz}$  and  $\vec{\Phi}''_{yz}$  (Figs. 4(c),4(d)).

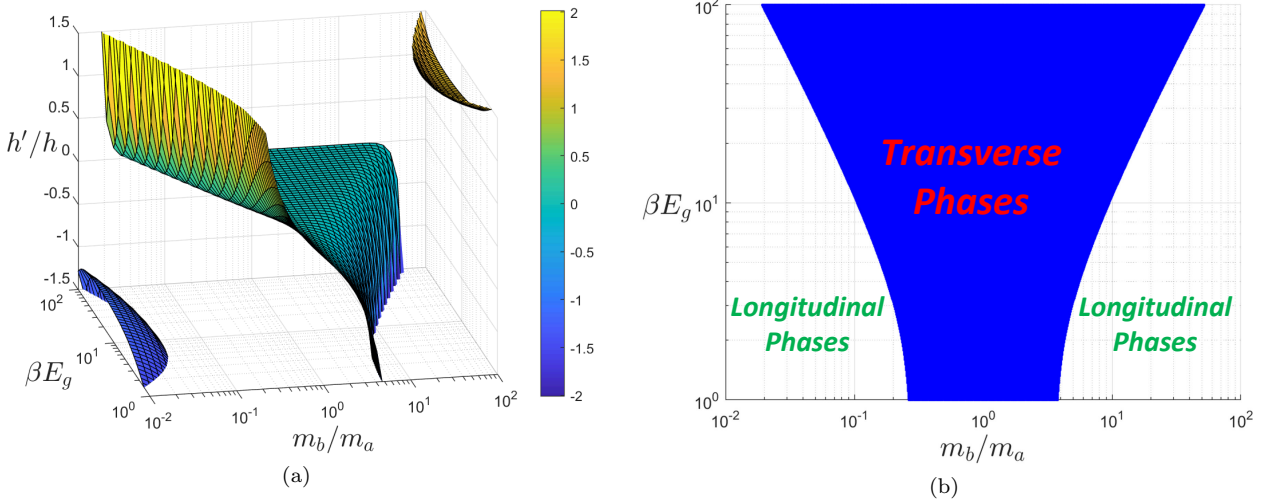


FIG. 3. (a) A ratio between  $h'$  and  $h$  depends on a ratio between the two effective mass ( $m_a$  and  $m_b$ ), temperature and band inversion parameter  $E_g$ . The ratio  $h'/h$  is plotted as a function of  $m_b/m_a$ , and the band inversion parameter normalized by the temperature. (b) When  $|h'/h| < 1$  ( $|h'/h| > 1$ ), the classical ground state is transverse (longitudinal) phases. Combining this with Fig. (a), we show the phase diagram as a function of  $m_b/m_a$  and  $\beta E_g$ .

We first minimize the third term of Eq. (B.1) that depends on  $\eta_1$ ,  $\eta_2$ ,  $\alpha_1$  and  $\alpha_2$  for fixed  $\Phi'$  and  $\Phi''$ . Namely, we maximize the following function for fixed  $\Phi'$  and  $\Phi''$ ,

$$g(\eta_1, \eta_2, \alpha_1, \alpha_2) = 2B\Phi'\Phi''(\cos\eta_1\cos\eta_2\cos\alpha_1 + \sin\eta_1\sin\eta_2\cos\alpha_2)^2 - h'\cos\eta_1\cos\eta_2\sin\alpha_1 + h\sin\eta_1\sin\eta_2\sin\alpha_2. \quad (\text{B.2})$$

The function is a sum of quadratic functions of  $x \equiv \cos(\eta_1 - \eta_2)$  and  $y \equiv \cos(\eta_1 + \eta_2)$ ,

$$g = C\left(\frac{\cos\alpha_1 + \cos\alpha_2}{2}x + \frac{\cos\alpha_1 - \cos\alpha_2}{2}y\right)^2 + \frac{h\sin\alpha_2 - h'\sin\alpha_1}{2}x - \frac{h\sin\alpha_2 + h'\sin\alpha_1}{2}y, \quad (\text{B.3})$$

with  $C \equiv 2B\Phi'\Phi'' > 0$ ,  $\frac{\partial^2 g}{\partial x^2} \geq 0$  and  $\frac{\partial^2 g}{\partial y^2} \geq 0$ . Since a domain of  $x$  and  $y$  is bounded by  $(x, y) \in [-1, 1] \times [-1, 1]$ , the function takes a maximum value at either one of the four corners of the domain;  $(x, y) = \{(-1, -1), (-1, 1), (1, -1), (1, 1)\}$ . By definition,  $(\alpha_1, \alpha_2, x, y)$  and  $(\alpha_1 + \pi, \alpha_2 + \pi, -x, -y)$  represent the same vectors. Thus, we take  $(x, y)$  at  $(1, 1)$  or at  $(1, -1)$  and maximize  $g$  with respect to  $\alpha_1$  and  $\alpha_2$ . When  $x = y = 1$ ,  $\eta_1 = \eta_2 = 0$ , and  $g = -C\sin^2\alpha_1 - h'\sin\alpha_1 + C$ ; When  $x = -y = 1$ ,  $\eta_1 = \eta_2 = \frac{\pi}{2}$ , and  $g = -C\sin^2\alpha_2 + h\sin\alpha_2 + C$ . Such  $g$  is maximized with respect to  $\alpha_1$  and/or  $\alpha_2$  at the following points,

$$\begin{cases} \eta_1 = \eta_2 = \frac{\pi}{2}, \alpha_1 \text{ undefined}, \sin\alpha_2 = \frac{h}{2C}, g = C + \frac{h^2}{4C}, (|h'| < |h| < 2C), \\ \eta_1 = \eta_2 = 0, \sin\alpha_1 = -\frac{h'}{2C}, \alpha_2 \text{ undefined}, g = C + \frac{h^2}{4C}, (|h| < |h'| < 2C), \\ \eta_1 = \eta_2 = \frac{\pi}{2}, \alpha_1 \text{ undefined}, \sin\alpha_2 = \frac{h}{|h|}, g = |h|, (|h'| < |h|, 2C < |h|), \\ \eta_1 = \eta_2 = 0, \sin\alpha_1 = -\frac{h'}{|h|}, \alpha_2 \text{ undefined}, g = |h'|, (|h| < |h'|, 2C < |h'|). \end{cases} \quad (\text{B.4})$$

Eq. (B.4) is symmetric with respect to an exchange between  $h$  and  $-h'$  and between  $\alpha_1$  and  $\alpha_2$ . We consider a case of  $|h| > |h'|$  first, where  $\vec{\Phi}'$  and  $\vec{\Phi}''$  are on a  $yz$  plane subtended by  $\vec{e}_y$  and  $\vec{e}_z$  ( $\eta_1 = \eta_2 = \pi/2$ ) and an angle between  $\vec{\Phi}'$  and  $\vec{\Phi}''$  is  $\alpha_2$  (Figs. 4(a), 4(b), 4(d)).  $g$  in Eq. (B.4) is substituted into Eq. (B.1),

$$\begin{cases} \mathcal{L} = -|A|(\Phi'^2 + \Phi''^2) + B(\Phi'^2 + \Phi''^2)^2 - \frac{h^2}{4B} & (2\Phi'\Phi'' \geq \frac{|h|}{2B}), \\ \mathcal{L} = -|A|(\Phi'^2 + \Phi''^2) + B(\Phi'^2 + \Phi''^2)^2 + 4B\Phi'^2\Phi''^2 - 2|h|\Phi'\Phi'' & (2\Phi'\Phi'' \leq \frac{|h|}{2B}). \end{cases} \quad (\text{B.5})$$

The Lagrangian in Eq. (B.5) is further minimized in  $\Phi'$  and  $\Phi''$ . First,  $\mathcal{L}$  is decomposed into a function of  $a \equiv \Phi'^2 + \Phi''^2$  and a function of  $b \equiv 2\Phi'\Phi''$ , each of which can be separately minimized;

$$\mathcal{L} \equiv \mathcal{L}_1(a) + \mathcal{L}_2(b), \quad \mathcal{L}_1(a) = -|A|a + Ba^2, \quad \mathcal{L}_2(b) = \begin{cases} -\frac{h^2}{4B} & (b \geq \frac{|h|}{2B}), \\ Bb^2 - |h|b & (b \leq \frac{|h|}{2B}). \end{cases} \quad (\text{B.6})$$

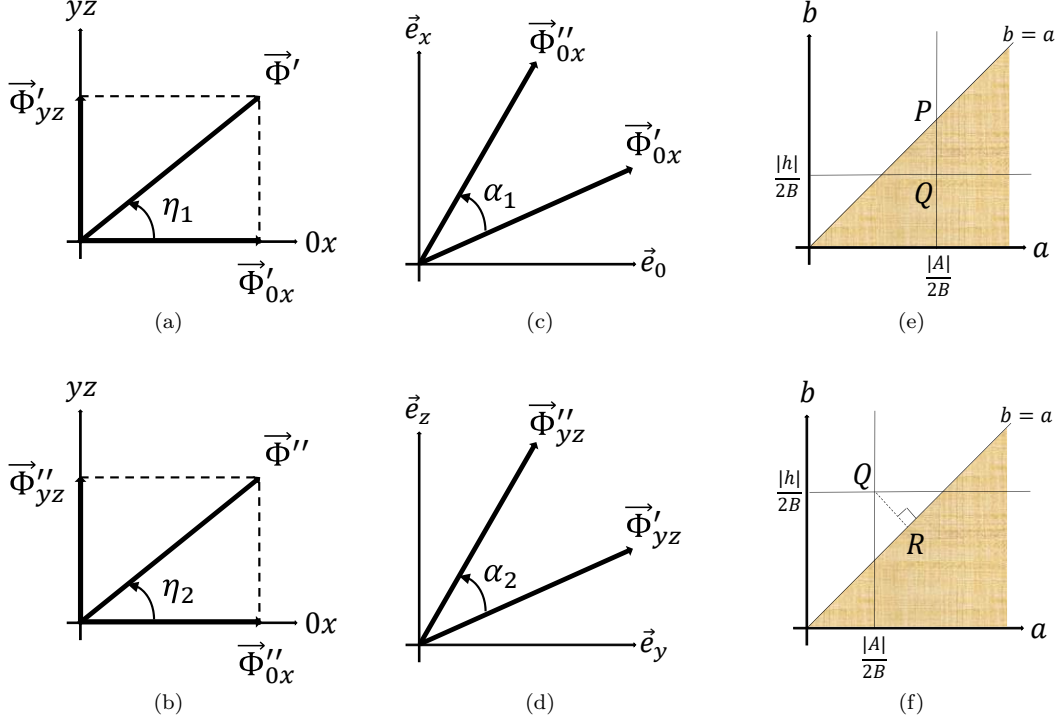


FIG. 4. (a-d) Definitions of  $\eta_1$ ,  $\eta_2$ ,  $\alpha_1$  and  $\alpha_2$ . (e,f) Minimization of  $\mathcal{L}_1(a) + \mathcal{L}_2(b)$  in a domain of  $0 \leq b \leq a$ .  $\mathcal{L}_1(a)$  is minimized along a line of  $a = |A|/2B$ .  $\mathcal{L}_2(b)$  is minimized in a region of  $b \geq |h|/2B$ . When  $|A| > |h|$ ,  $\mathcal{L}_1(a) + \mathcal{L}_2(b)$  is minimized along a finite length of line:  $a = |A|/2B$  and  $|A|/2B \geq b \geq |h|/2B$  (a line of PQ in Fig. (e)). When  $|A| < |h|$ ,  $\mathcal{L}_1(a) + \mathcal{L}_2(b)$  is minimized at a point on the domain boundary:  $a = b = \frac{1}{2}(\frac{|h|}{2B} + \frac{|A|}{2B})$  (a point of R in Fig. (f)).

$\mathcal{L}_1(a)$  and  $\mathcal{L}_2(b)$  take respective minimum at the following point or region,

$$a \equiv \Phi'^2 + \Phi''^2 = \frac{|A|}{2B}, \quad b \equiv 2\Phi'\Phi'' \equiv a \sin 2\theta \geq \frac{|h|}{2B}. \quad (\text{B.7})$$

with  $(\Phi', \Phi'') \equiv \sqrt{a}(\cos \theta, \sin \theta)$  and  $0 < \theta < \pi/2$ . Noting that a domain of  $a$  and  $b$  is limited by  $0 < b < a$  together with  $|A| \equiv h_c$ ,  $B \equiv |\gamma|$ , we complete the minimization of the Lagrangian with a help of Figs. 4(e), 4(f).

**Case 1:**  $h_c \geq |h|$  and  $|h| > |h'|$ , the global minimum of the action is achieved on a finite length of a line defined as:

$$a \sin \alpha_2 \sin 2\theta = \frac{h}{2|\gamma|}, \quad a \equiv \Phi'^2 + \Phi''^2 = \frac{h_c}{2|\gamma|}, \quad \frac{|h|}{2|\gamma|} \leq b \equiv a \sin 2\theta \leq \frac{h_c}{2|\gamma|}. \quad (\text{B.8})$$

**Case 2:**  $h_c \leq |h|$  and  $|h| > |h'|$ , the global minimum in the domain is achieved at a point on the domain boundary,  $a = b = \frac{a+b}{2} = \frac{h_c+|h|}{4|\gamma|}$ :

$$\sin \alpha_2 = \frac{h}{|h|}, \quad a \equiv \Phi'^2 + \Phi''^2 = \frac{h_c + |h|}{4|\gamma|}, \quad \theta = \frac{\pi}{4}. \quad (\text{B.9})$$

In the case of  $|h| < |h'|$ ,  $\vec{\Phi}'$  and  $\vec{\Phi}''$  are on the  $0x$  plane subtended by  $\vec{e}_0$  and  $\vec{e}_x$  ( $\eta_1 = \eta_2 = 0$ ) and the angle between  $\vec{\Phi}'$  and  $\vec{\Phi}''$  is  $\alpha_1$  (Figs. 4(a), 4(b), 4(c)). Following the same argument, we obtain the other two cases.

**Case 3:**  $h_c \geq |h'|$  and  $|h| < |h'|$ , the global minimum of the action is achieved on a finite length of a line given by:

$$a \sin \alpha_1 \sin 2\theta = -\frac{h'}{2|\gamma|}, \quad a \equiv \Phi'^2 + \Phi''^2 = \frac{h_c}{2|\gamma|}, \quad \frac{|h'|}{2|\gamma|} \leq b \equiv a \sin 2\theta \leq \frac{h_c}{2|\gamma|}. \quad (\text{B.10})$$

**Case 4:**  $h_c \leq |h'|$  and  $|h| < |h'|$ , the global minimum in the domain is achieved at a point on the domain boundary,

$$a = b = \frac{a+b}{2} = \frac{h_c + |h|}{4|\gamma|}:$$

$$\sin \alpha_1 = -\frac{h'}{|h'|}, \quad a \equiv \Phi'^2 + \Phi''^2 = \frac{h_c + |h'|}{4|\gamma|}, \quad \theta = \frac{\pi}{4}. \quad (\text{B.11})$$

To summarize these four cases, we have the following four phases.

**For  $|h'| < |h| < h_c$  (normal transverse phase: Case 1 with  $\alpha_2 = \varphi$ ):**

$$\begin{aligned} \vec{\phi} &= \rho \cos \theta (\cos \varphi_0 \vec{e}_y + \sin \varphi_0 \vec{e}_z) + i \rho \sin \theta [\cos(\varphi + \varphi_0) \vec{e}_y + \sin(\varphi + \varphi_0) \vec{e}_z], \\ \rho &= \sqrt{\frac{h_c}{2|\gamma|}}, \quad \sin \varphi \sin 2\theta = \frac{h}{h_c}. \end{aligned} \quad (\text{B.12})$$

**For  $|h| < |h'| < h_c$  (normal longitudinal phase: case 3 with  $\alpha_1 = \varphi$ ):**

$$\begin{aligned} \vec{\phi} &= \rho [-\sin \theta \cos(\varphi + \varphi_0) \vec{e}_0 + \cos \theta \sin \varphi_0 \vec{e}_x] + i \rho [\cos \theta \cos \varphi_0 \vec{e}_0 + \sin \theta \sin(\varphi + \varphi_0) \vec{e}_x], \\ \rho &= \sqrt{\frac{h_c}{2|\gamma|}}, \quad \sin \varphi \sin 2\theta = -\frac{h'}{h_c}. \end{aligned} \quad (\text{B.13})$$

**For  $|h'| < |h|, h_c < |h|$  (saturated transverse phase: case 2 with  $\alpha_2 = \text{sgn}(h) \frac{\pi}{2}$ ):**

$$\vec{\phi} = \rho (\cos \varphi_0 \vec{e}_y + \sin \varphi_0 \vec{e}_z) - i \rho \text{sgn}(h) [\sin \varphi_0 \vec{e}_y - \cos \varphi_0 \vec{e}_z], \quad \rho = \sqrt{\frac{h_c + |h|}{8|\gamma|}}. \quad (\text{B.14})$$

**For  $|h| < |h'|, h_c < |h'|$  (saturated longitudinal phase: case 4 with  $\alpha_1 = -\text{sgn}(h') \frac{\pi}{2}$ ):**

$$\vec{\phi} = \rho [\text{sgn}(-h') \sin \varphi_0 \vec{e}_0 + \sin \varphi_0 \vec{e}_x] + i \rho [\cos \varphi_0 \vec{e}_0 + \text{sgn}(-h') \cos \varphi_0 \vec{e}_x], \quad \rho = \sqrt{\frac{h_c + |h'|}{8|\gamma|}}. \quad (\text{B.15})$$

From Eqs. (B.12-B.15), we obtain a classical ground-state phase diagram at  $D = 0$  (Fig. 5(a)). The phase boundaries at  $|h| = |h'|$  are of the first order. The phase boundaries at  $|h| = h_c$  and at  $|h'| = h_c$  are of the second order. As the exchange field  $H$  is supposed to be small, we focus on the normal transverse phase and the normal longitudinal phase in the main text (Eqs. (3-5)).

### C. Spin rotational symmetry of the excitonic condensate system

In this section, we clarify what continuous spin-rotational symmetry is broken in the normal transverse and longitudinal phases, i.e. Eq. (6) in the main text. Let us begin with the longitudinal phase:

$$\begin{aligned} \vec{\phi}_{0x}(\theta, \varphi, \varphi_0) \cdot \vec{\sigma} &\equiv -\rho \sin \theta [\sigma_0 \cos(\varphi + \varphi_0) - i \sigma_x \sin(\varphi + \varphi_0)] + i \rho \cos \theta [\sigma_0 \cos \varphi_0 - i \sigma_x \sin \varphi_0] \\ &= -\rho \sin \theta e^{-i(\varphi + \varphi_0) \sigma_x} + i \rho \cos \theta e^{-i\varphi_0 \sigma_x} = [-\rho \sin \theta e^{-i\varphi \sigma_x} + i \rho \cos \theta] e^{-i\varphi_0 \sigma_x} = \vec{\phi}_{0x}(\theta, \varphi, 0) \cdot \vec{\sigma} e^{-i\varphi_0 \sigma_x}. \end{aligned} \quad (\text{C.1})$$

A change of  $\varphi_0$  by  $\delta \varphi_0$  can be absorbed by spin rotations around the  $x$  axis in the electron and hole layers through a mean-field coupling term,

$$\vec{\phi}_{0x}(\varphi_0 + \delta \varphi_0) \cdot \mathbf{a}^\dagger \vec{\sigma} \mathbf{b} = \vec{\phi}_{0x}(\varphi_0) \cdot \mathbf{a}^\dagger \vec{\sigma} e^{-i\delta \varphi_0 \sigma_x} \mathbf{b} = \vec{\phi}_{0x}(\varphi_0) \cdot \mathbf{a}^\dagger e^{-i\delta \varphi_0 \sigma_x} \vec{\sigma} \mathbf{b}. \quad (\text{C.2})$$

Namely, the mean-field term  $\vec{\phi}_{0x} \cdot \mathbf{a}^\dagger \vec{\sigma} \mathbf{b}$  is invariant under the followings;

$$\mathbf{a} \rightarrow e^{i\varphi_a \sigma_x} \mathbf{a}, \quad \mathbf{b} \rightarrow e^{i\varphi_b \sigma_x} \mathbf{b}, \quad \vec{\phi}_{0x}(\varphi_0) \rightarrow \vec{\phi}(\varphi_0 + \varphi_b - \varphi_a). \quad (\text{C.3})$$

Similarly, the transverse phase is given by the following classical configuration:

$$\begin{aligned} \vec{\phi}_{yz}(\theta, \varphi, \varphi_0) \cdot \vec{\sigma} &\equiv \rho \cos \theta \sigma_y e^{i\varphi_0 \sigma_x} + i \rho \sin \theta \sigma_y e^{i(\varphi + \varphi_0) \sigma_x} \\ &= \vec{\phi}_{yz}(\theta, \varphi, 0) \cdot \vec{\sigma} e^{i\varphi_0 \sigma_x} = e^{-i\varphi_0 \sigma_x} \vec{\phi}_{yz}(\theta, \varphi, 0) \cdot \vec{\sigma}. \end{aligned} \quad (\text{C.4})$$

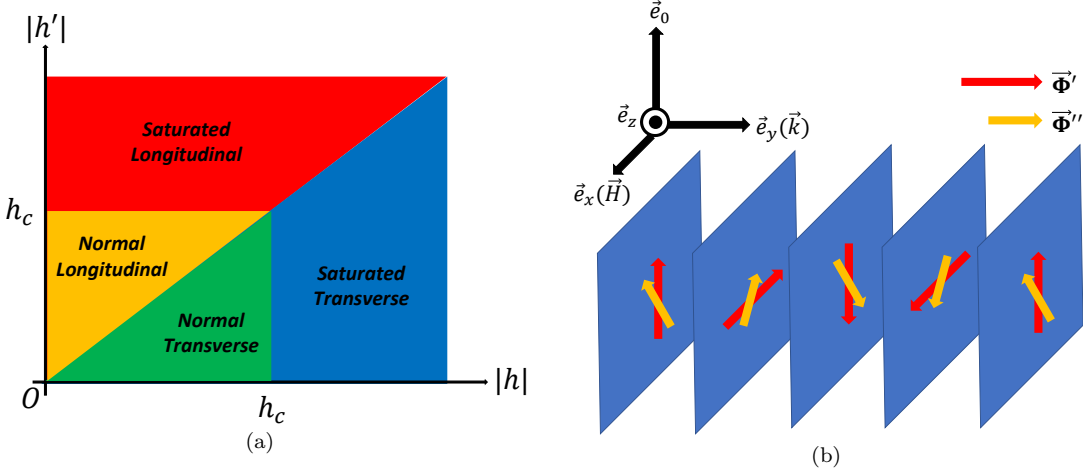


FIG. 5. (a) Classical ground-state phase diagram of the EHD excitons under magnetic exchange fields without Rashba interaction. The phase diagram remains unchanged with Rashba interaction, except the transverse/longitudinal phases are substituted by corresponding helicoidal/helical phases. (b) A schematic picture of the helical structure of condensed excitons. The real ( $\vec{\Phi}'$ ) and imaginary ( $\vec{\Phi}''$ ) parts are depicted by red and yellow arrows respectively. The propagation direction  $\vec{k}(\vec{e}_y)$  is along the in-plane direction perpendicular to the magnetic field, and  $\vec{\Phi}'$  and  $\vec{\Phi}''$  rotate in the plane (depicted by blue planes) subtended by a direction of spin singlet ( $\vec{e}_0$ ) and a direction of magnetic field  $\vec{H}(\vec{e}_x)$ . An angle between  $\vec{\Phi}'$  and  $\vec{\Phi}''$  is acute for the normal helical phase. The angle becomes 0 for  $h' = 0$  and  $\pi/2$  for  $|h'| \geq |h|$  (saturated helical phase). The length of  $\vec{\Phi}'$  and that of  $\vec{\Phi}''$  become identical to each other for the saturated helical phase.

A variation of  $\varphi_0$  by  $\delta\varphi_0$  transforms the mean-field coupling term as

$$\vec{\phi}_{yz}(\varphi_0 + \delta\varphi_0) \cdot \mathbf{a}^\dagger \vec{\sigma} \mathbf{b} = \vec{\phi}_{yz}(\varphi_0) \cdot \mathbf{a}^\dagger \vec{\sigma} e^{i\delta\varphi_0 \sigma_x} \mathbf{b} = \vec{\phi}_{yz}(\varphi_0) \cdot \mathbf{a}^\dagger e^{-i\delta\varphi_0 \sigma_x} \vec{\sigma} \mathbf{b}. \quad (\text{C.5})$$

The variation can be absorbed by the following spin rotations around the  $x$  axis in the electron and hole layers,

$$\mathbf{a} \rightarrow e^{i\varphi_a \sigma_x} \mathbf{a}, \quad \mathbf{b} \rightarrow e^{i\varphi_b \sigma_x} \mathbf{b}, \quad \vec{\phi}_{yz}(\varphi_0) \rightarrow \vec{\phi}_{yz}(\varphi_0 - \varphi_b - \varphi_a). \quad (\text{C.6})$$

Eqs. (C.3, C.6) are equivalent to Eq. (6) in the main text.

#### D. Relation between the Goldstone modes and the $U(1)$ gauge symmetry

In this section, we show that the relative  $U(1)$  gauge transformation can be absorbed into a combination of changes of  $\theta$ ,  $\varphi$  and  $\varphi_0$  that satisfies the constraint Eq. (5);

$$\begin{cases} e^{i\psi} \vec{\phi}_\lambda(\theta, \varphi, \varphi_0) = \vec{\phi}_\lambda(\theta(\psi), \varphi(\psi), \varphi_0(\psi)), \\ \sin 2\theta(\psi) \sin \varphi(\psi) = \sin 2\theta \sin \varphi = h \equiv \begin{cases} \frac{h}{h_c} & (\lambda = yz), \\ -\frac{h'}{h_c} & (\lambda = 0x), \end{cases} \end{cases} \quad (\text{D.1})$$

for both the transverse phase ( $\lambda = yz$ ) and the longitudinal phase ( $\lambda = 0x$ ). We can generalize the argument into the helical and helicoidal phase by replacing  $\varphi_0$  by  $\varphi_0 - Ky$ . In the following, we only sketch the argument for the transverse phase, while the argument for the longitudinal phase goes as well. Without loss of generality, we take  $\varphi_0$  to be  $-\varphi$  in Eq. (3) of the main text and apply the gauge transformation on Eq. (3) as,

$$\vec{\phi}_{yz}(\theta, \varphi, \varphi_0) = \rho(\cos\theta \cos\varphi + i\sin\theta \sin\varphi) \vec{e}_y - \rho \cos\theta \sin\varphi \vec{e}_z, \quad (\text{D.2})$$

$$\begin{aligned} e^{i\psi} \vec{\phi}_{yz}(\theta, \varphi, \varphi_0) &= \rho(\cos\theta \cos\varphi \cos\psi - \sin\theta \sin\psi) \vec{e}_y + i\rho(\sin\theta \cos\psi + \cos\theta \sin\varphi \sin\psi) \vec{e}_y \\ &\quad - \rho \cos\theta \sin\varphi \cos\psi \vec{e}_z - i\rho \cos\theta \sin\varphi \sin\psi \vec{e}_z. \end{aligned} \quad (\text{D.3})$$

In terms of  $\theta'$ ,  $\varphi'$ ,  $\varphi'_0$  ( $\varphi''_0 \equiv \varphi' + \varphi'_0$ ), Eq. (D.3) is equated to

$$\vec{\phi}_{yz}(\theta', \varphi', \varphi'_0) = \rho \cos\theta' \cos(\varphi' - \varphi''_0) \vec{e}_y + i\rho \sin\theta' \cos\varphi''_0 \vec{e}_y - \rho \cos\theta' \sin(\varphi' - \varphi''_0) \vec{e}_z + i\rho \sin\theta' \sin\varphi''_0 \vec{e}_z. \quad (\text{D.4})$$

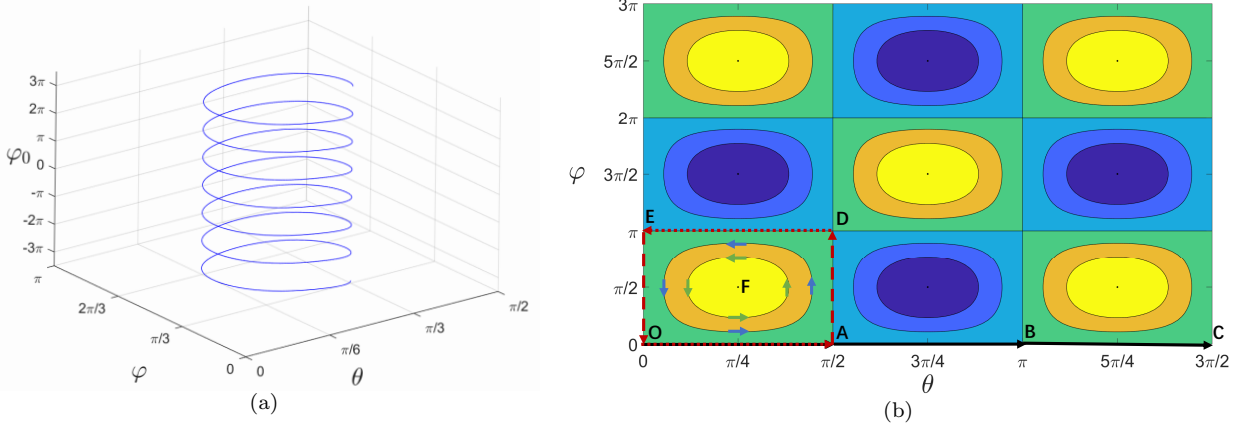


FIG. 6. (a) A parameter plot of  $(\theta(\psi), \varphi(\psi), \varphi_0(\psi))$  where the initial point  $(\theta(0), \varphi(0), \varphi_0(0))$  satisfy  $h = \sin 2\theta(0) \sin \varphi(0) = 0.75$ ,  $\sin \varphi(0) = 0.8$ , and  $\varphi_0(0) = 0$ . When  $\psi$  increases by  $\pi$ ,  $\varphi$  decreases by  $\pi$ , while  $(\theta, \varphi)$  goes along a closed curve ( $\tilde{h} \equiv \sin 2\theta \sin \varphi = h$ ) at one time. (b) The contour plot of  $\tilde{h} = h$  for different values of  $h$ . When  $h = 1$ , the projection becomes a point (F). When  $h = 0$ , the projection tends to a rectangle (O  $\rightarrow$  A  $\rightarrow$  D  $\rightarrow$  E  $\rightarrow$  O), but it is also equivalent to go along a straight line (O  $\rightarrow$  A  $\rightarrow$  B  $\rightarrow$  C  $\rightarrow$  O), as different values of  $(\psi, \theta, \varphi, \varphi_0)$  may be equivalent in the special case of  $\tilde{h} = 0$ .

The comparison of (D.4) with (D.3) gives four equations:

$$\cos \theta' \cos(\varphi' - \varphi_0'') = \cos \theta \cos \varphi \cos \psi - \sin \theta \sin \psi, \quad (\text{D.5})$$

$$\sin \theta' \cos \varphi_0'' = \sin \theta \cos \psi + \cos \theta \cos \varphi \sin \psi, \quad (\text{D.6})$$

$$\cos \theta' \sin(\varphi' - \varphi_0'') = \cos \theta \sin \varphi \cos \psi, \quad (\text{D.7})$$

$$-\sin \theta' \sin \varphi_0'' = \cos \theta \sin \varphi \sin \psi. \quad (\text{D.8})$$

Note first that  $(\text{D.5})^2 + (\text{D.6})^2 + (\text{D.7})^2 + (\text{D.8})^2$  are trivially satisfied, so that Eqs. (D.5–D.8) have only three independent equations. Three unknown variables  $(\theta', \varphi', \varphi_0')$  can be solved in favor for  $(\theta, \varphi, \varphi_0 = -\varphi)$  and  $\psi$ .

From Eqs. (D.6,D.8), we get:

$$-\tan \varphi_0'' = \frac{\cos \theta \sin \varphi \sin \psi}{\sin \theta \cos \psi + \cos \theta \cos \varphi \sin \psi}, \quad (\text{D.9})$$

From Eqs. (D.5,D.7), we get:

$$\tan(\varphi' - \varphi_0'') = \frac{\cos \theta \sin \varphi \cos \psi}{\cos \theta \cos \varphi \cos \psi - \sin \theta \sin \psi}, \quad (\text{D.10})$$

Using Eqs. (D.9,D.10) together with  $\sin 2\theta \sin \varphi = h$ , we have

$$\tan \varphi' = \frac{\tan(\varphi' - \varphi_0'') + \tan \varphi_0''}{1 - \tan(\varphi' - \varphi_0'') \tan \varphi_0''} = \frac{h}{\sin 2\theta \cos \varphi \cos 2\psi + \cos 2\theta \sin 2\psi}. \quad (\text{D.11})$$

From Eqs. (D.5,D.7), we get:

$$\cos^2 \theta' = \frac{1}{2}(1 + \cos 2\theta \cos 2\psi - \sin 2\theta \sin 2\psi \cos \varphi), \quad (\text{D.12})$$

From Eqs. (D.6,D.8), we get:

$$\sin^2 \theta' = \frac{1}{2}(1 - \cos 2\theta \cos 2\psi + \sin 2\theta \sin 2\psi \cos \varphi). \quad (\text{D.13})$$

Eqs. (D.9,D.11,D.12,D.13) are nothing but the solutions of  $\theta'$ ,  $\varphi'$ ,  $\varphi'_0$  in favor for  $\theta$ ,  $\varphi$ ,  $\varphi_0 = -\varphi$  and  $\psi$ . To see that such  $\theta'$  and  $\varphi'$  satisfy the same condition as  $\theta$  and  $\varphi$ , i.e.  $\sin 2\theta' \sin \varphi' = h$ , we multiply Eq. (D.12) by Eq. (D.13), to have

$$\sin^2 2\theta' = 4 \sin^2 \theta' \cos^2 \theta' = 1 - (\cos 2\theta \cos 2\psi - \sin 2\theta \sin 2\psi \cos \varphi)^2, \quad (\text{D.14})$$

and we square Eq. (D.11), to have

$$\sin^2 \varphi' = \frac{\tan^2 \varphi'}{1 + \tan^2 \varphi'} = \frac{h^2}{(\sin 2\theta \cos \varphi \cos 2\psi + \cos 2\theta \sin 2\psi)^2 + h^2}. \quad (\text{D.15})$$

Combining these two, we get:

$$\sin^2 2\theta' \sin^2 \varphi' = h^2 \frac{1 - (\cos 2\theta \cos 2\psi - \sin 2\theta \sin 2\psi \cos \varphi)^2}{(\sin 2\theta \cos \varphi \cos 2\psi + \cos 2\theta \sin 2\psi)^2 + h^2} = h^2. \quad (\text{D.16})$$

Because  $\theta'$  and  $\varphi'$  can be regarded as smooth functions of  $\psi$  that reduce to  $\theta$  and  $\varphi$  at  $\psi = 0$  respectively, we can conclude that  $\sin 2\theta' \sin \varphi' = h$ . This completes the proof of Eq. (D.1) for the transverse phase. In other words, the gapless Goldstone mode associated with the symmetry breaking of the relative gauge symmetry is given by a combination of the  $\varphi_0$  mode and a variation of  $\theta$  and  $\varphi$  within the constraint of Eq. (5) in the main text.

A parameter-plot of  $(\theta(\psi), \varphi(\psi), \varphi_0(\psi))$  is given in Fig. 6(a) for a given  $(\theta(0), \varphi(0), \varphi_0(0))$ . The plot takes a form of a helical curve in the  $(\theta, \varphi, \varphi_0)$  space. A projection of the curve onto the  $(\theta, \varphi)$  plane is a circle that is defined by  $\tilde{h} \equiv \sin 2\theta \sin \varphi = h$ . When  $\psi$  changes by  $\pi$ ,  $(\theta, \varphi)$  goes around the circle once and  $\varphi_0$  changes by  $-\pi$ . When  $h = 1$  ( $h = h_c$ ), the circle reduces to a point of  $\theta = \pi/4 + n\pi/2$  and  $\varphi = \pi/2 + n\pi$ , and the helical curve reduces to a straight line of  $\psi = -\varphi_0$ . When  $h = 0$ , the parameter plot of  $(\theta(\psi), \varphi(\psi), \varphi_0(\psi))$  still preserves the periodicity in a trickly way. To see this, we take an initial point at  $\psi = 0$  as  $(\theta, \varphi, \varphi_0) = (0, 0, 0)$ . When  $\psi$  changes from 0 to  $\pi/2$ ,  $(\theta(\psi), \varphi(\psi), \varphi_0(\psi)) = (\psi, 0, 0)$ . At  $\psi = \pi/2$ ,  $\varphi(\psi)$  jumps from 0 to  $\pi$ . When  $\psi$  changes from  $\pi/2$  to  $\pi$ ,  $(\theta(\psi), \varphi(\psi), \varphi_0(\psi)) = (\pi - \psi, \pi, 0)$ . At  $\psi = \pi$ ,  $\varphi(\psi)$  jumps from  $\pi$  to 0, and  $\varphi_0(\psi)$  jumps from 0 to  $-\pi$ . Thus, the periodicity is still true: when  $\psi$  changes by  $\pi$ ,  $\varphi_0$  changes by  $-\pi$ , and  $(\theta, \varphi)$  comes back to the same point.

## E. Derivation of the spin-charge coupled Josephson equations without Rashba interaction

In this section, we derive the spin-charge coupled Josephson equation for the transverse and longitudinal phases. In the main text, we introduced a quantum-dot junction model (Eqs. (10)-(12)). Applying local (time-dependent) gauge transformations in the electron and hole layers, we obtain

$$\mathcal{S}_{\text{mf}} = \int d\tau \sum_{i=1,2} \sum_{\alpha} \left\{ \mathbf{a}_{i\alpha}^\dagger [\partial_\tau + \mathbf{H}_{a\alpha} - \mu] \mathbf{a}_{i\alpha} + \mathbf{b}_{i\alpha}^\dagger [\partial_\tau + \mathbf{H}_{b\alpha} - \mu - i \frac{\eta_i}{2} (V_C + V_S \boldsymbol{\sigma}_x)] \mathbf{b}_{i\alpha} - \vec{\phi}_\lambda(\psi_i, \varphi_{0i}) \cdot \mathbf{a}_{i\alpha}^\dagger \vec{\sigma} \mathbf{b}_{i\alpha} + \text{h.c.} \right\} \quad (\text{E.1})$$

with  $\lambda = yz, 0x$  and  $\eta_1 = -\eta_2 = 1$ . Here  $V_C$  is charge voltage difference between the electron and hole layers respectively, while  $V_S$  is the sum of (difference between) the spin voltage in the electron layer and the spin voltage in the hole layer for the transverse (longitudinal) phase;

$$V_C = V_{Cb} - V_{Ca}, \quad V_S = V_{Sb} \pm V_{Sa}. \quad (\text{E.2})$$

Namely, “+” is for transverse ( $\lambda = yz$ ) and “-” for longitudinal ( $\lambda = 0x$ ). Note that we treat  $V_C$  and  $V_S$  as external fields. The excitonic mean fields in the two regions are identical to each other except for the two gapless U(1) phase variables;

$$\vec{\phi}_\lambda(\psi_i, \varphi_{0i}) \cdot \vec{\sigma} = \vec{\phi}_\lambda(\psi = 0, \varphi_0 = 0) \cdot \vec{\sigma} e^{i\psi_i \pm i\varphi_{0i} \boldsymbol{\sigma}_x} \quad (\text{E.3})$$

with  $\pm$  for  $\lambda = yz, 0x$  respectively. Note that  $V_C$ ,  $V_S$ , and  $\vec{\phi}_\lambda(\psi = 0, \varphi_0 = 0) \equiv \vec{\phi}_\lambda$  are treated as given (e.g. external) static variables, and the gapless U(1) phase variables,  $\psi_i$  and  $\varphi_{0i}$  ( $i = 1, 2$ ), are treated as dynamical variables. In terms of a global gauge transformation in the hole layer,  $e^{i\psi_i \pm i\varphi_{0i} \boldsymbol{\sigma}_x} \mathbf{b}_{i\alpha} \rightarrow \mathbf{b}_{i\alpha}$ , the dependence on the gapless phase variables can be removed from the mean field coupling. After the transformation, the phase variables appear in the tunneling part  $S_T$ ; accordingly, we have

$$\mathcal{S}[\Psi, \Psi^\dagger, \psi_i, \varphi_{0i}; V_C, V_S] \equiv \mathcal{S}_{\text{mf}}[\Psi, \Psi^\dagger, \psi_i, \varphi_{0i}; V_C, V_S] + \mathcal{S}_T[\Psi, \Psi^\dagger, \psi_i, \varphi_{0i}] = \int d\tau \sum_{\alpha\beta} \Psi_\alpha^\dagger (\mathcal{G}^{-1})_{\alpha\beta} \Psi_\beta, \quad (\text{E.4})$$

$$(\mathcal{G}^{-1})_{\alpha\beta} = \begin{pmatrix} \mathbf{G}_{a\alpha}^{-1} \delta_{\alpha\beta} & -\vec{\phi}_\lambda \cdot \vec{\sigma} \delta_{\alpha\beta} & T_{\alpha\beta}^{(a)} & 0 \\ -\vec{\phi}_\lambda^* \cdot \vec{\sigma} \delta_{\alpha\beta} & (\mathbf{G}_{b\alpha}^{-1} + \Delta_1) \delta_{\alpha\beta} & 0 & T_{\alpha\beta}^{(b)} e^{i(\tilde{\psi} \pm \tilde{\varphi}_0 \sigma_x)} \\ T_{\beta\alpha}^{(a)*} & 0 & \mathbf{G}_{a\alpha}^{-1} \delta_{\alpha\beta} & -\vec{\phi}_\lambda \cdot \vec{\sigma} \delta_{\alpha\beta} \\ 0 & T_{\beta\alpha}^{(b)*} e^{-i(\tilde{\psi} \pm \tilde{\varphi}_0 \sigma_x)} & -\vec{\phi}_\lambda^* \cdot \vec{\sigma} \delta_{\alpha\beta} & (\mathbf{G}_{b\alpha}^{-1} + \Delta_2) \delta_{\alpha\beta} \end{pmatrix}, \quad (\text{E.5})$$

where  $\vec{\phi}_\lambda \equiv \vec{\phi}_\lambda(\psi = 0, \varphi_0 = 0)$ ,  $\tilde{\psi} \equiv \psi_1 - \psi_2$ ,  $\tilde{\varphi}_0 \equiv \varphi_{01} - \varphi_{02}$ , and

$$\mathbf{G}_{a\alpha}^{-1} \equiv \partial_\tau + \mathbf{H}_{a\alpha} - \mu, \quad \mathbf{G}_{b\alpha}^{-1} \equiv \partial_\tau + \mathbf{H}_{b\alpha} - \mu, \quad (\text{E.6})$$

$$\Delta_i \equiv -i(\dot{\psi}_i + \eta_i \frac{V_C}{2}) - i(\pm \dot{\varphi}_{0i} + \eta_i \frac{V_S}{2}) \sigma_x, \quad (\text{E.7})$$

with  $\dot{\psi}_i \equiv \partial_\tau \psi_i$  and  $\dot{\varphi}_{0i} \equiv \partial_\tau \varphi_{0i}$  ( $i = 1, 2$ ). The multiple signs in the tunneling matrix element in the hole layer are chosen as “+” for the transverse phase and “-” for the longitudinal phase.  $\Psi_\alpha \equiv (\mathbf{a}_{1\alpha}, \mathbf{b}_{1\alpha}, \mathbf{a}_{2\alpha}, \mathbf{b}_{2\alpha})^T$  is an eight-components vectors with the domain ( $i = 1, 2$ ), the layer ( $a, b$ ), and the spin ( $\uparrow, \downarrow$ ) indices. The phase variables are decomposed into their average parts ( $\bar{\psi} \equiv \frac{\psi_1 + \psi_2}{2}$  and  $\bar{\varphi}_0 \equiv \frac{\varphi_{01} + \varphi_{02}}{2}$ ) and their difference parts ( $\tilde{\psi} \equiv \psi_1 - \psi_2$  and  $\tilde{\varphi}_0 \equiv \varphi_{01} - \varphi_{02}$ ), i.e.

$$\psi_i = \bar{\psi} + \eta_i \frac{\tilde{\psi}}{2}, \quad \varphi_{0i} = \bar{\varphi}_0 + \eta_i \frac{\tilde{\varphi}_0}{2}. \quad (\text{E.8})$$

The difference parts,  $\tilde{\psi}$  and  $\tilde{\varphi}_0$ , together with  $V_C$  and  $V_S$ , are coupled with charge and spin density differences  $N_C$  and  $N_S$  respectively;

$$N_C \equiv \frac{1}{2} \sum_{\alpha} \left[ \mathbf{b}_{1\alpha}^\dagger \mathbf{b}_{1\alpha} - \mathbf{b}_{2\alpha}^\dagger \mathbf{b}_{2\alpha} \right], \quad N_S \equiv \frac{1}{2} \sum_{\alpha} \left[ \mathbf{b}_{1\alpha}^\dagger \sigma_x \mathbf{b}_{1\alpha} - \mathbf{b}_{2\alpha}^\dagger \sigma_x \mathbf{b}_{2\alpha} \right]. \quad (\text{E.9})$$

To see this coupling, we follow a standard procedure and introduce  $N_C$  and  $N_S$  and their canonical conjugate variables  $\mu_C$  and  $\mu_S$ ,

$$\begin{aligned} \mathcal{Z}[V_C, V_S] &\equiv \int \mathcal{D}\psi_i \mathcal{D}\varphi_{0i} \mathcal{D}\Psi^\dagger \mathcal{D}\Psi e^{-\mathcal{S}[\Psi, \Psi^\dagger, \psi_i, \varphi_{0i}; V_C, V_S]} \\ &= \int \mathcal{D}N_C \mathcal{D}N_S \mathcal{D}\psi_i \mathcal{D}\varphi_{0i} \mathcal{D}\Psi^\dagger \mathcal{D}\Psi \delta(N_C - \sum_{i\alpha} \eta_i \mathbf{b}_{i\alpha}^\dagger \mathbf{b}_{i\alpha}/2) \delta(N_S - \sum_{i\alpha} \eta_i \mathbf{b}_{i\alpha}^\dagger \sigma_x \mathbf{b}_{i\alpha}/2) e^{-\mathcal{S}[\Psi, \Psi^\dagger, \psi_i, \varphi_{0i}; V_C, V_S]} \\ &= \int \mathcal{D}\mu_C \mathcal{D}\mu_S \mathcal{D}N_C \mathcal{D}N_S \mathcal{D}\psi_i \mathcal{D}\varphi_{0i} \mathcal{D}\Psi^\dagger \mathcal{D}\Psi e^{i \int d\tau [\mu_C (N_C - \sum_{i\alpha} \eta_i \mathbf{b}_{i\alpha}^\dagger \mathbf{b}_{i\alpha}/2) + \mu_S (N_S - \sum_{i\alpha} \eta_i \mathbf{b}_{i\alpha}^\dagger \sigma_x \mathbf{b}_{i\alpha}/2)] - \mathcal{S}[\Psi, \Psi^\dagger, \psi_i, \varphi_{0i}; V_C, V_S]}, \\ &= \int \mathcal{D}\mu_C \mathcal{D}\mu_S \mathcal{D}N_C \mathcal{D}N_S \mathcal{D}\psi_i \mathcal{D}\varphi_{0i} \mathcal{D}\Psi^\dagger \mathcal{D}\Psi e^{\int d\tau (i\mu_C N_C + i\mu_S N_S) - \mathcal{S}[\Psi, \Psi^\dagger, \psi_i, \varphi_{0i}; V_C + \mu_C, V_S + \mu_S]}, \end{aligned} \quad (\text{E.10})$$

where  $\delta(N_C - \sum_{i\alpha} \eta_i \mathbf{b}_{i\alpha}^\dagger \mathbf{b}_{i\alpha}/2)$  and  $\delta(N_S - \sum_{i\alpha} \eta_i \mathbf{b}_{i\alpha}^\dagger \sigma_x \mathbf{b}_{i\alpha}/2)$  are delta functions defined between real numbers and bilinear Grassmann numbers, whose definition and properties are discussed in Sec. J. An integration over  $\Psi_\alpha$  and  $\Psi_\alpha^\dagger$  leads to an effective action of the dynamical variables,  $\psi_i$ ,  $\varphi_{0i}$ ,  $N_C$ ,  $N_S$ ,  $\mu_C$ , and  $\mu_S$ ,

$$\mathcal{Z}[V_C, V_S] = \int \mathcal{D}\mu_C \mathcal{D}\mu_S \mathcal{D}N_C \mathcal{D}N_S \mathcal{D}\psi_i \mathcal{D}\varphi_{0i} e^{i \int d\tau (\mu_C N_C + \mu_S N_S) + \text{Tr} \ln \mathcal{G}_\mu^{-1}}, \quad (\text{E.11})$$

where the subscript “ $\mu$ ” in  $\mathcal{G}_\mu^{-1}$  represents that  $V_C$  and  $V_S$  in  $\mathcal{G}^{-1}$  in Eq. (E.5) are replaced by  $V_C + \mu_C$  and  $V_S + \mu_S$  in  $\mathcal{G}_\mu^{-1}$ . Tr includes the integral over the time and the summation over single-particle energy-levels as well as a trace of  $8 \times 8$  matrix associated with domain, layer and spin indices. The  $8 \times 8$  matrix-formed  $\mathcal{G}_\mu^{-1}$  can be decomposed into four parts:

$$\mathcal{G}_\mu^{-1} = \tilde{\mathcal{G}}_{\mu 0}^{-1} + \mathcal{T}, \quad \tilde{\mathcal{G}}_{\mu 0}^{-1} = \mathcal{G}_0^{-1} + \Phi + \Delta_\mu, \quad (\text{E.12})$$

$$(\mathcal{G}_0^{-1})_{\alpha\beta} = \delta_{\alpha\beta} \begin{pmatrix} \mathbf{G}_{a\alpha}^{-1} & 0 & 0 & 0 \\ 0 & \mathbf{G}_{b\alpha}^{-1} & 0 & 0 \\ 0 & 0 & \mathbf{G}_{a\alpha}^{-1} & 0 \\ 0 & 0 & 0 & \mathbf{G}_{b\alpha}^{-1} \end{pmatrix}, \quad (\text{E.13})$$

$$\Phi_{\alpha\beta} = \delta_{\alpha\beta} \begin{pmatrix} 0 & -\vec{\phi}_\lambda \cdot \vec{\sigma} & 0 & 0 \\ -\vec{\phi}_\lambda^* \cdot \vec{\sigma} & 0 & 0 & 0 \\ 0 & 0 & 0 & -\vec{\phi}_\lambda \cdot \vec{\sigma} \\ 0 & 0 & -\vec{\phi}_\lambda^* \cdot \vec{\sigma} & 0 \end{pmatrix}, \quad (\text{E.14})$$

$$(\Delta_\mu)_{\alpha\beta} = \delta_{\alpha\beta} \begin{pmatrix} 0 & 0 & 0 & 0 \\ 0 & \Delta_{\mu 1} & 0 & 0 \\ 0 & 0 & 0 & 0 \\ 0 & 0 & 0 & \Delta_{\mu 2} \end{pmatrix}, \quad (\text{E.15})$$

$$\mathcal{T}_{\alpha\beta} = \begin{pmatrix} 0 & 0 & T_{\alpha\beta}^{(a)} & 0 \\ 0 & 0 & 0 & T_{\alpha\beta}^{(b)} e^{i(\tilde{\psi} \pm \tilde{\varphi}_0 \sigma_x)} \\ T_{\beta\alpha}^{(a)*} & 0 & 0 & 0 \\ 0 & T_{\beta\alpha}^{(b)*} e^{-i(\tilde{\psi} \pm \tilde{\varphi}_0 \sigma_x)} & 0 & 0 \end{pmatrix}, \quad (\text{E.16})$$

where

$$\Delta_{\mu i} \equiv -i\left(\dot{\psi}_i + \eta_i \frac{V_C - \mu_C}{2}\right) - i\left(\pm \dot{\varphi}_{0i} + \eta_i \frac{V_S - \mu_S}{2}\right) \sigma_x, \quad (\text{E.17})$$

for  $i = 1, 2$ . As the tunneling matrix elements  $\mathcal{T}$  are small quantities, the effective action can be expanded in  $\mathcal{T}$ :

$$-\text{Trln}\mathcal{G}_\mu^{-1} = -\text{Trln}\tilde{\mathcal{G}}_{\mu 0}^{-1} - \text{Trln}(1 + \tilde{\mathcal{G}}_{\mu 0}\mathcal{T}) = -\text{Trln}\tilde{\mathcal{G}}_{\mu 0}^{-1} + \frac{1}{2}\text{Tr}(\tilde{\mathcal{G}}_{\mu 0}\mathcal{T})^2 + \frac{1}{4}\text{Tr}(\tilde{\mathcal{G}}_{\mu 0}\mathcal{T})^4 + \dots \quad (\text{E.18})$$

In the expansion, only the even-order terms remains, as  $\mathcal{T}$  is off-diagonal in the domain index ( $i = 1, 2$ ).

The couplings between  $N_C, N_S, \partial_\tau \tilde{\psi} + V_C$  and  $\pm \partial_\tau \tilde{\varphi}_0 + V_S$  are encoded in the zeroth-order term in  $\mathcal{T}$  in Eq. (E.18). To see this coupling, we further expand the zero-order term in  $\Delta_\mu$ ,

$$\begin{aligned} -\text{Trln}\tilde{\mathcal{G}}_{\mu 0}^{-1} &= -\text{Trln}(\mathcal{G}_0^{-1} + \Phi) - \text{Trln}[1 + (\mathcal{G}_0^{-1} + \Phi)^{-1}\Delta_\mu)] \\ &= -\text{Trln}(\mathcal{G}_0^{-1} + \Phi) - \text{Tr}[(\mathcal{G}_0^{-1} + \Phi)^{-1}\Delta_\mu] + \frac{1}{2}\text{Tr}[(\mathcal{G}_0^{-1} + \Phi)^{-1}\Delta_\mu(\mathcal{G}_0^{-1} + \Phi)^{-1}\Delta_\mu] + \dots \end{aligned} \quad (\text{E.19})$$

The first term is constant in variables. The second term is proportional to  $\int d\tau (\Delta_{\mu 1}(\tau) + \Delta_{\mu 2}(\tau)) = -2i \int d\tau (\partial_\tau \tilde{\psi} + \partial_\tau \tilde{\varphi}_0)$ , that vanishes after the integral over the time. The third term forms a saddle point in a space of  $\partial_\tau \tilde{\psi}, \partial_\tau \tilde{\varphi}_0, \partial_\tau \tilde{\psi} + V_C - \mu_C$ , and  $\pm \partial_\tau \tilde{\varphi}_0 + V_S - \mu_S$ ,

$$\begin{aligned} \text{Tr}[(\mathcal{G}_0^{-1} + \Phi)^{-1}\Delta_\mu(\mathcal{G}_0^{-1} + \Phi)^{-1}\Delta_\mu] &= \\ &\int \int d\tau_1 d\tau_2 \chi_{00}(\tau_1 - \tau_2) \left( (\dot{\tilde{\psi}})_{\tau_1} (\dot{\tilde{\psi}})_{\tau_2} + \frac{1}{4} (\dot{\tilde{\psi}} + V_C - \mu_C)_{\tau_1} (\dot{\tilde{\psi}} + V_C - \mu_C)_{\tau_2} \right) \\ &+ \int \int d\tau_1 d\tau_2 \chi_{xx}(\tau_1 - \tau_2) \left( (\dot{\tilde{\varphi}}_0)_{\tau_1} (\dot{\tilde{\varphi}}_0)_{\tau_2} + \frac{1}{4} (\pm \dot{\tilde{\varphi}}_0 + V_S - \mu_S)_{\tau_1} (\pm \dot{\tilde{\varphi}}_0 + V_S - \mu_S)_{\tau_2} \right) \\ &+ \int \int d\tau_1 d\tau_2 \chi_{0x}(\tau_1 - \tau_2) \left( (\dot{\tilde{\psi}})_{\tau_1} (\dot{\tilde{\varphi}}_0)_{\tau_2} + \frac{1}{4} (\dot{\tilde{\psi}} + V_C - \mu_C)_{\tau_1} (\pm \dot{\tilde{\varphi}}_0 + V_S - \mu_S)_{\tau_2} \right) \\ &+ \int \int d\tau_1 d\tau_2 \chi_{x0}(\tau_1 - \tau_2) \left( (\dot{\tilde{\varphi}}_0)_{\tau_1} (\dot{\tilde{\psi}})_{\tau_2} + \frac{1}{4} (\pm \dot{\tilde{\varphi}}_0 + V_S - \mu_S)_{\tau_1} (\dot{\tilde{\psi}} + V_C - \mu_C)_{\tau_2} \right). \end{aligned} \quad (\text{E.20})$$

As the higher-order expansion terms in Eq. (E.19) do not change this saddle-point structure, we can fairly conclude that  $-\text{Trln}\tilde{\mathcal{G}}_{\mu 0}^{-1}$  has the following saddle point,

$$-\mu_C + \dot{\tilde{\psi}} + V_C = 0, \quad -\mu_S \pm \dot{\tilde{\varphi}}_0 + V_S = 0, \quad \dot{\tilde{\psi}} = 0, \quad \dot{\tilde{\varphi}}_0 = 0. \quad (\text{E.21})$$

Due to a term of  $\mu_C N_C + \mu_S N_S$  in the action, the saddle point of the whole action in Eq. (E.11) is deviated from Eq. (E.21) by  $\mathcal{O}(N_C, N_S)$ . Given  $N_C(0) = N_S(0) = 0$ , however, the deviation is on the order  $\mathcal{O}(\mathcal{T}^2)$ , so that the correction term results in higher-order effects in Josephson equations and we can ignore them legitimately.

Then an integration over  $\mu_C$ ,  $\mu_S$ ,  $\tilde{\psi}$  and  $\tilde{\varphi}_0$  in Eq. (E.11) under the saddle-point approximation leads to the following effective action for  $\tilde{\psi}$ ,  $\tilde{\varphi}_0$ ,  $N_C$  and  $N_S$ ;

$$\mathcal{Z}[V_C, V_S] = \int \mathcal{D}N_C \mathcal{D}N_S \mathcal{D}\tilde{\psi} \mathcal{D}\tilde{\varphi}_0 e^{i \int d\tau [N_C(\tilde{\psi} + V_C) + N_S(\pm \tilde{\varphi}_0 + V_S)] - \frac{1}{2} \text{Tr}[(\mathcal{G}_0^{-1} + \Phi)^{-1} \mathcal{T})^2] - \frac{1}{4} \text{Tr}[(\mathcal{G}_0^{-1} + \Phi)^{-1} \mathcal{T})^4] + \dots}, \quad (\text{E.22})$$

where  $\mu_C$  and  $\mu_S$  in Eq. (E.11) were replaced by  $\partial_\tau \tilde{\psi} + V_C$  and  $\pm \partial_\tau \tilde{\psi} + V_S$  respectively, and  $\tilde{\mathcal{G}}_{\mu 0}^{-1}$  in Eq. (E.18) was replaced by  $\mathcal{G}_0^{-1} + \Phi$ . In Eq. (E.22), one can clearly see that  $\partial_\tau \tilde{\psi} + V_C$  and  $\partial_\tau \tilde{\varphi}_0 + V_S$  are coupled only with  $N_C$  and  $N_S$  respectively. The couplings result in the second Josephson equations.

The first Josephson equation comes from the the second-order term in the tunneling part,  $\mathcal{T}$  in Eq. (E.18), which can be further expanded in  $\Phi$ ;

$$\begin{aligned} \frac{1}{2} \text{Tr}(\tilde{\mathcal{G}}_{\mu 0} \mathcal{T})^2 &= \frac{1}{2} \text{Tr}[(\mathcal{G}_0^{-1} + \Phi)^{-1} \mathcal{T}(\mathcal{G}_0^{-1} + \Phi)^{-1} \mathcal{T}] \\ &= \frac{1}{2} \text{Tr}[(\mathcal{G}_0 - \mathcal{G}_0 \Phi \mathcal{G}_0 + (\mathcal{G}_0 \Phi)^2 \mathcal{G}_0 - (\mathcal{G}_0 \Phi)^3 \mathcal{G}_0 + \dots) \mathcal{T}(\mathcal{G}_0 - \mathcal{G}_0 \Phi \mathcal{G}_0 + (\mathcal{G}_0 \Phi)^2 \mathcal{G}_0 - (\mathcal{G}_0 \Phi)^3 \mathcal{G}_0 + \dots) \mathcal{T}] \\ &= \frac{1}{2} \text{Tr} \mathcal{G}_0 \mathcal{T} \mathcal{G}_0 \mathcal{T} + \text{Tr} \mathcal{G}_0 \Phi \mathcal{G}_0 \Phi \mathcal{G}_0 \mathcal{T} \mathcal{G}_0 \mathcal{T} + \frac{1}{2} \text{Tr} \mathcal{G}_0 \Phi \mathcal{G}_0 \mathcal{T} \mathcal{G}_0 \Phi \mathcal{G}_0 \mathcal{T} + \dots \end{aligned} \quad (\text{E.23})$$

The first two terms do not depend on  $\tilde{\psi}$  and  $\tilde{\varphi}_0$ , when dissipation effect is neglected from the Josephson equation. Namely,  $\mathbf{G}_b^{-1}$  commutes with  $\boldsymbol{\sigma}_x$  and the dissipation effect comes from the time-dependence of  $\psi$  and  $\tilde{\varphi}_0$ . The (dissipationless) Josephson equation comes from the third term in the right hand side, in which the spin-charge coupled nature of the Josephson equations are encoded;

$$\begin{aligned} &\text{Tr}[(\mathcal{G}_0 \Phi)(\mathcal{G}_0 \mathcal{T})(\mathcal{G}_0 \Phi)(\mathcal{G}_0 \mathcal{T})] \\ &= \text{tr}[\mathbf{G}_{a\alpha}(\vec{\phi}_\lambda \cdot \vec{\sigma}) \mathbf{G}_{b\alpha} T_{\alpha\beta}^{(b)} e^{i(\tilde{\psi} \pm \tilde{\varphi}_0 \boldsymbol{\sigma}_x)} \mathbf{G}_{b\beta}(\vec{\phi}_\lambda^* \cdot \vec{\sigma}) \mathbf{G}_{a\beta} T_{\alpha\beta}^{(a)*}] + \text{Tr}[\mathbf{G}_{b\alpha}(\vec{\phi}_\lambda^* \cdot \vec{\sigma}) \mathbf{G}_{a\alpha} T_{\alpha\beta}^{(a)} \mathbf{G}_{a\beta}(\vec{\phi}_\lambda \cdot \vec{\sigma}) \mathbf{G}_{b\beta} T_{\alpha\beta}^{(b)*} e^{-i(\tilde{\psi} \pm \tilde{\varphi}_0 \boldsymbol{\sigma}_x)}] \\ &+ \text{Tr}[\mathbf{G}_{a\alpha}(\vec{\phi}_\lambda \cdot \vec{\sigma}) \mathbf{G}_{b\alpha} T_{\beta\alpha}^{(b)*} e^{-i(\tilde{\psi} \pm \tilde{\varphi}_0 \boldsymbol{\sigma}_x)} \mathbf{G}_{b\beta}(\vec{\phi}_\lambda^* \cdot \vec{\sigma}) \mathbf{G}_{a\beta} T_{\beta\alpha}^{(a)}] + \text{Tr}[\mathbf{G}_{b\alpha}(\vec{\phi}_\lambda^* \cdot \vec{\sigma}) \mathbf{G}_{a\alpha} T_{\beta\alpha}^{(a)*} \mathbf{G}_{a\beta}(\vec{\phi}_\lambda \cdot \vec{\sigma}) \mathbf{G}_{b\beta} T_{\beta\alpha}^{(b)} e^{i(\tilde{\psi} \pm \tilde{\varphi}_0 \boldsymbol{\sigma}_x)}] \\ &= 2 T_{\beta\alpha}^{(b)} T_{\beta\alpha}^{(a)*} \text{Tr}[(\vec{\phi}_\lambda \cdot \vec{\sigma}) e^{-i(\tilde{\psi} \pm \tilde{\varphi}_0 \boldsymbol{\sigma}_x)} (\vec{\phi}_\lambda^* \cdot \vec{\sigma}) \bar{\mathbf{G}}_{b\alpha} \mathbf{G}_{a\alpha} \mathbf{G}_{a\beta} \bar{\mathbf{G}}_{b\beta}] + \text{c.c.} \end{aligned} \quad (\text{E.24})$$

Here  $\mathbf{G}_{ca}^{-1} \equiv \partial_\tau + E_{ca} \boldsymbol{\sigma}_0 + H \boldsymbol{\sigma}_x - \mu$  and  $\bar{\mathbf{G}}_{ca}^{-1} \equiv \partial_\tau + E_{ca} \boldsymbol{\sigma}_0 \mp H \boldsymbol{\sigma}_x - \mu$  for  $c = a, b$ , and the upper and lower signs of the multiple sign are for the transvere ( $\lambda = yz$ ) and longitudinal ( $\lambda = 0x$ ) phases respectively. In Eq. (E.24), a product between two tunneling matrix element picks up an external magnetic flux  $\Psi$  that penetrates through the junction area in the transversal direction;

$$T_{\beta\alpha}^{(b)} T_{\beta\alpha}^{(a)*} = |T_{\beta\alpha}|^2 e^{i\Psi}. \quad (\text{E.25})$$

Using Eq. (E.25) together with  $\bar{\mathbf{G}}_{b\beta} \mathbf{G}_{a\beta} \mathbf{G}_{a\alpha} \bar{\mathbf{G}}_{b\alpha} = \bar{\mathbf{G}}_{b\alpha} \mathbf{G}_{a\alpha} \mathbf{G}_{a\beta} \bar{\mathbf{G}}_{b\beta}$ , we obtain a tunneling term  $\mathcal{S}_{\text{tun}}$  in the effective action as;

$$\begin{aligned} \mathcal{S}_{\text{tun}} &\equiv \frac{1}{2} \text{Tr}[(\mathcal{G}_0 \Phi)(\mathcal{G}_0 \mathcal{T})(\mathcal{G}_0 \Phi)(\mathcal{G}_0 \mathcal{T})] \\ &= 2 |T_{\beta\alpha}|^2 \text{Tr}[(\vec{\phi}_\lambda \cdot \vec{\sigma})(\cos(\tilde{\psi} - \Psi) \cos \tilde{\varphi}_0 \mp \sin(\tilde{\psi} - \Psi) \sin \tilde{\varphi}_0 \boldsymbol{\sigma}_x)(\vec{\phi}_\lambda^* \cdot \vec{\sigma}) \bar{\mathbf{G}}_{b\alpha} \mathbf{G}_{a\alpha} \mathbf{G}_{a\beta} \bar{\mathbf{G}}_{b\beta}]. \end{aligned} \quad (\text{E.26})$$

Note that

$$\begin{aligned} &(\vec{\phi}_\lambda \cdot \vec{\sigma})(\cos(\tilde{\psi} - \Psi) \cos \tilde{\varphi}_0 \mp \sin(\tilde{\psi} - \Psi) \sin \tilde{\varphi}_0 \boldsymbol{\sigma}_x)(\vec{\phi}_\lambda^* \cdot \vec{\sigma}) \\ &= (\vec{\phi}_\lambda \cdot \vec{\sigma})(\vec{\phi}_\lambda^* \cdot \vec{\sigma})(\cos(\tilde{\psi} - \Psi) \cos \tilde{\varphi}_0 + \sin(\tilde{\psi} - \Psi) \sin \tilde{\varphi}_0 \boldsymbol{\sigma}_x) \\ &= (\boldsymbol{\sigma}_0 + \tilde{h} \boldsymbol{\sigma}_x) \left( \cos(\tilde{\psi}(\tau) - \Psi) \cos(\tilde{\varphi}_0(\tau)) + \sin(\tilde{\psi}(\tau) - \Psi) \sin(\tilde{\varphi}_0(\tau)) \boldsymbol{\sigma}_x \right) \equiv \mathcal{F}_\lambda(\tau), \end{aligned} \quad (\text{E.27})$$

where  $\tilde{h} = h \equiv h/h_c$  for  $\lambda = yz$  and  $\tilde{h} = \hbar \equiv -h'/h_c$  for  $\lambda = 0x$ . Since we do not include the dissipation effect in the Josephson equation, we take the zero Matsubara frequency component of  $\mathcal{F}_\lambda(\tau)$ . This leads to

$$\mathcal{S}_{\text{tun}} = \int d\tau \text{tr}[\mathcal{F}_\lambda(\tau) \sum_{\alpha, \beta} 2 |T_{\beta\alpha}|^2 \frac{1}{\beta} \sum_{i\omega_n} \bar{\mathbf{G}}_{b\alpha}(i\omega_n) \mathbf{G}_{a\alpha}(i\omega_n) \mathbf{G}_{a\beta}(i\omega_n) \bar{\mathbf{G}}_{b\beta}(i\omega_n)] \equiv \int d\tau \text{tr}[\mathcal{F}_\lambda(\tau) \mathcal{G}], \quad (\text{E.28})$$

where  $\text{tr}$  is an trace of 2 by 2 matrices associated with the spin index. A 2 by 2 matrix  $\mathcal{G}$  can be evaluated up to the first order in the exchange field,

$$\begin{aligned}\mathcal{G} &= \frac{1}{\beta} \sum_{i\omega_n} \sum_{\alpha, \beta} 2|T_{\beta\alpha}|^2 g_{b\alpha} (1 \pm g_{b\alpha} H \boldsymbol{\sigma}_x) g_{a\alpha} (1 - g_{a\alpha} H \boldsymbol{\sigma}_x) g_{a\beta} (1 - g_{a\beta} H \boldsymbol{\sigma}_x) g_{b\beta} (1 \pm g_{b\beta} H \boldsymbol{\sigma}_x) + \mathcal{O}(H^2), \\ &= \frac{1}{\beta} \sum_{i\omega_n} \sum_{\alpha, \beta} g_{a\alpha} g_{b\alpha} g_{a\beta} g_{b\beta} |T_{\beta\alpha}|^2 - \frac{H\boldsymbol{\sigma}_x}{\beta} \sum_{i\omega_n} \sum_{\alpha, \beta} (g_{a\alpha} \mp g_{b\alpha} + g_{a\beta} \mp g_{b\beta}) g_{a\alpha} g_{b\alpha} g_{a\beta} g_{b\beta} |T_{\beta\alpha}|^2 + \mathcal{O}(H^2), \\ &\equiv A_0 \boldsymbol{\sigma}_0 + A_x \hbar \boldsymbol{\sigma}_x + \mathcal{O}(H^2),\end{aligned}\quad (\text{E.29})$$

with

$$A_0 \equiv \frac{1}{\beta} \sum_{i\omega_n} \sum_{\alpha, \beta} g_{a\alpha} g_{b\alpha} g_{a\beta} g_{b\beta} |T_{\beta\alpha}|^2, \quad A_x \equiv -\frac{1}{\hbar} \frac{H}{\beta} \sum_{i\omega_n} \sum_{\alpha, \beta} (g_{a\alpha} \mp g_{b\alpha} + g_{a\beta} \mp g_{b\beta}) g_{a\alpha} g_{b\alpha} g_{a\beta} g_{b\beta} |T_{\beta\alpha}|^2. \quad (\text{E.30})$$

Substituting Eqs. (E.29, E.27) into Eq. (E.28), we obtain the following spin-charge coupled potential term from the second order expansion in  $\mathcal{T}$ :

$$\mathcal{S}_{\text{tun}} = \int d\tau \text{tr}[\mathcal{F}(\tau) (A_0 + A_x \hbar \boldsymbol{\sigma}_x)] = -I_0 \int d\tau \left( \cos(\tilde{\psi}(\tau) - \Psi) \cos(\tilde{\varphi}_0(\tau)) + \bar{h} \sin(\tilde{\psi}(\tau) - \Psi) \sin(\tilde{\varphi}_0(\tau)) \right), \quad (\text{E.31})$$

with

$$I_0 \equiv -\rho^2 A_0, \quad \bar{h} \equiv \hbar (1 + \frac{A_x}{A_0}). \quad (\text{E.32})$$

Substituting Eq. (E.31) into Eq. (E.22), we finally obtain the effective action for  $N_C$ ,  $N_S$ ,  $\tilde{\psi}$  and  $\tilde{\varphi}_0$ :

$$\begin{aligned}\mathcal{S}_{\text{eff}}[\tilde{\psi}, \tilde{\varphi}_0, N_C, N_S; V_C, V_S] &= \int d\tau \left[ iN_C (-\hbar \dot{\tilde{\psi}} - eV_C) + iN_S (\mp \hbar \dot{\tilde{\varphi}}_0 - eV_S) \right. \\ &\quad \left. - \hbar I_0 \left( \cos(\tilde{\psi}(\tau) - \frac{e}{\hbar c} \Psi) \cos(\tilde{\varphi}_0(\tau)) + \bar{h} \sin(\tilde{\psi}(\tau) - \frac{e}{\hbar c} \Psi) \sin(\tilde{\varphi}_0(\tau)) \right) \right],\end{aligned}\quad (\text{E.33})$$

where we recover  $\hbar$  as base unit of the action, unit charge  $e$  in front of  $V_C$  and  $V_S$ , and the inverse of magnetic flux unit  $e/\hbar c$ . A variation of the effective action with respect to these variables lead to the spin-charge coupled Josephson equations:

$$\dot{\tilde{\psi}} = -\frac{e}{\hbar} V_C, \quad \dot{\tilde{\varphi}}_0 = \mp \frac{e}{\hbar} V_S, \quad (\text{E.34})$$

$$\dot{N}_C = iI_0 \left( \sin(\tilde{\psi} - \frac{e}{\hbar c} \Psi) \cos(\tilde{\varphi}_0) - \bar{h} \cos(\tilde{\psi} - \frac{e}{\hbar c} \Psi) \sin(\tilde{\varphi}_0) \right), \quad (\text{E.35})$$

$$\dot{N}_S = \pm iI_0 \left( \sin(\tilde{\varphi}_0) \cos(\tilde{\psi} - \frac{e}{\hbar c} \Psi) - \bar{h} \cos(\tilde{\varphi}_0) \sin(\tilde{\psi} - \frac{e}{\hbar c} \Psi) \right). \quad (\text{E.36})$$

Under the Wick rotation from the imaginary time to the real time,

$$\tau = it, \quad I_C = (-e)(-\partial_t N_C) = ie\dot{N}_C, \quad I_S = (-e)(-\partial_t N_S) = ie\dot{N}_S, \quad (\text{E.37})$$

we obtain

$$I_C = -eI_0 \left( \sin(\tilde{\psi} - \frac{e}{\hbar c} \Psi) \cos(\tilde{\varphi}_0) - \bar{h} \cos(\tilde{\psi} - \frac{e}{\hbar c} \Psi) \sin(\tilde{\varphi}_0) \right), \quad (\text{E.38})$$

$$I_S = \mp eI_0 \left( \sin(\tilde{\varphi}_0) \cos(\tilde{\psi} - \frac{e}{\hbar c} \Psi) - \bar{h} \cos(\tilde{\varphi}_0) \sin(\tilde{\psi} - \frac{e}{\hbar c} \Psi) \right), \quad (\text{E.39})$$

$$\frac{d\tilde{\psi}}{dt} = -\frac{e}{\hbar} V_C, \quad \frac{d\tilde{\varphi}_0}{dt} = \mp \frac{e}{\hbar} V_S. \quad (\text{E.40})$$

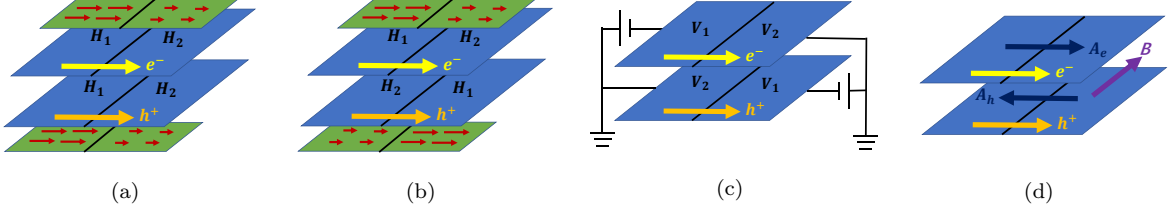


FIG. 7. Four ways to induce the counterflow charge Josephson currents. (a) By a spin voltage across the junction,  $V_S = V_{Sb} + V_{Sa}$  in the transverse phase. (b) By a spin voltage across the junction,  $V_S = V_{Sb} - V_{Sa}$  in the longitudinal phase. (c) By a charge voltage across the junction,  $V_C = V_{Cb} - V_{Ca}$ . (d) By the transverse magnetic flux through the junction,  $\Psi$ .

Note that  $V_C$  and  $V_S$  in Eqs. (E.34) should be multiplied by  $i$  to have the conventional voltages (see Eqs. (11) in the main text and Eq. (E.1)).  $I_C$  and  $I_S$  are the charge and spin currents in the hole layer. The charge current in the electron layer must be along in the opposite direction to that in the hole layer,

$$I_C^{(a)} = -I_C^{(b)} = -I_C. \quad (\text{E.41})$$

The spin current  $I_S$  is defined as a difference between the charge current of the hole layer with up spin (along  $+x$ ) and the charge current of the hole layer with down spin,

$$I_S = e\partial_t N_S = \frac{\partial}{\partial t} \left\langle \frac{e}{2} \sum_{\alpha} (\mathbf{b}_{1\alpha}^\dagger \boldsymbol{\sigma}_x \mathbf{b}_{1\alpha} - \mathbf{b}_{2\alpha}^\dagger \boldsymbol{\sigma}_x \mathbf{b}_{2\alpha}) \right\rangle. \quad (\text{E.42})$$

Thus,  $I_S$  is always equal to the  $+x$ -component spin current in the hole layer, i.e.  $I_S = I_S^{(b)}$ . The  $+x$ -component spin current in the electron layer can have the same sign as or opposite sign to  $I_S$ , depending on whether the pseudospin superfluid phase is either the transverse phase or the longitudinal phase. The transverse phase breaks the continuous symmetry of the spin rotation that rotates spin in the electron layer and spin in the hole layer in the same direction around the  $x$  axis in the spin space. Accordingly,

$$I_S^{(a)} = I_S^{(b)} = I_S, \quad (\text{E.43})$$

for the transverse phase. The longitudinal phase breaks the continuous symmetry of the spin rotation that rotates spin in the electron layer and spin in the hole layer in the opposite direction around the  $x$  axis. Thus,

$$-I_S^{(a)} = I_S^{(b)} = I_S, \quad (\text{E.44})$$

for the longitudinal phase. Eqs. (E.43, E.44) are consistent with our intuition. Namely, the electron with spin polarized along  $+x$  and the hole with spin polarized along  $\mp x$  form a excitonic pairing in the transverse/longitudinal phases, where  $I_S^{(b)}$  must have the same sign as / opposite sign to  $I_S^{(a)}$  respectively. In conclusion, we obtain Eqs. (13,14,15) in the main text from Eqs. (E.38, E.39, E.40, E.43, E.44).

Suppose that charge or spin voltages are applied across the two dots in the both electron and hole layers. Then, we can decompose the charge and spin voltages,  $V_{Ca}$ ,  $V_{Cb}$ ,  $V_{Sa}$ , and  $V_{Sb}$ , into the two components,  $V_{Ca} \pm V_{Cb}$  and  $V_{Sa} \pm V_{Sb}$ . According to Eq. (E.2), only one out of the two induces the AC Josephson currents. We summarize these voltage components in Fig. 7.

#### F. Solutions of the spin-charge coupled Josephson equations: $V_S$ - $I_C$ conversion

In this section, we solve the spin-charge coupled Josephson equations under a particular physical circumstance depicted in Fig. 2(a) of the main text. Thereby, the electron layer is externally connected to a closed electric circuit with an electric resistance  $R_a$ , and the hole layer is connected to another external circuit with an electric resistance  $R_b$ . An exchange field is induced in the hole layer through a magnetic proximity effect. By using a spatial variation of the exchange field, we apply a spin voltage across the junction between two domains;  $V_{Sb} \neq 0$ ,  $V_{Sa} = 0$ . According to the Josephson equations, the spin voltage results in a linear increase of  $\dot{\varphi}_0$  in time, which leads to both AC charge supercurrent  $I_C$  and AC spin supercurrent  $I_S$ . Leads in the external circuits do not conserve spin angular momenta

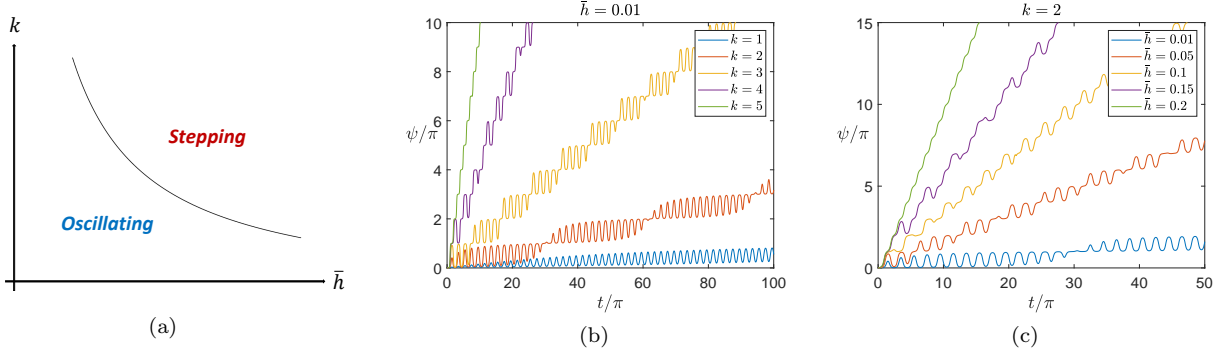


FIG. 8. (a) Schematic crossover diagram of a solution of Eq. (F.3) in favor for  $\psi(t)$ . In a ‘oscillating region’ ( $k\bar{h} \ll 1$ ),  $\psi(t)$  comprises of two oscillations with short periodicity  $T_1 = 2\pi$  and a longer periodicity  $T_2 = \mathcal{O}(\pi/(k\bar{h}))$ . In a ‘stepping region’ ( $k\bar{h} \geq 1$ ),  $\psi(t)$  takes a constant value of  $n\pi$  around  $t = n\pi$  and  $\psi(t)$  increases abruptly from  $n\pi$  to  $(n+1)\pi$  around  $t = (2n+1)\pi/2$ . (b,c) A crossover from the oscillating region to the stepping region.

in general. Thus, the spin component of the supercurrents injected into the external circuits shall decay quickly and it has no significant impact on the spin voltage. In this respect, we can assume that the spin voltage is determined only by the static exchange field by the proximity effect.  $V_S = V_{Sb} \pm V_{Sa}$  thus given is constant in time. On the one hand, the charge component of the supercurrents induce an AC charge voltages in both electron and hole layers;  $V_{Ca} = I_C^{(a)} R_a$  and  $V_{Cb} = I_C^{(b)} R_b$ . From  $V_C = V_{Cb} - V_{Ca}$  and  $I_C^{(a)} = -I_C^{(b)} = -I_C$ , Eqs. (E.38,E.40) lead to a closed equation of motion for  $\tilde{\psi}(t)$ ,

$$\frac{d\tilde{\psi}}{dt} = -I_0 R \left( \sin(\tilde{\psi}) \cos(\mp V_S t) - \bar{h} \cos(\tilde{\psi}) \sin(\mp V_S t) \right), \quad (\text{F.1})$$

with  $R \equiv R_a + R_b$ . With rescaling of the relevant variables,

$$V_S t \equiv s, \quad k \equiv \frac{I_0 R}{V_s}, \quad (\text{F.2})$$

we have

$$\frac{d\tilde{\psi}}{ds} = -k \left( \sin(\tilde{\psi}) \cos(s) \pm \bar{h} \cos(\tilde{\psi}) \sin(s) \right). \quad (\text{F.3})$$

In this section, we will describe (numerical) solution of this non-linear differential equation in favor for  $\tilde{\psi}(s)$ . Without loss of generality, we take the minus sign, i.e. the longitudinal phase (Eq. (B.13)) in Eq. (F.3), and  $k$  and  $\bar{h}$  can be assumed to be positive.  $\bar{h} \equiv h(1 + A_x/A_0)$  is supposed to be much small than 1;  $|h| \equiv |h'/h_c| \ll 1$  and  $A_x/A_0 = \mathcal{O}(1)$ . Thus, we discuss the solution only in a region of  $0 \leq \bar{h} \ll 1$ . For simplicity, we remove the tilde from  $\tilde{\psi}(s)$  and call  $s$  as  $t$ ,  $\tilde{\psi}(s) \rightarrow \psi(t)$ .

When  $\bar{h} = 0$ , the solution is oscillatory in time with  $2\pi$  periodicity ( $T_1 = 2\pi$ );

$$\frac{\psi(t)}{2} = \arctan \left( \tan \left( \frac{\psi(0)}{2} \right) e^{-k \sin(t)} \right). \quad (\text{F.4})$$

The solution respects a time-reversal symmetry  $\psi(\pi - t) = \psi(t)$ . The amplitude of the oscillation gets larger for larger  $k$ , while it is always bounded by  $\pi$ ;  $\psi(t)$  is in the same branch of the arctan function of Eq. (F.4). A finite  $\bar{h}$  breaks the time-reversal symmetry, and the solution acquires a  $t$ -asymmetric component that increases linearly in time  $t$ . The form of the differential equation indicates that the  $t$ -asymmetric component must be scaled by  $k\bar{h}t$  for  $k\bar{h} \ll 1$ ; without loss of generality, we take  $\psi(0) = 0$ , such that  $\langle \psi(t) \rangle \sim k\bar{h}t$ , where  $\langle \psi(t) \rangle$  is an average of  $\psi(t)$  over a time scale much longer than  $T_1$  and much shorter than  $1/(k\bar{h})$ .  $\langle \psi(t) \rangle$  modifies the short-periodicity ( $T_1$ ) oscillating amplitude by the factor  $\sin(\psi)$  in front of  $\cos(t)$ . Overall behaviours of numerical solutions are consistent with this indication (see Fig. 9). Due to the  $t$ -asymmetric component, the solution with finite  $\bar{h}$  with  $k\bar{h} \ll 1$  comprises of two oscillations: one with the shorter periodicity  $T_1 = 2\pi$ , and the other with a longer periodicity,  $T_2 = \mathcal{O}(\pi/(k\bar{h}))$  (Figs. 9,10).

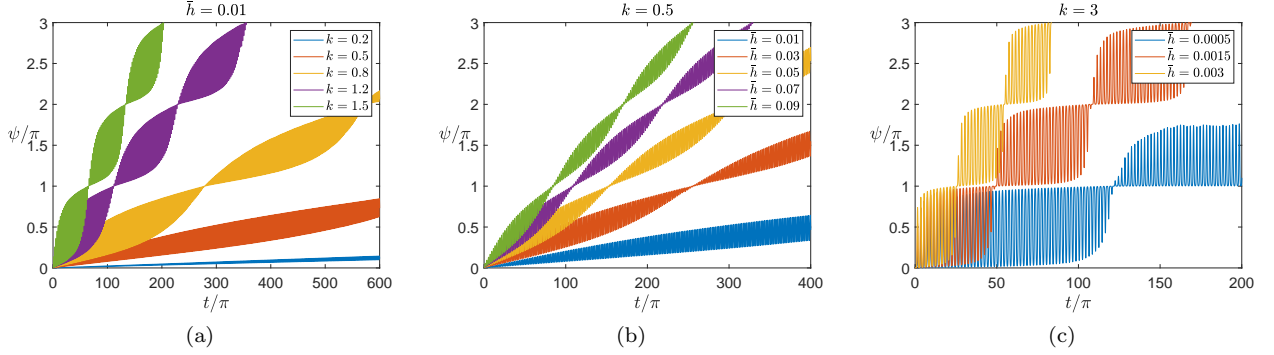


FIG. 9.  $\psi(t)$  in the oscillating region in a longer time scale.  $\psi(t)$  comprises of two oscillations with a short periodicity and a longer periodicity. The short periodicity is  $T_1 = 2\pi$  (see Fig. 10), while the longer periodicity changes with  $kh$ .

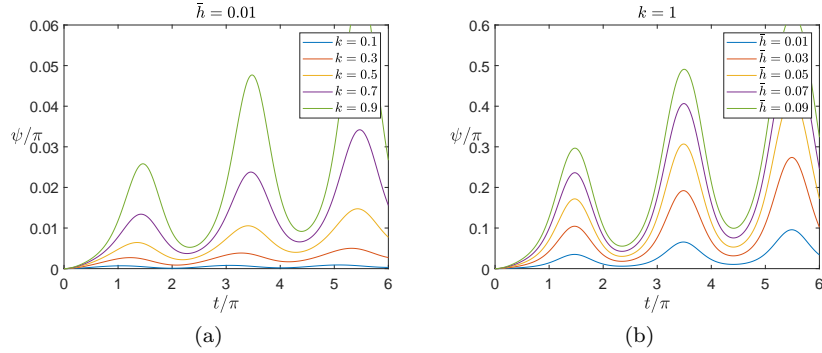


FIG. 10.  $\psi(t)$  in the oscillating region in a shorter time scale. The short periodicity  $T_1$  is around  $2\pi$ .

When  $k\bar{h} \ll 1$ , the two oscillations are clearly distinguishable ('oscillating region'). When  $k\bar{h} = \mathcal{O}(1)$ , the two periodicities become on the same order and the solution shows a crossover from the oscillating region to a 'stepping region' (Figs. 8(b), 8(c)). When  $k \gg k\bar{h} > 1$ , the solution converges into the stepping behavior, where  $\psi(t)$  shows a plateau ( $\psi(t) = n\pi$ ) around  $t = n\pi$ , and  $\psi(t)$  increases abruptly from  $n\pi$  to  $(n+1)\pi$  around  $t = (2n+1)\pi/2$  (Fig. 11).

#### G. Derivation of classical ground-state phase diagram with Rashba interaction

In this section, we describe the minimization of the Lagrangian in the presence of the antisymmetric vector-product (AVP) type interaction ( $D \neq 0$ ), Eq. (A.14). In the absence of the AVP type interaction ( $D = 0$ ), the classical Lagrangian is minimized by spatial uniform configurations of  $\vec{\Phi}'(\vec{r})$  and  $\vec{\Phi}''(\vec{r})$ . To discuss the minimization in the presence of the AVP type interaction, let us decompose these four-component vectors into their amplitude parts ( $\Phi'(\vec{r})$  and  $\Phi''(\vec{r})$ ) and four-component unit vector parts ( $\vec{\psi}'(\vec{r})$  and  $\vec{\psi}''(\vec{r})$ );  $\vec{\Phi}'(\vec{r}) \equiv \Phi'(\vec{r})\vec{\psi}'(\vec{r})$  and  $\vec{\Phi}''(\vec{r}) \equiv \Phi''(\vec{r})\vec{\psi}''(\vec{r})$ . Spatial gradients of the amplitude parts do not lower the AVP type interaction energy because of its anti-symmetric form, e.g.

$$D[(\Phi'\psi'_z)\partial_x(\Phi'\psi'_x) - (\Phi'\psi'_x)\partial_x(\Phi'\psi'_z)] = D(\Phi')^2[\psi'_z\partial_x(\psi'_x) - \psi'_x\partial_x(\psi'_z)]. \quad (\text{G.1})$$

Thus, we take the amplitude parts to be spatially uniform,  $\vec{\Phi}'(\vec{r}) \equiv \Phi'\vec{\psi}'(\vec{r})$  and  $\vec{\Phi}''(\vec{r}) \equiv \Phi''\vec{\psi}''(\vec{r})$ .

The classical Lagrangian of Eq. (A.14) consists of three parts:

$$\frac{S}{\beta} = S_0[\vec{\Phi}', \vec{\Phi}'] + S_1[\vec{\Phi}'] + S_1[\vec{\Phi}'''] \equiv \int d^2\vec{r}[\mathcal{L}_0(\vec{\Phi}', \vec{\Phi}'') + \mathcal{L}_1(\vec{\Phi}', \partial_i\vec{\Phi}') + \mathcal{L}_1(\vec{\Phi}'', \partial_i\vec{\Phi}'')]. \quad (i = x, y) \quad (\text{G.2})$$

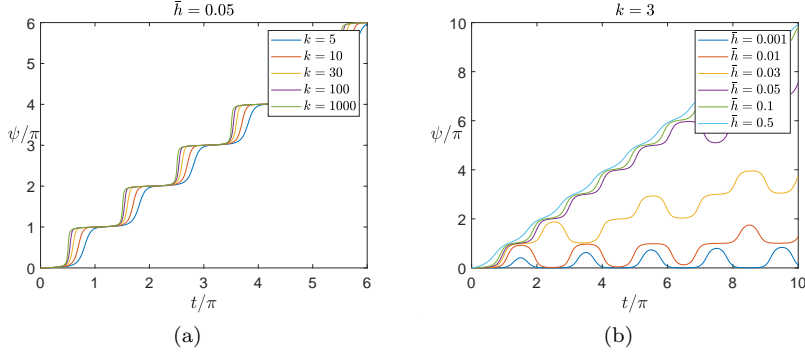


FIG. 11. (a)  $\psi(t)$  in the stepping region.  $\psi(t)$  takes a constant value of  $n\pi$  around  $t = n\pi$ , while it changes abruptly from  $n\pi$  to  $(n+1)\pi$  around  $t = (2n+1)\pi/2$ . (b)  $\psi(t)$  in the stepping region ( $\bar{h} = 0.5, 0.1, 0.05$ ), in the crossover region ( $\bar{h} = 0.03$ ) and in the oscillating region ( $\bar{h} = 0.01, 0.001$ ).

The first part describes a coupling between  $\vec{\Phi}'(\vec{r})$  and  $\vec{\Phi}''(\vec{r})$ . It is free from the spatial gradients of the fields,

$$S_0[\vec{\Phi}', \vec{\Phi}'] \equiv \int d^2\vec{r} \mathcal{L}_0(\vec{\Phi}', \vec{\Phi}''),$$

$$\mathcal{L}_0(\vec{\Phi}', \vec{\Phi}'') = A(\Phi'^2 + \Phi''^2) + B[\Phi'^4 + \Phi''^4 + 6\Phi'^2\Phi''^2] - 2\Phi'\Phi''g(\Phi', \Phi'', \vec{\psi}', \vec{\psi}''),$$

$$g(\Phi', \Phi'', \vec{\psi}', \vec{\psi}'') = 2B\Phi'\Phi''(\vec{\psi}'(\vec{r}) \cdot \vec{\psi}''(\vec{r}))^2 + h(\psi'_y(\vec{r})\psi''_z(\vec{r}) - \psi'_z(\vec{r})\psi''_y(\vec{r})) - h'(\psi'_0(\vec{r})\psi''_x(\vec{r}) - \psi'_x(\vec{r})\psi''_0(\vec{r})). \quad (G.3)$$

The other two parts depend on  $\vec{\Phi}'(\vec{r})$  and  $\vec{\Phi}''(\vec{r})$  separately and they depend on their spatial gradients, e.g.

$$S_1[\Phi'\vec{\psi}'] = \Phi'^2 \int d^2\vec{r} \{ \lambda(\nabla\psi'_\mu) \cdot (\nabla\psi'_\mu) - D(\psi'_z \partial_x \psi'_x - \psi'_x \partial_x \psi'_z - \psi'_y \partial_y \psi'_z + \psi'_z \partial_y \psi'_y + \psi'_x \partial_y \psi'_0 - \psi'_y \partial_x \psi'_0 + \psi'_0 \partial_x \psi'_y - \psi'_0 \partial_y \psi'_x) \}. \quad (G.4)$$

We first minimize  $S_1[\Phi'\vec{\psi}']$  and  $S_1[\Phi''\vec{\psi}'']$  in terms of the four-component vectors  $\vec{\psi}'$  and  $\vec{\psi}''$  respectively. We then show that  $\vec{\Phi}'$  and  $\vec{\Phi}''$  thus determined also maximally minimize  $S_0[\vec{\Phi}', \vec{\Phi}']$  by optimizing the amplitude parts,  $\Phi'$  and  $\Phi''$ .

To minimize  $S_1[\Phi'\vec{\psi}']$  in terms of  $\vec{\psi}'(\vec{r}) \equiv (\psi'_0(\vec{r}), \psi'_x(\vec{r}), \psi'_y(\vec{r}), \psi'_z(\vec{r}))$ , take the Fourier transformation of  $\psi'_\mu(\vec{r})$ ,

$$\psi'_{\mu, \vec{k}} = \int d^2\vec{r} e^{-i\vec{k} \cdot \vec{r}} \psi'_\mu(\vec{r}), \quad \psi'_\mu(\vec{r}) = \frac{1}{V} \sum_{\vec{k}} e^{i\vec{k} \cdot \vec{r}} \psi'_{\mu, \vec{k}}, \quad (G.5)$$

for  $\mu = 0, x, y, z$  with  $\psi'^*_{\mu, \vec{k}} = \psi'_{\mu, -\vec{k}}$ . The Fourier component  $\psi'_{\mu, \vec{k}}$  is given by two real-valued functions  $\alpha_{\mu, \vec{k}}$  and  $\beta_{\mu, \vec{k}}$  as  $\psi'_{\mu, \vec{k}} \equiv \alpha_{\mu, \vec{k}} + i\beta_{\mu, \vec{k}}$ . They are even and odd functions in  $\vec{k}$  respectively.  $S_1[\Phi'\vec{\psi}']$  is given by these two functions:

$$S_1[\Phi'\vec{\psi}'] = \frac{2\Phi'^2\lambda}{V} \sum_{k_x > 0} k^2 w_{\vec{k}}^2 + \frac{4\Phi'^2 D}{V} \sum_{k_x > 0} f(\alpha_{\mu, \vec{k}}, \beta_{\mu, \vec{k}}), \quad (G.6)$$

$$f(\alpha_{\mu, \vec{k}}, \beta_{\mu, \vec{k}}) \equiv k_x(\alpha_{z, \vec{k}}\beta_{x, \vec{k}} - \alpha_{x, \vec{k}}\beta_{z, \vec{k}} + \alpha_{0, \vec{k}}\beta_{y, \vec{k}} - \alpha_{y, \vec{k}}\beta_{0, \vec{k}}) + k_y(\alpha_{z, \vec{k}}\beta_{y, \vec{k}} - \alpha_{y, \vec{k}}\beta_{z, \vec{k}} + \alpha_{x, \vec{k}}\beta_{0, \vec{k}} - \alpha_{0, \vec{k}}\beta_{x, \vec{k}}), \quad (G.7)$$

with  $w_{\vec{k}}^2 \equiv \sum_\mu (\alpha_{\mu, \vec{k}}\alpha_{\mu, \vec{k}} + \beta_{\mu, \vec{k}}\beta_{\mu, \vec{k}})$ . For given  $w_{\vec{k}}$ ,  $f(\alpha_{\mu, \vec{k}}, \beta_{\mu, \vec{k}})$  in Eq. (G.6) shall be minimized for each  $\hat{\vec{k}}$  (the subscript  $\vec{k}$  will be omitted for convenience):

$$f(\alpha_\mu, \beta_\mu) = k_x(\alpha_z\beta_x - \alpha_x\beta_z + \alpha_0\beta_y - \alpha_y\beta_0) + k_y(\alpha_z\beta_y - \alpha_y\beta_z - \alpha_0\beta_x + \alpha_x\beta_0) = -\hat{\vec{k}} \cdot (\hat{\alpha}' \times \hat{\beta}' + \alpha'_0 \hat{\beta}' - \beta'_0 \hat{\alpha}'). \quad (G.8)$$

In the right hand side of Eq. (G.8), the three-component vectors  $\hat{\alpha}'$ ,  $\hat{\beta}'$ ,  $\hat{\vec{k}}$  are introduced as,

$$\begin{aligned} \hat{\alpha}' &\equiv (\alpha'_x, \alpha'_y, \alpha'_z), \quad \hat{\beta}' \equiv (\beta'_x, \beta'_y, \beta'_z), \quad \hat{\vec{k}} \equiv (k_x, k_y, 0) \equiv (\vec{k}, 0), \\ \alpha_x &= \alpha'_y, \quad \alpha_y = -\alpha'_x, \quad \alpha_z = \alpha'_z, \quad \alpha_0 = \alpha'_0; \\ \beta_x &= \beta'_y, \quad \beta_y = -\beta'_x, \quad \beta_z = \beta'_z, \quad \beta_0 = \beta'_0. \end{aligned} \quad (G.9)$$

The function  $f(\alpha_\mu, \beta_\mu)$  can be easily minimized for the special  $\vec{k}$ . For  $\vec{k} = k\vec{e}_x$ , it is minimized by

$$\begin{aligned}\alpha'_y &= \frac{w}{\sqrt{2}} \cos \zeta \cos \delta_1, & \beta'_y &= -\frac{w}{\sqrt{2}} \cos \zeta \sin \delta_1, & \alpha'_z &= \frac{w}{\sqrt{2}} \cos \zeta \sin \delta_1, & \beta'_z &= \frac{w}{\sqrt{2}} \cos \zeta \cos \delta_1, \\ \alpha'_0 &= \frac{w}{\sqrt{2}} \sin \zeta \cos \delta_2, & \beta'_0 &= -\frac{w}{\sqrt{2}} \sin \zeta \sin \delta_2, & \alpha'_x &= \frac{w}{\sqrt{2}} \sin \zeta \sin \delta_2, & \beta'_x &= \frac{w}{\sqrt{2}} \sin \zeta \cos \delta_2,\end{aligned}\quad (\text{G.10})$$

with arbitrary U(1) variables  $\zeta$ ,  $\delta_1$  and  $\delta_2$ . For  $\vec{k} = k\vec{e}_y$ , we take a substitution of  $\alpha'_1 \rightarrow \alpha'_2$ ,  $\alpha'_2 \rightarrow -\alpha'_1$ ,  $\alpha'_3 \rightarrow \alpha'_3$ ,  $\alpha'_0 \rightarrow \alpha'_0$  in Eq. (G.10), and change  $\beta'$  similarly. For general  $\vec{k} = k(\cos \omega \vec{e}_x + \sin \omega \vec{e}_y)$ , the function  $f(\alpha_\mu, \beta_\mu)$  is minimized by a combination of these two,

$$\vec{\alpha}' = \frac{w}{\sqrt{2}} [(-\sin \omega \cos \zeta \cos \delta_1 + \cos \omega \sin \zeta \sin \delta_2) \vec{e}_x + (\sin \omega \sin \zeta \sin \delta_2 + \cos \omega \cos \zeta \cos \delta_1) \vec{e}_y + \cos \zeta \sin \delta_1 \vec{e}_z + \sin \zeta \cos \delta_2 \vec{e}_0], \quad (\text{G.11})$$

$$\vec{\beta}' = \frac{w}{\sqrt{2}} [(\sin \omega \cos \zeta \sin \delta_1 + \cos \omega \sin \zeta \cos \delta_2) \vec{e}_x + (\sin \omega \sin \zeta \cos \delta_2 - \cos \omega \cos \zeta \sin \delta_1) \vec{e}_y + \cos \zeta \cos \delta_1 \vec{e}_z - \sin \zeta \sin \delta_2 \vec{e}_0]. \quad (\text{G.12})$$

With the solution Eqs. (G.11-G.12),  $S_1[\Phi' \vec{\psi}'(\vec{r})]$  is minimized by the following  $\vec{\psi}'(\vec{r})$  for a given  $\Phi'$  and  $w_{\vec{k}}$ :

$$\begin{aligned}\vec{\psi}'(\vec{r}) &= \frac{1}{V} \sum_{k_x > 0} \sqrt{2} w_{\vec{k}} \{ [-\sin \omega \sin \zeta \sin(\vec{k} \cdot \vec{r} - \delta_2) + \cos \omega \cos \zeta \cos(\vec{k} \cdot \vec{r} - \delta_1)] \vec{e}_x \\ &\quad + [\sin \omega \cos \zeta \cos(\vec{k} \cdot \vec{r} - \delta_1) + \cos \omega \sin \zeta \sin(\vec{k} \cdot \vec{r} - \delta_2)] \vec{e}_y - \cos \zeta \sin(\vec{k} \cdot \vec{r} - \delta_1) \vec{e}_z + \sin \zeta \cos(\vec{k} \cdot \vec{r} - \delta_2) \vec{e}_0\},\end{aligned}\quad (\text{G.13})$$

$$S_1[\Phi' \vec{\psi}'(\vec{r})] = \frac{2\Phi'^2}{V} \sum_{k_x > 0} (\lambda k^2 - Dk) w_{\vec{k}}^2. \quad (\text{G.14})$$

Here  $\omega$  in Eq. (G.13) is a function of  $\vec{k}/k$ ;  $\vec{k} \equiv k(\cos \omega \vec{e}_x + \sin \omega \vec{e}_y)$ , while  $\zeta$ ,  $\delta_1$  and  $\delta_2$  are arbitrary functions of  $\vec{k}$ . From Eq. (G.14),  $S_1[\Phi' \vec{\psi}'(\vec{r})]$  can be maximally minimized by those  $w_{\vec{k}}$  that is non-zero only when  $k = D/(2\lambda)$ ;

$$\vec{k} = k(\cos \omega \vec{e}_x + \sin \omega \vec{e}_y) = \frac{D}{2\lambda} (\cos \omega \vec{e}_x + \sin \omega \vec{e}_y). \quad (\text{G.15})$$

The action thus minimized depends only on  $\Phi'$ ,

$$S_1[\Phi' \vec{\psi}'(\vec{r})] = -\frac{\Phi'^2 D^2}{2\lambda V} \sum_{k_x > 0} w_{\vec{k}}^2 = -\frac{\Phi'^2 D^2 V}{4\lambda}. \quad (\text{G.16})$$

In the right hand side, we use a global constraint,  $\sum_{\vec{k}} w_{\vec{k}}^2 = V^2$ , that comes from the local constraint  $\sum_{\mu} \psi'_{\mu}(\vec{r}) \psi'_{\mu}(\vec{r}) = 1$ ,

$$\sum_{\mu} \int d^2 \vec{r} \psi'_{\mu}(\vec{r}) \psi'_{\mu}(\vec{r}) = \frac{1}{V} \sum_{\mu, \vec{k}} \psi'^*_{\mu, \vec{k}} \psi'_{\mu, \vec{k}} = \frac{1}{V} \sum_{\vec{k}} w_{\vec{k}}^2 = V. \quad (\text{G.17})$$

In Sec. K, we show that it is impossible that  $\psi_{\mu}(\vec{r})$  given by Eq. (G.13) consists of two wavevector Fourier components. Specifically, we prove that if  $\vec{\psi}(\vec{r})$  in Eq. (G.13) consists of the two wavevector Fourier components,  $\vec{k}_1$  and  $\vec{k}_2$ ;

$$w_{\vec{k}} = \begin{cases} 0 & \text{for } \vec{k} \neq \vec{k}_1 \text{ and } \vec{k} \neq \vec{k}_2, \\ w_1 \neq 0 & \text{for } \vec{k} = \vec{k}_1, \\ w_2 \neq 0 & \text{for } \vec{k} = \vec{k}_2 \neq \vec{k}_1, -\vec{k}_1, \end{cases} \quad (\text{G.18})$$

$\vec{\psi}(\vec{r})$  thus given cannot satisfy the local constraint  $(\vec{\psi}(\vec{r}) \cdot \vec{\psi}(\vec{r}) = 1)$  in any way. The conclusion can be generalized into a case with more than the two momenta. Thus, we regard  $\vec{\psi}(\vec{r})$  is composed only of one component of momentum  $\vec{k}$  on  $|\vec{k}| = D/(2\lambda)$  and take  $w = \frac{V}{\sqrt{2}}$  from the global constraint. In conclusion,  $S_1[\Phi' \vec{\psi}'(\vec{r})]$  is maximally minimized by,

$$\begin{aligned}\vec{\psi}'(\vec{r}) &= \{ [-\sin \omega' \sin \zeta \sin(\vec{k}' \cdot \vec{r} - \delta'_2) + \cos \omega' \cos \zeta \cos(\vec{k}' \cdot \vec{r} - \delta'_1)] \vec{e}_x \\ &\quad + [\sin \omega' \cos \zeta \cos(\vec{k}' \cdot \vec{r} - \delta'_1) + \cos \omega' \sin \zeta \sin(\vec{k}' \cdot \vec{r} - \delta'_2)] \vec{e}_y - \cos \zeta \sin(\vec{k}' \cdot \vec{r} - \delta'_1) \vec{e}_z + \sin \zeta \cos(\vec{k}' \cdot \vec{r} - \delta'_2) \vec{e}_0\},\end{aligned}\quad (\text{G.19})$$

with  $\vec{k}' = \frac{D}{2\lambda}(\cos\omega'\vec{e}_x + \sin\omega'\vec{e}_y)$  together with arbitrary U(1) phase variables,  $\zeta'$ ,  $\delta'_1$  and  $\delta'_2$ . Note that this satisfies the local constraint,  $\vec{\psi}(\vec{r}) \cdot \vec{\psi}(\vec{r}) = 1$ . Likewise,  $S_1[\Phi''\vec{\psi}''(\vec{r})]$  is maximally minimized by  $\psi''(\vec{r})$  given by the same type of the unit vector as Eq. (G.19) with another set of the U(1) variables of  $\omega''(\vec{k}'')$ ,  $\zeta''$ ,  $\delta''_1$  and  $\delta''_2$ .

Finally, we minimize  $S_0[\vec{\Phi}', \vec{\Phi}'']$  within a ‘manifold’ of Eq. (G.19) for  $\vec{\Phi}'(\vec{r}) \equiv \Phi'\vec{\psi}'(\vec{r})$  and that for  $\vec{\Phi}''(\vec{r}) \equiv \Phi''\vec{\psi}''(\vec{r})$ . The minimization is carried out in a parameter space subtended by  $\omega'(\vec{k}')$ ,  $\zeta'$ ,  $\delta'_1$ ,  $\delta'_2$ ,  $\omega''(\vec{k}'')$ ,  $\zeta''$ ,  $\delta''_1$ ,  $\delta''_2$ ,  $\Phi'$  and  $\Phi''$ . To begin with, we consider to maximize  $g$  in Eq. (G.3) at a given spatial point  $\vec{r}$ . The maximization leads to  $\omega' = \omega'' = \pi/2$  ( $\vec{k}' = \vec{k}'' = \frac{D}{2\lambda}\vec{e}_y$ ), while  $\zeta' = \zeta'' = \pi/2$  for  $|h| \leq |h'|$ , and  $\zeta' = \zeta'' = 0$  for  $|h'| \leq |h|$ . For each of these two cases, we then maximize  $g$  in Eq. (G.3) in terms of  $\delta'_2 - \delta''_2$  and  $\delta'_1 - \delta''_1$  respectively, and finally minimize the whole action in terms of  $\Phi'$  and  $\Phi''$ ;

$$s \equiv \frac{S}{V} = A'(\Phi'^2 + \Phi''^2) + B(\Phi'^4 + \Phi''^4 + 6\Phi'^2\Phi''^2) - 2\Phi'\Phi''g,$$

$$g \equiv \begin{cases} 2B\Phi'\Phi'' \cos(\delta'_1 - \delta''_1) + h \sin(\delta'_1 - \delta''_1) & \text{when } |h'| < |h|, \\ 2B\Phi'\Phi'' \cos(\delta'_2 - \delta''_2) - h' \sin(\delta'_2 - \delta''_2) & \text{when } |h| < |h'|, \end{cases} \quad (\text{G.20})$$

with  $A' = -(\alpha - \frac{2}{g} + \frac{D^2}{4\lambda})$ . Here the  $D^2$  term in  $A'$  comes from Eq. (G.16). The maximization of  $g$  in terms of  $\delta'_2 - \delta''_2 = \alpha_1$  and  $\delta'_1 - \delta''_1 = \alpha_2$  and the minimization of the classical action  $s$  in terms of  $\Phi'$  and  $\Phi''$  are essentially same as in Eqs. (B.4-B.11). Thereby, Eqs. (B.12-B.15) are still valid classical solutions, except for the following substitutions,

$$\varphi_0 \rightarrow \varphi_0 - Ky, \quad K \equiv \frac{D}{2\lambda}, \quad (\text{G.21})$$

$$h_c = \alpha - \frac{2}{g} \rightarrow h_c = \alpha - \frac{2}{g} + \frac{D^2}{4\lambda}. \quad (\text{G.22})$$

To summarize, we have the following four phases.

**For  $|h'| < |h| < h_c$  (normal helicoidal phase):**

$$\vec{\phi} = \rho \cos\theta (\cos(\varphi_0 - Ky)\vec{e}_y + \sin(\varphi_0 - Ky)\vec{e}_z) + i\rho \sin\theta [\cos(\varphi + \varphi_0 - Ky)\vec{e}_y + \sin(\varphi + \varphi_0 - Ky)\vec{e}_z],$$

$$\rho = \sqrt{\frac{h_c}{2|\gamma|}}, \quad \sin\varphi \sin 2\theta = \frac{h}{h_c}. \quad (\text{G.23})$$

**For  $|h| < |h'| < h_c$  (normal helical phase):**

$$\vec{\phi} = \rho [-\sin\theta \cos(\varphi + \varphi_0 - Ky)\vec{e}_0 + \cos\theta \sin(\varphi_0 - Ky)\vec{e}_x] + i\rho [\cos\theta \cos(\varphi_0 - Ky)\vec{e}_0 + \sin\theta \sin(\varphi + \varphi_0 - Ky)\vec{e}_x],$$

$$\rho = \sqrt{\frac{h_c}{2|\gamma|}}, \quad \sin\varphi \sin 2\theta = -\frac{h'}{h_c}. \quad (\text{G.24})$$

**For  $|h'| < |h|$ ,  $h_c < |h|$  (saturated helicoidal phase):**

$$\vec{\phi} = \rho (\cos(\varphi_0 - Ky)\vec{e}_y + \sin(\varphi_0 - Ky)\vec{e}_z) - i\rho \text{sgn}(h) [\sin(\varphi_0 - Ky)\vec{e}_y - \cos(\varphi_0 - Ky)\vec{e}_z], \quad \rho = \sqrt{\frac{h_c + |h|}{8|\gamma|}}. \quad (\text{G.25})$$

**For  $|h| < |h'|$ ,  $h_c < |h'|$  (saturated helical phase):**

$$\vec{\phi} = \rho [\text{sgn}(-h') \sin(\varphi_0 - Ky)\vec{e}_0 + \sin(\varphi_0 - Ky)\vec{e}_x] + i\rho [\cos(\varphi_0 - Ky)\vec{e}_0 + \text{sgn}(-h') \cos(\varphi_0 - Ky)\vec{e}_x], \quad \rho = \sqrt{\frac{h_c + |h'|}{8|\gamma|}}. \quad (\text{G.26})$$

Here we call ground-state configurations of Eqs. (G.23, G.25) with the substitutions as normal and saturated helicoidal phase and those of Eqs. (G.24, G.26) as normal and saturated helical phase. Both helical and helicoidal phases have a nonzero momentum  $K$ , breaking the translational symmetry along  $y$ -axis. The phase diagram with  $D \neq 0$  is given by Fig. 5(a) where ‘transverse’ and ‘longitudinal’ are replaced by ‘helicoidal’ and ‘helical’ respectively. The helicoidal phases were introduced and studied in Ref. [69]. A schematic picture of the helical phase is shown in Fig. 5(b).

## H. Derivation of spin-charge coupled Josephson equation with Rashba interaction

In this section, we derive spin-charge coupled Josephson equations in helicoidal and helical phases, Eqs. (18,19) in the main text. We first apply the Noether theorem to the  $\phi^4$ -type effective Lagrangian, Eq. (A.13), to express (conserved) charge and spin currents in terms of the four-components excitonic fields and their spatial gradient terms. We then substitute the classical solutions, Eqs. (G.23,G.24,G.25,G.26), into the expressions. This leads to the spin-charge coupled Josephson equations in the helical and heliodial phases.

In practice, the magnetic exchange fields within the  $xy$  plane can be experimentally controlled by an external magnetic field in the plane. The magnetic field causes magnetic vector potentials in the electron and hole layers. In the presence of the vector potentials,  $\partial_i$  in Eqs. (1,17) in the main text ( $i = x, y$ ) is replaced by  $\partial_i + iA_{a,i}$  in the electron layer and by  $\partial_i + iA_{b,i}$  in the hole layer. The two vector potentials,  $A_{a,i}$  and  $A_{b,i}$ , are generally different from each other, as the electron and hole layers are spatially separated along the  $z$  direction. An integral of the difference between them,  $\tilde{A}_i \equiv A_{b,i} - A_{a,i}$ , is the magnetic flux penetrating through the separation layer. The difference appears in the  $\phi^4$ -type effective Lagrangian in a covariant way;  $\partial_i$  in Eq. (A.13) is replaced by  $\partial_i - i\tilde{A}_i$ .

The Noether theorem associates a global continuous symmetry in Lagrangian  $\mathcal{L}(\vec{\phi}, \partial_i \vec{\phi})$  with a conserved current. [83] Suppose that a Lagrangian is invariant under the following transformation,

$$\phi_\nu \rightarrow \phi_\nu + \epsilon \Delta \phi_\nu, \quad \phi_\nu^* \rightarrow \phi_\nu^* + \epsilon \Delta \phi_\nu^*, \quad (\text{H.1})$$

with a small  $\epsilon$ . The Noether's theorem dictates that a system must have a conserved current defined as follows:

$$J_\mu = \frac{\partial \mathcal{L}}{\partial(\partial_\mu \phi_\nu)} \Delta \phi_\nu + \frac{\partial \mathcal{L}}{\partial(\partial_\mu \phi_\nu^*)} \Delta \phi_\nu^*. \quad (\text{H.2})$$

The effective  $\phi^4$ -type lagrangian has the pseudospin rotational symmetry around  $x$  axis;

$$\begin{cases} \begin{pmatrix} -i\phi_0 \\ \phi_x \end{pmatrix} \rightarrow \begin{pmatrix} -i\tilde{\phi}_0 \\ \tilde{\phi}_x \end{pmatrix} = \begin{pmatrix} \cos(\delta\varphi_0) & -\sin(\delta\varphi_0) \\ \sin(\delta\varphi_0) & \cos(\delta\varphi_0) \end{pmatrix} \begin{pmatrix} -i\phi_0 \\ \phi_x \end{pmatrix}, \\ \begin{pmatrix} \phi_y \\ \phi_z \end{pmatrix} \rightarrow \begin{pmatrix} \tilde{\phi}_y \\ \tilde{\phi}_z \end{pmatrix} = \begin{pmatrix} \cos(\delta\varphi_0) & -\sin(\delta\varphi_0) \\ \sin(\delta\varphi_0) & \cos(\delta\varphi_0) \end{pmatrix} \begin{pmatrix} \phi_y \\ \phi_z \end{pmatrix}, \end{cases} \quad (\text{H.3})$$

and the relative U(1) gauge symmetry;

$$\vec{\phi} \rightarrow \vec{\phi}' = e^{i\psi} \vec{\phi}. \quad (\text{H.4})$$

Note that in the presence of the Rashba interaction  $\xi_e \neq 0$ , the pseudospin rotational symmetry around the  $x$  axis is nothing but the spin rotational symmetry in the hole layer in Eqs. (1,17) in the main text; taking  $\varphi_a = 0$  and  $\varphi_b = \mp\delta\varphi_0$  in Eq. (6) of the main text leads to Eq. (H.3). For the relative  $U(1)$  gauge symmetry, taking  $\psi_b - \psi_a = -\psi$  in Eq. (7) of the main text leads to Eq. (H.4).

To calculate charge and spin Noether current in the hole layer, we choose  $\varphi_b$  and  $\psi_b - \psi_a$  to be positive. Namely, taking  $\delta\varphi_0$  and  $\psi$  in Eqs. (H.3,H.4) to be  $\mp\epsilon$  and  $-\epsilon$  with infinitesimally small positive  $\epsilon$ , we obtain

$$\phi_y \rightarrow \phi_y \pm \epsilon \phi_z, \quad \phi_z \rightarrow \phi_z \mp \epsilon \phi_y, \quad (\text{H.5})$$

$$-i\phi_0 \rightarrow -i\phi_0 \pm \epsilon \phi_x, \quad \phi_x \rightarrow \phi_x \mp \epsilon (-i\phi_0), \quad (\text{H.6})$$

(and  $\phi_\nu^*$  changes accordingly) for the spin rotational symmetry and

$$\phi_\nu \rightarrow \phi_\nu - i\epsilon \phi_\nu, \quad \phi_\nu^* \rightarrow \phi_\nu^* + i\epsilon \phi_\nu^*, \quad (\text{H.7})$$

for the relative gauge symmetry respectively. Accordingly, the corresponding conserved currents are calculated from the Noether theorem:

$$J_\mu^C = -\frac{\partial \mathcal{L}}{\partial(\partial_\mu \phi_\nu)} i\phi_\nu + \frac{\partial \mathcal{L}}{\partial(\partial_\mu \phi_\nu^*)} i\phi_\nu^*, \quad (\text{H.8})$$

and

$$\begin{aligned} J_\mu^S = & \pm \left\{ \frac{\partial \mathcal{L}}{\partial(\partial_\mu \phi_y)} \phi_z - \frac{\partial \mathcal{L}}{\partial(\partial_\mu \phi_z)} \phi_y + \frac{\partial \mathcal{L}}{\partial(\partial_\mu \phi_y^*)} \phi_z^* - \frac{\partial \mathcal{L}}{\partial(\partial_\mu \phi_z^*)} \phi_y^* \right. \\ & \left. + \frac{\partial \mathcal{L}}{\partial[\partial_\mu(-i\phi_0)]} \phi_x - \frac{\partial \mathcal{L}}{\partial(\partial_\mu \phi_x)} (-i\phi_0) + \frac{\partial \mathcal{L}}{\partial[\partial_\mu(i\phi_0^*)]} \phi_x^* - \frac{\partial \mathcal{L}}{\partial(\partial_\mu \phi_x^*)} (i\phi_0^*) \right\}, \end{aligned} \quad (\text{H.9})$$

respectively. Here  $\mathcal{L}$  is the  $\phi^4$ -type Lagrangian density (see Eq. (A.13)).

A substitution of the magnetic vector potentials into Eq. (A.13) leads to the following Lagrangian density:

$$\begin{aligned}\mathcal{L} = & -\eta\phi_\nu^*(\partial_\tau - i\tilde{A}_\tau)\phi_\nu + \lambda[(\partial_i + i\tilde{A}_i)\phi_\nu^*][(\partial_i - i\tilde{A}_i)\phi_\nu] \\ & - D[\phi_z^*(\partial_x\phi_x) - \phi_x^*(\partial_x\phi_z) - \phi_y^*(\partial_y\phi_z) + \phi_z^*(\partial_y\phi_y) - i\phi_x^*(\partial_y\phi_0) + i\phi_y^*(\partial_x\phi_0) + i\phi_0^*(\partial_x\phi_y) - i\phi_0^*(\partial_y\phi_x)] + \dots, \quad (\text{H.10})\end{aligned}$$

where  $D = 2K\lambda$  from Eq. (A.18),  $i = x, y$  and  $\nu = 0, x, y, z$ . Here “...” denotes other terms without the spatial gradients of  $\phi_\nu$  and  $\phi_\nu^*$ ; they do not contribute to the Noether currents. Putting Eq. (H.10) into Eq. (H.8), we get the (hole-layer) charge Noether current:

$$J_i^C = 2i\lambda\phi_\nu^*(\partial_i - i\tilde{A}_i)\phi_\nu + iD[\delta_{i,x}(\phi_z^*\phi_x - \phi_x^*\phi_z) - \delta_{i,y}(\phi_y^*\phi_z - \phi_z^*\phi_y) + i\delta_{i,x}(\phi_0^*\phi_y + \phi_y^*\phi_0) - i\delta_{i,y}(\phi_0^*\phi_x + \phi_x^*\phi_0)], \quad (\text{H.11})$$

where we have used  $\phi_\nu\partial_i\phi_\nu^* = -\phi_\nu^*\partial_i\phi_\nu$ . Putting Eq. (H.10) into Eq. (H.9), we get the (hole-layer) spin Noether current:

$$\begin{aligned}J_i^S = & \pm 2\lambda[\phi_z^*(\partial_i - i\tilde{A}_i)\phi_y - \phi_y^*(\partial_i - i\tilde{A}_i)\phi_z - i\phi_x^*(\partial_i - i\tilde{A}_i)\phi_0 - i\phi_0^*(\partial_i - i\tilde{A}_i)\phi_x] \\ & \mp D[\delta_{i,x}(i\phi_0^*\phi_z + \phi_x^*\phi_y) + \delta_{i,y}(\phi_z^*\phi_z + \phi_y^*\phi_y) + \delta_{i,x}(i\phi_z^*\phi_0 - \phi_y^*\phi_x) + \delta_{i,y}(\phi_z^*\phi_z + \phi_0^*\phi_0)]. \quad (\text{H.12})\end{aligned}$$

Let us next substitute the classical solutions of Eqs. (G.23, G.24, G.25, G.26) into these expressions for the Noether currents. Thereby, the spatial gradients in the expressions apply not only to an explicit spatial-coordinate dependence of the classical solutions but also to the slowly-varying gapless modes,  $\varphi_0$  and  $\psi$ . Thus, the spatial derivatives in Eqs. (H.11, H.12) can be decomposed into:

$$\partial_i = (\partial_i\psi)\frac{\partial}{\partial\psi} + (\partial_i\varphi_0)\frac{\partial}{\partial\varphi_0} + \partial'_i, \quad (\text{H.13})$$

where  $\partial'_i$  applies only to the explicit spatial-coordinate dependence. From Eqs. (G.23, G.25), these partial derivatives take the following forms in the helicoidal phases,

$$\frac{\partial\phi_y}{\partial\psi} = i\phi_y, \quad \frac{\partial\phi_z}{\partial\psi} = i\phi_z, \quad \frac{\partial\phi_y}{\partial\varphi_0} = -\phi_z, \quad \frac{\partial\phi_z}{\partial\varphi_0} = \phi_y, \quad \partial'_i\phi_y = K\phi_z\delta_{i,y}, \quad \partial'_i\phi_z = -K\phi_y\delta_{i,y}. \quad (\text{H.14})$$

From Eqs. (G.24, G.26), we obtain a set of similar relations for the helical phases. Using them in Eqs. (H.11, H.12) together with  $D = 2K\lambda$ , and recover units by substitutions  $\tilde{A}_i \rightarrow e\tilde{A}_i/\hbar c$ , we finally obtain Eqs. (18, 19) of the main text.

## I. Local magnetic moment induced by excitonic condensations

For a 2D system in  $xy$  plane, effective confinement potential along  $z$  direction may break spatial inversion symmetry. This results in an effective electric field along  $z$  direction, which leads to Rashba SOC interaction in the electron layer (Eq. (17) of the main text). This kind of the SOC is called structural inversion asymmetry (SIA). As mentioned in the main text, the SIA in the electron-hole double-layer semiconductor systems results not only in the Rashba interaction in the electron layer with  $S_z = \pm 1/2$ , but also Rashba interaction in the hole layer with  $J_z = \pm 3/2$ . As the Pauli matrices  $\sigma_x$  and  $\sigma_y$  connect between the  $J_z = \pm 3/2$  Kramers doublet in the hole layer, the SOC for the hole layer is proportional to a cubic in the momentum  $k$  and atomic spin-orbit interaction strength and it is therefore negligibly small especially around the  $\Gamma$  point.

However, the hole layer is still not completely free from SOC interaction at the linear order of momentum  $k$ . The bulk crystal structure itself may break spatial inversion symmetry, and this kind of the SOC is called bulk inversion asymmetry (BIA). The BIA leads to Dirac-type SOC interaction in the hole layer [78–81]:

$$H_D = \Delta_h \int d^2\vec{r} \mathbf{b}^\dagger(\vec{r}) (-i\partial_x\sigma_x - i\partial_y\sigma_y) \mathbf{b}(\vec{r}). \quad (\text{I.1})$$

For a typical system,  $\Delta_h \sim 0.01\xi_e$  [81, 84], and it is therefore quantitatively negligible. Nonetheless, the Dirac interaction in the hole layer breaks the pseudospin rotational symmetry, endowing the gapless spin rotational modes with a finite gap. The gap causes a finite dissipation in the spin-charge conversion phenomena proposed in this paper. In the presence of the Dirac-type interaction, the classical ground state becomes a linear combination of helical and helicoidal textures. In other words, the first-order phase transition between the helical and helicoidal phases in the phase diagram in Fig. 5(a) becomes a crossover boundary. More importantly, the excitonic condensation under the

exchange field brings about a finite local magnetism in electron and hole layers respectively. In this section, we will evaluate the local magnetism in the electron layer by treating the excitonic order parameter perturbatively.

To this end, we treat the excitonic order parameter as a static mean field and include both the Dirac interaction in the hole layer and the Rashba interaction in the electron layer;

$$K = H - \mu N = \sum_{\vec{k}} \mathbf{a}_{\vec{k}}^\dagger (\xi_{\vec{k}}^a \boldsymbol{\sigma}_0 + \xi_e (k_y \boldsymbol{\sigma}_x - k_x \boldsymbol{\sigma}_y) + H \boldsymbol{\sigma}_a) \mathbf{a}_{\vec{k}} + \sum_{\vec{k}} \mathbf{b}_{\vec{k}}^\dagger (\xi_{\vec{k}}^b \boldsymbol{\sigma}_0 + \Delta_h (k_x \boldsymbol{\sigma}_x + k_y \boldsymbol{\sigma}_y) + H \boldsymbol{\sigma}_b) \mathbf{b}_{\vec{k}} \\ - \int d^2 \vec{r} \vec{\phi}_\lambda^* (\vec{r}) \cdot \mathbf{b}^\dagger (\vec{r}) \vec{\sigma} \mathbf{a} (\vec{r}) - \int d^2 \vec{r} \vec{\phi}_\lambda (\vec{r}) \cdot \mathbf{a}^\dagger (\vec{r}) \vec{\sigma} \mathbf{b} (\vec{r}), \quad (\text{I.2})$$

Here  $\xi_{\vec{k}}^{a/b} \equiv \mathcal{E}_{a/b}(\vec{k}) - \mu$ . An imaginary-time time-ordered Green's function for the electron layer is defined by this mean-field Hamiltonian:

$$\mathbf{G}_{\alpha\beta}^a (\vec{r}, \tau; \vec{r}', \tau') = - \frac{\text{Tr}[e^{-\beta K} \mathcal{T}_\tau \{ \mathbf{a}_\alpha (\vec{r}, \tau) \mathbf{a}_\beta^\dagger (\vec{r}', \tau') \}]}{\text{Tr}[e^{-\beta K}]}, \quad (\text{I.3})$$

with  $\mathbf{a}_\alpha (\vec{r}, \tau) \equiv e^{\tau K} \mathbf{a}_\alpha (\vec{r}) e^{-\tau K}$  and  $\mathbf{a}_\beta^\dagger (\vec{r}', \tau') \equiv e^{\tau' K} \mathbf{a}_\beta^\dagger (\vec{r}') e^{-\tau' K}$ . The local magnetic moment and local charge density in the electron layer are given by the Green function:

$$\vec{m}^{(e)} (\vec{r}) = \frac{1}{2} \text{Tr}[\vec{\sigma} \mathbf{G}^a (\vec{r}, \tau; \vec{r}, \tau + 0)], \quad \rho^{(e)} (\vec{r}) = \text{Tr}[\mathbf{G}^a (\vec{r}, \tau; \vec{r}, \tau + 0)], \quad (\text{I.4})$$

We will calculate these two quantities perturbatively in the excitonic fields. Since the excitonic field connects between electron and hole layers, the lowest order starts from the second order. A detailed perturbative calculation process was described in Ref. [69]. Here we only describe the results;

$$\vec{m}^{(e)} (\vec{r}) = A (\cos^2 \theta \cos(2K y - 2\varphi_0) + \sin^2 \theta \cos(2K y - 2\varphi - 2\varphi_0)) \vec{e}_y \\ - B (\cos^2 \theta \sin(2K y - 2\varphi_0) + \sin^2 \theta \sin(2K y - 2\varphi - 2\varphi_0)) \vec{e}_z + \frac{1}{2} (D \vec{e}_x + E \vec{e}_y) + \mathcal{O}(\Delta_h^2), \quad (\text{I.5})$$

$$\rho^{(e)} (\vec{r}) = C + \mathcal{O}(\Delta_h^2). \quad (\text{I.6})$$

The magnetic moment has similar propagating structure as the excitonic field, while the wavevector becomes  $2K \vec{e}_y$  instead of  $K \vec{e}_y$ . All the four excitonic phases in Eqs. (G.23, G.24, G.25, G.26) share this expression, while the coefficients ( $A, B, C, D, E$ ) are different. The leading-order proportionality relations are:

$$C \propto \rho^2, \quad D \propto \rho^2 H, \quad A, B, E \propto \rho^2 \Delta_h \xi_e H. \quad (\text{I.7})$$

When  $\vec{\phi}_\lambda (\vec{r})$  in Eq. (I.2) takes purely the normal helicoidal structure (Eq. (G.23)), the coefficients are calculated as:

$$\begin{pmatrix} A \\ B \end{pmatrix} \equiv \frac{\rho^2 \Delta_h}{V} \sum_{\vec{q}} \frac{1}{\beta} \sum_{i\omega_m} e^{i\omega_m 0+} q_y f(q, H) \begin{pmatrix} t^2 + s^2 \\ t^2 - s^2 \end{pmatrix}, \quad (\text{I.8})$$

$$\begin{pmatrix} C \\ D \end{pmatrix} \equiv \frac{\rho^2}{V} \sum_{\vec{q}} \frac{1}{\beta} \sum_{i\omega_m} e^{i\omega_m 0+} \sum_{\sigma=\pm} (1 + \sigma \sin \varphi \sin 2\theta) (i\omega_m - \xi_{\vec{q}}^b - \sigma H) g_\sigma(q, H) \begin{pmatrix} u_\sigma^2 + s^2 \\ \sigma(u_\sigma^2 - s^2) \end{pmatrix}, \quad (\text{I.9})$$

$$E \equiv \frac{\rho^2 \Delta_h}{V} \sum_{\vec{q}} \frac{1}{\beta} \sum_{i\omega_m} e^{i\omega_m 0+} \xi_e q_x^2 \sum_{\sigma=\pm} (1 + \sigma \sin \varphi \sin 2\theta) g_\sigma(q, H) u_\sigma \eta_\sigma, \quad (\text{I.10})$$

where

$$f(q, H) \equiv \frac{1}{(i\omega_m - \xi_{\vec{q}}^b)^2 - H^2} \prod_{\sigma=\pm} \frac{1}{(i\omega_m - \xi_{\vec{q}+\vec{\sigma}}^a)^2 - [(\xi_e q_x)^2 + (\xi_e (q_y + \sigma K) + H)^2]}, \quad (\text{I.11})$$

	$\Delta_h$	$\xi_e$	$H_x$	$\Delta_h \xi_e H_x$	$m_y$
$\sigma_{yz}$	—	+	+	—	—
$\sigma_{zx}$	—	+	—	+	+
$R_x^\pi$	+	—	+	—	—
$R_y^\pi$	+	—	—	+	+
$R_z^\pi$	+	+	—	—	—
$\mathcal{T}$	+	+	—	—	—

TABLE I. A list of parities of Rashba-type interaction ( $\xi_e$ ), Dirac-type interaction ( $\Delta_h$ ), magnetic exchange field along  $x$  ( $H_x$ ), and the magnetization along  $y$  ( $m_y$ ) under all the possible symmetry transformations in the Hamiltonian of Eqs. (1,17,I.1).  $\sigma_{\mu\nu}$  denotes the  $\mu\nu$ -plane mirror reflection.  $R_\mu^\pi$  denotes the  $\pi$ -rotation along  $\mu$ -axis.  $\mathcal{T}$  denotes time reversal operation. “+” means that the corresponding term or observable remains unchanged (even), while “—” means that the sign changes (odd). The list concludes that symmetry properties of  $m_y$  and  $\Delta_h \xi_e H_x$  are consistent with each other.

$$g_\sigma(q, H) \equiv \frac{1}{(\mathrm{i}\omega_m - \xi_{\vec{q}}^b)^2 - H^2} \left( \frac{1}{(\mathrm{i}\omega_m - \xi_{\vec{q}+\vec{\sigma}}^a)^2 - [(\xi_e q_x)^2 + (\xi_e(q_y + \sigma K) + H)^2]} \right)^2, \quad (\text{I.12})$$

$$t^2 \equiv [(\mathrm{i}\omega_m - \xi_{\vec{q}+}^a) + (\xi_e(q_y + K) + H)][(\mathrm{i}\omega_m - \xi_{\vec{q}-}^a) - (\xi_e(q_y - K) + H)], \quad s \equiv \xi_e q_x, \quad (\text{I.13})$$

$$u_\sigma \equiv (\mathrm{i}\omega_m - \xi_{\vec{q}+\vec{\sigma}}^a) + \sigma(\xi_e(q_y + \sigma K) + H), \quad \eta_\sigma = 2[\sigma - \frac{2(\mathrm{i}\omega_m - \xi_{\vec{q}}^b - \sigma H)H}{(\mathrm{i}\omega_m - \xi_{\vec{q}}^b)^2 - H^2}], \quad (\text{I.14})$$

$$\vec{q} + \vec{\sigma} \equiv (q_x, q_y + \sigma K) \quad (\sigma = \pm). \quad (\text{I.15})$$

When  $\vec{\phi}_\lambda(\vec{r})$  in Eq. (I.2) takes purely the normal helical structure (Eq. (G.24)), the coefficients  $A$  and  $B$  are the same as above, while  $C$ ,  $D$ , and  $E$  should be replaced by the followings:

$$\begin{pmatrix} C \\ D \end{pmatrix} \equiv \frac{\rho^2}{V} \sum_{\vec{q}} \frac{1}{\beta} \sum_{\mathrm{i}\omega_m} \mathrm{e}^{\mathrm{i}\omega_m 0+} \sum_{\sigma=\pm} (1 + \sigma \sin \varphi \sin 2\theta) (\mathrm{i}\omega_m - \xi_{\vec{q}}^b + \sigma H) g_\sigma(\vec{q}, H) \begin{pmatrix} u_\sigma^2 + s^2 \\ \sigma(u_\sigma^2 - s^2) \end{pmatrix}, \quad (\text{I.16})$$

$$E \equiv \frac{\rho^2 \Delta_h}{V} \sum_{\vec{q}} \frac{1}{\beta} \sum_{\mathrm{i}\omega_m} \mathrm{e}^{\mathrm{i}\omega_m 0+} \xi_e q_x^2 \sum_{\sigma=\pm} (1 + \sigma \sin \varphi \sin 2\theta) g_\sigma(\vec{q}, H) u_\sigma \eta'_\sigma, \quad (\text{I.17})$$

where

$$\eta'_\sigma = 2[-\sigma - \frac{2(\mathrm{i}\omega_m - \xi_{\vec{q}}^b + \sigma H)H}{(\mathrm{i}\omega_m - \xi_{\vec{q}}^b)^2 - H^2}]. \quad (\text{I.18})$$

When  $H = 0$ , both  $D$  and  $E$  vanish, because the following symmetries enable cancellations between  $(q_x, q_y, \sigma)$  and  $(q_x, -q_y, -\sigma)$  in Eqs. (I.9, I.10, I.16, I.17);

$$\sin \varphi \sin 2\theta = \frac{h}{h_c} = 0, \quad \eta_\sigma = 2\sigma, \quad \eta'_\sigma = -2\sigma \quad \xi_{q_x, q_y}^{a/b} = \xi_{q_x, -q_y}^{a/b}, \quad (\text{I.19})$$

$$u_\sigma(q_x, q_y, \mathrm{i}\omega_m) = u_{-\sigma}(q_x, -q_y, \mathrm{i}\omega_m), \quad g_\sigma(q_x, q_y, 0) = g_{-\sigma}(q_x, -q_y, 0). \quad (\text{I.20})$$

In the presence of finite exchange field along  $x$ , however, the excitonic condensation induces a uniform magnetization along the  $y$  direction, i.e.  $E \neq 0$ . The transverse magnetization along  $y$  does not contradict the symmetries of the EHDL systems under the exchange field along  $x$  (Table. I).

### J. Delta functions between real numbers and bilinear Grassmann numbers in Eq. (E.10)

In this section, we define a delta function between a real number and a bilinear Grassmann number, and discuss its properties. The discussion can be regarded as a proof for Eq. (E.10). For simplicity, we discuss normal integrals (i.e.

zero-dimensional field theory), and the results are easy to be generalized for path integrals (i.e. finite-dimensional field theory). Below  $(\psi, \psi^*)$  is a pair of conjugate Grassmann numbers, while  $N$  and  $\mu$  are real numbers. We define a delta function:

$$\delta(N - \psi^* \psi) \equiv \delta(N) - \delta'(N) \psi^* \psi, \quad (\text{J.1})$$

where  $\delta(N)$  is a delta function for real numbers,  $\delta'(N) \equiv d\delta(N)/dN$ . It leads to following two equations:

$$\int dN \delta(N - \psi^* \psi) f(N) = \int [\delta(N) f(N) + \psi^* \psi \delta(N) f'(N)] = f(0) + \psi^* \psi f'(0) = f(\psi^* \psi). \quad (\text{J.2})$$

$$\int \frac{d\mu}{2\pi} e^{i\mu(N - \psi^* \psi)} = \int \frac{d\mu}{2\pi} e^{i\mu N} (1 - i\mu \psi^* \psi) = \int \frac{d\mu}{2\pi} (1 - \psi^* \psi \frac{\partial}{\partial N}) e^{i\mu N} = \delta(N) - \psi^* \psi \delta'(N) = \delta(N - \psi^* \psi). \quad (\text{J.3})$$

Eq. (J.2) and Eq. (J.3) lead to the second line and the third line of Eq. (E.10) respectively. Note that the delta function thus defined does not satisfy a reciprocal equation of Eq. (J.2):

$$\int d\psi^* d\psi \delta(N - \psi^* \psi) g(\psi^* \psi) \neq \int d\psi^* d\psi \bar{\delta}(N - \psi^* \psi) g(\psi^* \psi) = g(N), \quad (\text{J.4})$$

where we define a reciprocal delta function as:

$$\bar{\delta}(N - \psi^* \psi) \equiv -N - \psi^* \psi. \quad (\text{J.5})$$

The right hand side of Eq. (J.4) holds true for an arbitrary linear function  $g(x) \equiv a + bx$ ,

$$\int d\psi^* d\psi \bar{\delta}(N - \psi^* \psi) g(\psi^* \psi) = \int d\psi d\psi^* (N + \psi^* \psi) (a + b\psi^* \psi) = a + bN = g(N), \quad (\text{J.6})$$

where we used  $d\psi d\psi^* = -d\psi^* d\psi$ .

Although Eq. (E.10) is verified, the physical meanings of  $N_C$  and  $N_S$  are still not apparent due to the uncommon properties of the delta function (Eq. (J.4)). Below we further verify Eq. (E.9) in the sense of expectation values, i.e.

$$\langle N_C - \frac{1}{2} \sum_{\alpha} [\mathbf{b}_{1\alpha}^\dagger \mathbf{b}_{1\alpha} - \mathbf{b}_{2\alpha}^\dagger \mathbf{b}_{2\alpha}] \rangle = \langle N_S - \frac{1}{2} \sum_{\alpha} [\mathbf{b}_{1\alpha}^\dagger \boldsymbol{\sigma}_x \mathbf{b}_{1\alpha} - \mathbf{b}_{2\alpha}^\dagger \boldsymbol{\sigma}_x \mathbf{b}_{2\alpha}] \rangle = 0, \quad (\text{J.7})$$

where the expectations values are taken with respect to the partition function in the last line of Eq. (E.10). We can verify it by a proof of a equation:

$$\langle N - \psi^* \psi \rangle = -i \frac{1}{Z[0]} \frac{\delta Z[\mu']}{\delta \mu'}|_{\mu'=0} = 0, \quad (\text{J.8})$$

where

$$Z[\mu'] \equiv \int \mathcal{D}\mu \mathcal{D}N \mathcal{D}\psi^* \mathcal{D}\psi e^{i \int d\tau (\mu + \mu') (N - \psi^* \psi) - \mathcal{S}[\psi, \psi^*]}. \quad (\text{J.9})$$

Eq. (J.8) can be proved by identities of variations and path integrals;

$$\begin{aligned} \langle N - \psi^* \psi \rangle &= \frac{-i}{Z[0]} \int \mathcal{D}\mu \frac{\delta}{\delta \mu'}|_{\mu'=0} \int \mathcal{D}N \mathcal{D}\psi^* \mathcal{D}\psi e^{i \int d\tau (\mu + \mu') (N - \psi^* \psi) - \mathcal{S}[\psi, \psi^*]} \\ &= \frac{-i}{Z[0]} \int \mathcal{D}\mu \frac{\delta}{\delta \mu} \int \mathcal{D}N \mathcal{D}\psi^* \mathcal{D}\psi e^{i \int d\tau \mu (N - \psi^* \psi) - \mathcal{S}[\psi, \psi^*]} = 0, \end{aligned} \quad (\text{J.10})$$

where the last equation holds because it is a surface term. Eq. (J.8) can be easily generalized to Eq. (J.7), so  $N_{C/S}$  indeed has the physical meaning of the charge/spin density difference in the hole layer.

### K. Impossibility that Eq. (G.13) consists of two wavevector Fourier components

In this section, we show it impossible that  $\psi'_\mu(\vec{r})$  in Eq. (G.13) is given by two wavevectors Fourier components. To be specific, we show that  $\psi'_\mu(\vec{r})$  thus given cannot satisfy the local constraint,  $\vec{\psi}'(\vec{r}) \cdot \vec{\psi}'(\vec{r}) = 1$ . For simplicity of the notation, we omit the prime in  $\vec{\psi}'(\vec{r})$  in this section:  $\vec{\psi}'(\vec{r}) \rightarrow \vec{\psi}(\vec{r})$ . Suppose that  $\vec{\psi}(\vec{r})$  is given by two wavevector Fourier components,  $\vec{k}$  and  $\vec{k}'$  with  $k_x > 0$ ,  $k'_x > 0$ ;

$$\vec{\psi}(\vec{r}) = \frac{2}{V} \text{Re}(\vec{\psi}_{\vec{k}} e^{i\vec{k} \cdot \vec{r}} + \vec{\psi}_{\vec{k}'} e^{i\vec{k}' \cdot \vec{r}}) \equiv \frac{\sqrt{2}}{V} (w \vec{\psi}_{\vec{k}}(\vec{r}) + w' \vec{\psi}_{\vec{k}'}(\vec{r})), \quad (\text{K.1})$$

Here  $\vec{\psi}_{\vec{k}}(\vec{r})$  is a unit vector defined by Eq. (G.13),

$$\begin{aligned} \vec{\psi}_{\vec{k}}(\vec{r}) = & [-\sin\omega\sin\zeta\sin(\vec{k} \cdot \vec{r} - \delta_2) + \cos\omega\cos\zeta\cos(\vec{k} \cdot \vec{r} - \delta_1)]\vec{e}_x \\ & + [\sin\omega\cos\zeta\cos(\vec{k} \cdot \vec{r} - \delta_1) + \cos\omega\sin\zeta\sin(\vec{k} \cdot \vec{r} - \delta_2)]\vec{e}_y - \cos\zeta\sin(\vec{k} \cdot \vec{r} - \delta_1)\vec{e}_z + \sin\zeta\cos(\vec{k} \cdot \vec{r} - \delta_2)\vec{e}_0, \end{aligned} \quad (\text{K.2})$$

with  $\vec{k} \equiv \frac{D}{2\lambda}(\cos\omega\vec{e}_x + \sin\omega\vec{e}_y)$  and arbitrary U(1) phase variables  $\zeta, \delta_1, \delta_2$ . The other unit vector  $\vec{\psi}_{\vec{k}'}(\vec{r})$  is defined in the same way with  $\vec{k}' \equiv \frac{D}{2\lambda}(\cos\omega'\vec{e}_x + \sin\omega'\vec{e}_y)$ ,  $\zeta', \delta'_1, \delta'_2$ . Since  $k_x > 0$ ,  $k'_x > 0$  and  $\vec{k} \neq \vec{k}'$ ,  $2\tau \equiv \omega - \omega'$  must satisfy  $\sin\tau \neq 0$  and  $\cos\tau \neq 0$ .

In the following, we will argue that it is impossible that  $\psi_\mu(\vec{r})$  thus given satisfies the local constraint. Firstly, the norm of  $\psi_\mu(\vec{r})$  is given by

$$\vec{\psi}(\vec{r}) \cdot \vec{\psi}(\vec{r}) = \frac{2}{V^2} (w^2 + w'^2) + \frac{4}{V^2} w w' \vec{\psi}_{\vec{k}}(\vec{r}) \cdot \vec{\psi}_{\vec{k}'}(\vec{r}), \quad (\text{K.3})$$

where the second term in the right hand side generally depends on spatial coordinate  $\vec{r}$ ,

$$\begin{aligned} 2\vec{\psi}_{\vec{k}}(\vec{r}) \cdot \vec{\psi}_{\vec{k}'}(\vec{r}) = & [(1 - \cos(\omega - \omega'))(\sin\zeta\sin\zeta'\cos(\delta_2 + \delta'_2) - \cos\zeta\cos\zeta'\cos(\delta_1 + \delta'_1)) \\ & + \sin(\omega - \omega')(\sin\zeta\cos\zeta'\sin(\delta_2 + \delta'_1) - \cos\zeta\sin\zeta'\sin(\delta'_2 + \delta_1))] \cos((\vec{k} + \vec{k}') \cdot \vec{r}) \\ & + [(1 - \cos(\omega - \omega'))(\sin\zeta\sin\zeta'\sin(\delta_2 + \delta'_2) - \cos\zeta\cos\zeta'\sin(\delta_1 + \delta'_1)) \\ & + \sin(\omega - \omega')(-\sin\zeta\cos\zeta'\cos(\delta_2 + \delta'_1) + \cos\zeta\sin\zeta'\cos(\delta'_2 + \delta_1))] \sin((\vec{k} + \vec{k}') \cdot \vec{r}) \\ & + [(1 + \cos(\omega - \omega'))(\sin\zeta\sin\zeta'\cos(\delta_2 - \delta'_2) + \cos\zeta\cos\zeta'\cos(\delta_1 - \delta'_1)) \\ & + \sin(\omega - \omega')(\sin\zeta\cos\zeta'\sin(\delta_2 - \delta'_1) - \cos\zeta\sin\zeta'\sin(\delta'_2 - \delta_1))] \cos((\vec{k} - \vec{k}') \cdot \vec{r}) \\ & + [(1 + \cos(\omega - \omega'))(\sin\zeta\sin\zeta'\sin(\delta_2 - \delta'_2) + \cos\zeta\cos\zeta'\sin(\delta_1 - \delta'_1)) \\ & + \sin(\omega - \omega')(-\sin\zeta\cos\zeta'\cos(\delta_2 - \delta'_1) - \cos\zeta\sin\zeta'\cos(\delta'_2 - \delta_1))] \sin((\vec{k} - \vec{k}') \cdot \vec{r}). \end{aligned} \quad (\text{K.4})$$

Thus, in order for  $\vec{\psi}(\vec{r})$  to satisfy the local constraint, the coefficients in front of  $\cos((\vec{k} + \vec{k}') \cdot \vec{r})$ ,  $\sin((\vec{k} + \vec{k}') \cdot \vec{r})$ ,  $\cos((\vec{k} - \vec{k}') \cdot \vec{r})$  and  $\sin((\vec{k} - \vec{k}') \cdot \vec{r})$  in Eq. (K.4) should be zero. Adding the coefficients in front of the first two terms together, we get:

$$2\sin^2\tau [\sin\zeta\sin\zeta'e^{i(\delta_2 + \delta'_2)} - \cos\zeta\cos\zeta'e^{i(\delta_1 + \delta'_1)}] - 2i\cos\tau\sin\tau [\sin\zeta\cos\zeta'e^{i(\delta_2 + \delta'_1)} - \cos\zeta\sin\zeta'e^{i(\delta_1 + \delta'_2)}] = 0. \quad (\text{K.5})$$

Adding the coefficients in front of the last two terms together, we get:

$$2\cos^2\tau [\sin\zeta\sin\zeta'e^{i(\delta_2 - \delta'_2)} + \cos\zeta\cos\zeta'e^{i(\delta_1 - \delta'_1)}] - 2i\cos\tau\sin\tau [\sin\zeta\cos\zeta'e^{i(\delta_2 - \delta'_1)} + \cos\zeta\sin\zeta'e^{i(\delta_1 - \delta'_2)}] = 0. \quad (\text{K.6})$$

As  $\sin\tau \neq 0$  and  $\cos\tau \neq 0$ , these two lead to either one of the following two constraints on  $\zeta, \zeta', \delta_1, \delta'_1, \delta_2, \delta'_2$  and  $2\tau \equiv \omega - \omega'$ . One is

$$\begin{aligned} \sin\zeta\sin\zeta'e^{i(\delta_2 + \delta'_2)} - \cos\zeta\cos\zeta'e^{i(\delta_1 + \delta'_1)} &= \sin\zeta\cos\zeta'e^{i(\delta_2 + \delta'_1)} - \cos\zeta\sin\zeta'e^{i(\delta_1 + \delta'_2)} \\ &= \sin\zeta\sin\zeta'e^{i(\delta_2 - \delta'_2)} + \cos\zeta\cos\zeta'e^{i(\delta_1 - \delta'_1)} = \sin\zeta\cos\zeta'e^{i(\delta_2 - \delta'_1)} + \cos\zeta\sin\zeta'e^{i(\delta_1 - \delta'_2)} = 0, \end{aligned} \quad (\text{K.7})$$

while the other is

$$\frac{\sin\zeta\cos\zeta'e^{i(\delta_2 + \delta'_1)} - \cos\zeta\sin\zeta'e^{i(\delta_1 + \delta'_2)}}{\sin\zeta\sin\zeta'e^{i(\delta_2 + \delta'_2)} - \cos\zeta\cos\zeta'e^{i(\delta_1 + \delta'_1)}} = -\frac{\sin\zeta\sin\zeta'e^{i(\delta_2 - \delta'_2)} + \cos\zeta\cos\zeta'e^{i(\delta_1 - \delta'_1)}}{\sin\zeta\cos\zeta'e^{i(\delta_2 - \delta'_1)} + \cos\zeta\sin\zeta'e^{i(\delta_1 - \delta'_2)}} = -i(\tan\tau). \quad (\text{K.8})$$

We first explore a possibility of the second constraint, Eq. (K.8). We simplify the first equation in Eq. (K.8), to get  $\sin^2\zeta e^{2i\delta_2} = \cos^2\zeta e^{2i\delta_1}$ . Thus, the second constraint leads to

$$\delta_2 = \delta_1 + n\pi, \quad \zeta = \frac{\pi}{4}, \frac{3\pi}{4}, \frac{5\pi}{4}, \frac{7\pi}{4}, \quad (\text{K.9})$$

with an integer  $n$ . Putting Eq. (K.9) back into Eq. (K.8) again, we end up with  $\pm 1 = i(\tan\tau)$ . This is clearly impossible. We next explore a possibility of the first constraint, Eq. (K.7). The first constraint is equivalent to the following eight equations

$$\begin{cases} \sin\zeta\sin\zeta'\cos(\delta_2 + \delta'_2) - \cos\zeta\cos\zeta'\cos(\delta_1 + \delta'_1) = 0, & \sin\zeta\cos\zeta'\sin(\delta_2 + \delta'_1) - \cos\zeta\sin\zeta'\sin(\delta_1 + \delta'_2) = 0, \\ \sin\zeta\sin\zeta'\sin(\delta_2 + \delta'_2) - \cos\zeta\cos\zeta'\sin(\delta_1 + \delta'_1) = 0, & \sin\zeta\cos\zeta'\cos(\delta_2 + \delta'_1) - \cos\zeta\sin\zeta'\cos(\delta_1 + \delta'_2) = 0, \\ \sin\zeta\sin\zeta'\cos(\delta_2 - \delta'_2) + \cos\zeta\cos\zeta'\cos(\delta_1 - \delta'_1) = 0, & \sin\zeta\cos\zeta'\sin(\delta_2 - \delta'_1) + \cos\zeta\sin\zeta'\sin(\delta_1 - \delta'_2) = 0, \\ \sin\zeta\sin\zeta'\sin(\delta_2 - \delta'_2) + \cos\zeta\cos\zeta'\sin(\delta_1 - \delta'_1) = 0, & \sin\zeta\cos\zeta'\cos(\delta_2 - \delta'_1) + \cos\zeta\sin\zeta'\cos(\delta_1 - \delta'_2) = 0. \end{cases} \quad (\text{K.10})$$

Eq. (K.10) leads to

$$\begin{cases} \tan(\delta_1 + \delta'_1) = \tan(\delta_2 + \delta'_2), & \tan(\delta_2 + \delta'_1) = \tan(\delta_1 + \delta'_2), \\ \tan(\delta_1 - \delta'_1) = \tan(\delta_2 - \delta'_2), & \tan(\delta_2 - \delta'_1) = \tan(\delta_1 - \delta'_2). \end{cases} \quad (\text{K.11})$$

Eq. (K.11) results in:

$$2(\delta_2 - \delta_1) = m\pi, \quad 2(\delta'_2 - \delta'_1) = n\pi, \quad (\text{K.12})$$

with integers  $m$  and  $n$ . Putting Eq. (K.12) into Eq. (K.11), we can see that  $m \pm n$  must be an even integer. Taking Eq. (K.12) into Eq. (K.10), we finally find the following four possibilities depending on the two integers  $\frac{m+n}{2}$  and  $\frac{m-n}{2}$ ,

$$\begin{cases} \cos(\zeta - \zeta') = \cos(\zeta + \zeta') = \sin(\zeta - \zeta') = \sin(\zeta + \zeta') = 0, & \text{when } \frac{m+n}{2} \text{ is odd (even) and } \frac{m-n}{2} \text{ is odd (even),} \\ \cos(\zeta - \zeta') = \sin(\zeta - \zeta') = 0, & \text{when } \frac{m+n}{2} \text{ is odd and } \frac{m-n}{2} \text{ is even,} \\ \cos(\zeta + \zeta') = \sin(\zeta + \zeta') = 0, & \text{when } \frac{m+n}{2} \text{ is even and } \frac{m-n}{2} \text{ is odd.} \end{cases} \quad (\text{K.13})$$

They are all impossible. This concludes that Eqs. (K.4) inevitably depends on the spatial coordinate, contradicting the local constraint. Thus, Eq. (K.1) cannot be true.

---